

# **For Reference**

---

**NOT TO BE TAKEN FROM THIS ROOM**



Ex LIBRIS  
UNIVERSITATIS  
ALBERTAENSIS





Digitized by the Internet Archive  
in 2019 with funding from  
University of Alberta Libraries

<https://archive.org/details/Tighe1979>











THE UNIVERSITY OF ALBERTA

RELEASE FORM

NAME OF AUTHOR ..... William G. Tighe .....  
TITLE OF THESIS ..... The Development of the Westward .....  
..... Travelling Surge during Magnetospheric .....  
..... Substorms .....  
DEGREE FOR WHICH THESIS WAS PRESENTED ..... Master of Science ...  
YEAR THIS DEGREE GRANTED ..... 1979 .....

Permission is hereby granted to THE UNIVERSITY OF ALBERTA LIBRARY to reproduce single copies of this thesis and to lend or sell such copies for private, scholarly or scientific research purposes only.

The author reserves other publication rights, and neither the thesis nor extensive extracts from it may be printed or otherwise reproduced without the author's written permission.





THE UNIVERSITY OF ALBERTA

The Development of the Westward Travelling Surge during  
Magnetospheric Substorms

by

William G. Tighe



A THESIS

SUBMITTED TO THE FACULTY OF GRADUATE STUDIES AND RESEARCH  
IN PARTIAL FULFILMENT OF THE REQUIREMENTS FOR THE DEGREE  
OF MASTER OF SCIENCE

DEPARTMENT OF PHYSICS

EDMONTON, ALBERTA

Fall, 1979





THE UNIVERSITY OF ALBERTA  
FACULTY OF GRADUATE STUDIES AND RESEARCH

The undersigned certify that they have read, and  
recommend to the Faculty of Graduate Studies and Research,  
for acceptance, a thesis entitled .....  
Westward Travelling Surge during Magnetospheric Substorms  
.....  
.....  
submitted by William G. Tighe .....  
in partial fulfilment of the requirements for the degree of  
Master of Science





## ABSTRACT

The westward travelling surge is a bulge-like auroral form which moves westward during the expansion phase of the auroral substorm. Using a network of ground-based magnetometers and some supporting all-sky photographic data, the magnetic variations associated with the westward travelling surge during three substorm events are analyzed. The development of the surge is described primarily in terms of longitude and latitude profiles of the magnetic data from the array and the magnetic signature of the surge is described in terms of these profiles. The magnetic signature of the surge is generally seen to be localized within 10 - 20 degrees of longitude, implying an associated current system with a 400 - 800 kilometer scale size. The evolution of the surge is seen through changes of its magnetic signature. The surge is often found to form and grow in a fixed location prior to moving westward and the westward motion can often be irregular in nature. To explain the features of the magnetic signature, a model current system for the surge is given. The model includes equatorward flowing current in the forward portion of the surge and poleward flowing current in the trailing portion of the surge. The model also incorporates the possibility of current systems being tilted with respect to lines of constant magnetic latitude. Good agreement is found between the model and the observations.



## ACKNOWLEDGEMENTS

I owe Dr. Gordon Rostoker, my supervisor, a tremendous amount of gratitude for his advice and support throughout the course of this research. He continually provided useful discussion and proved to be a remarkable source of information.

I would also like to extend my thanks to Dr. Terry Hughes, Dr. Koji Kawasaki, Dr. Jerry Kisabeth, and Dr. John Olson, all of whom provided extensive assistance. In particular, Jerry Kisabeth and Terry Hughes supplied the basic programs used in the model, John Olson supplied the basic programs for the handling of the data and Koji Kawasaki was always available for and always supplied valuable discussion. I am very grateful for their help and very proud of their friendship.





DEDICATION  
to my Parents



## TABLE OF CONTENTS

CHAPTER	PAGE
1. INTRODUCTION TO SUBSTORMS AND SURGES .....	1
1.1 The Magnetosphere .....	1
1.2 The Magnetospheric Substorm .....	7
1.2.1 The Auroral Substorm .....	8
1.2.2 The Polar Magnetic Substorm .....	9
1.2.3 The Substorm Model .....	14
1.3 The Westward Travelling Surge .....	18
1.3.1 The Auroral Behaviour .....	18
1.3.2 The Magnetic Behaviour and the Surge Model ..	21
1.4 The Thesis Objectives .....	25
2. DATA COLLECTING AND HANDLING .....	27
2.1 Data Collection and Processing .....	27
2.1.1 The Flux-Gate Magnetometer .....	27
2.1.2 The Riometer .....	28
2.1.3 The All-Sky Camera .....	29
2.1.4 The Station Network .....	31
2.1.5 Data Processing .....	35
2.2 Data Presentation .....	35
2.2.1 The Stacked Magnetogram Format .....	35
2.2.2 The Profile Format .....	36
3. EVENT ANALYSIS .....	39
3.1 Selection of the Events for Analysis .....	39





3.2 The Approach to the Analysis of the Events .....	40
3.3 Event Analysis: Day 214, 1974 .....	47
3.3.1 Introduction .....	47
3.3.2 Surge Onset and Development .....	55
3.3.3 Following the Passage of the Surge .....	63
3.3.4 Summary for Day 214, 1974 .....	64
3.4 Event Analysis: Day 307, 1974 .....	65
3.4.1 Introduction .....	65
3.4.2 Surge Onset and Development .....	73
3.4.3 Following the Passage of the Surge .....	87
3.4.4 Summary for Day 307, 1976 .....	87
3.5 Event Analysis: Day 223, 1977 .....	89
3.5.1 Introduction .....	89
3.5.2 Activity Prior to Onset .....	97
3.5.3 Surge Onset and Development .....	102
3.5.4 Following the Passage of the Surge .....	109
3.5.5 Summary of Day 223, 1977 .....	113
3.6 Summary .....	115
4. MODELLING OF THE SUBSTORM EVENTS .....	119
4.1 Introduction .....	119
4.2 The Model Current System .....	119
4.3 Justification of the Model .....	121
4.4 General Approach to the Modelling .....	123
4.5 Modelling the Data .....	124
4.5.1 The Day 214, 1974 Event .....	124
4.5.2 The Day 307, 1976 Event .....	128
4.5.3 The Day 223, 1977 Event .....	136



## TABLE OF CONTENTS continued

4.6 Summary .....	145
5. CONCLUSIONS AND DISCUSSION .....	148
5.1 Summary of Results .....	148
5.2 Comments and Discussion .....	151
5.3 Final Comments .....	157
BIBLIOGRAPHY .....	158





## LIST OF TABLES

Table	Description	Page
2.1	Locations of Stations used in this Study	32
4.1	Current System Parameters; Surge Model for Day 214, 1974	126
4.2	Current System Parameters; Surge Model for Day 307, 1976	129
4.3	Current System Parameters; Surge Model for Day 223, 1977	137
5.1	Ionospheric Surge Parameters Mapped to the Plasma Sheet	152



## LIST OF FIGURES

Figure		Page
1.1	Plasma regions in the Earth's magnetosphere (after Akasofu, 1977). Large arrows indicate plasma flow (after Axford and Hines, 1961).	2
1.2	The development of the auroral substorm shown in sequential plots (after Akasofu, 1964).	10
1.3	Location of eastward and westward electrojets. Region of overlap is known as the Harang Discontinuity. Location of field-aligned currents is also shown (after Iijima and Potemera, 1978).	12
1.4	Wiens-Rostoker model for the expansion of the westward electrojet showing stepping motion (after Wiens and Rostoker, 1975).	15
1.5	Model for magnetospheric substorms involving reconnection of magnetic field lines in the magnetotail (after Akasofu, 1978).	17
1.6	Model for magnetospheric substorms involving disruption of cross-tail current in the magnetotail (after Akasofu, 1978).	19
1.7	Summary of electron precipitation within the westward travelling surge (after Meng <u>et al</u> , 1978).	22
1.8	Surge model showing north-south shear and superposed ionospheric current (after Kisabeth and Rostoker, 1973).	24
1.9	Hughes model of westward electrojet development during a substorm including westward travelling surge (after Hughes, 1978).	26
2.1	Typical All-Sky camera and photograph (inset) (after Rostoker, 1975).	30
2.2	Map indicating locations of most stations used in this study	33



# LIST OF FIGURES continued

3.1	Theoretical latitude profile at various positions beneath a westward electrojet (after Kisabeth, 1972).	41
3.2	Diagram of surge model used in this study. The large arrows indicate a Birkeland current loop which is closed in the ionosphere with a westward current. The smaller arrows are used for loops with either equatorward or poleward ionospheric currents. White arrows are used in regions behind other current sheets. Dotted lines indicate a projection to the earth's surface where A, B, and C and 1, 2, and 3, indicate positions of longitude and latitude profiles shown in figure 3.3 .	44
3.3	Longitude and latitude profiles at locations indicated in figure 3.2 . of surge model used in this study.	45
3.4	Stacked magnetograms: H' component for Day 214, 1974. Arrows indicate times of interest referred to in text.	48
3.5	Stacked magnetograms: D' component for Day 214, 1974. Arrows indicate times of interest referred to in text.	49
3.6	Stacked magnetograms: Z component for Day 214, 1974. Arrows indicate times of interest referred to in text.	50
3.7	Corrected All-Sky camera images and associated longitude profiles at indicated times on Day 214, 1974. H, S, U refer to stations at Hay River, Fort Smith and Uranium City respectively. Arrows at the stations indicate geomagnetic north. LMN refers to Local Magnetic North. X, Y, Z refer to magnetic components H, D, Z, respectively.	53
3.8	Corrected All-Sky camera images and associated longitude profiles at indicated times on Day 214, 1974. Symbols as in figure 3.7 .	54
3.9	Graph of position versus time showing the motion of both the leading edge of the surge form and the D component cross-over point.	60
3.10	Contour plot of D component perturbation due to a simplified model for the surge.	62





# LIST OF FIGURES continued

3.11	Stacked magnetograms along east-west station chain: H' component for Day 307, 1976. Regions of interest referred to in text are indicated.	66
3.12	Stacked magnetograms along east-west station chain: D' component for Day 307, 1976. Regions of interest referred to in text are indicated.	67
3.13	Stacked magnetograms along east-west station chain: Z component for Day 307, 1976. Regions of interest referred to in text are indicated.	68
3.14	Stacked magnetograms along south-north station chain: H' component for Day 307, 1976. Regions of interest referred to in text are indicated.	69
3.15	Stacked magnetograms along south-north station chain: D' component for Day 307, 1976. Regions of interest referred to in text are indicated.	70
3.16	Stacked magnetograms along south-north station chain: Z component for Day 307, 1976. Regions of interest referred to in text are indicated.	71
3.17	Stacked riometer signals at available stations for Day 307, 1976. Regions of interest referred to in text are indicated.	72
3.18	Longitude profiles at indicated times for Day 307, 1976. Profiles are referred to in text by the indicated label. Note that X, Y, and Z refer to magnetic components H, D, and Z.	74
3.19	Latitude profiles at indicated times for Day 307, 1976. Profiles are referred to in text by the indicated label. Note that X, Y, and Z refer to magnetic components H, D, and Z.	75
3.20	Longitude profiles at indicated times for Day 307, 1976. Profiles are referred to in text by the indicated label. Note that X, Y, and Z refer to magnetic components H, D, and Z.	80
3.21	Latitude profiles at indicated times for Day 307, 1976. Profiles are referred to in text by the indicated label. Note that X, Y, and Z refer to magnetic components H, D, and Z.	81
3.22	Longitude profiles at indicated times for Day 307, 1976. Profiles are referred to in text by the indicated label. Note that X, Y, and Z refer to magnetic components H, D, and Z.	84



# LIST OF FIGURES continued

3.23	Stacked magnetograms along east-west station chain: H' component for Day 223, 1977. Regions of interest referred to in text are indicated.	90
3.24	Stacked magnetograms along east-west station chain: D' component for Day 223, 1977. Regions of interest referred to in text are indicated.	91
3.25	Stacked magnetograms along east-west station chain: Z component for Day 223, 1977. Regions of interest referred to in text are indicated.	92
3.26	Stacked magnetograms along south-north station chain: H' component for Day 223, 1977. Regions of interest referred to in text are indicated.	93
3.27	Stacked magnetograms along south-north station chain: D' component for Day 223, 1977. Regions of interest referred to in text are indicated.	94
3.28	Stacked magnetograms along south-north station chain: Z component for Day 223, 1977. Regions of interest referred to in text are indicated.	95
3.29	Stacked riometer signals at available stations for Day 223, 1977. Regions of interest referred to in text are indicated .	96
3.30	Magnetograms from Churchill and Whiteshell for Day 223, 1977.	98
3.31	Longitude profiles at indicated times for Day 223, 1977. Profiles are referred to in text by the indicated label. Note that X , Y, and Z refer to magnetic components H, D, and Z.	100
3.32	Latitude profiles at indicated times for Day 223, 1977. Profiles are referred to in text by the indicated label. Note that X , Y, and Z refer to magnetic components H, D, and Z.	101
3.33	Longitude profiles at indicated times for Day 223, 1977. Profiles are referred to in text by the indicated label. Note that X , Y, and Z refer to magnetic components H, D, and Z.	106
3.34	Latitude profiles at indicated times for Day 223, 1977. Profiles are referred to in text by the indicated label. Note that X , Y, and Z refer to magnetic components H, D, and Z.	107
3.35	Estimated locations of electrojets before ('A') and after ('B') onset of event on Day 223, 1977.	112





# LIST OF FIGURES continued

3.36	Magnetograms from station at Honolulu for event on Day 223, 1977 and also, for comparison, on a quiet day (Day 234, 1977)	114
4.1	Hall and Pederson current flow for electric fields expected in westward electrojet ('A') and surge ('B') regions. Subscripts H and P refer to Hall and Pederson, respectively. N, E, W, and S refer to directions north, east, west and south.	122
4.2	Observed and theoretical longitude profiles at indicated times for Day 214, 1974. Profiles are referred to in text by the indicated label. Note that X, Y, and Z refer to magnetic components H, D, and Z.	127
4.3	Observed and theoretical longitude profiles at indicated times for Day 307, 1976. Profiles are referred to in text by the indicated label. Note that X, Y, and Z refer to magnetic components H, D, and Z.	130
4.4	Observed and theoretical latitude profiles at indicated times for Day 307, 1976. Profiles are referred to in text by the indicated label. Note that X, Y, and Z refer to magnetic components H, D, and Z.	131
4.5	Observed and theoretical longitude profiles at indicated times for Day 307, 1976. Profiles are referred to in text by the indicated label. Note that X, Y, and Z refer to magnetic components H, D, and Z.	132
4.6	Observed and theoretical latitude profiles at indicated times for Day 307, 1976. Profiles are referred to in text by the indicated label. Note that X, Y, and Z refer to magnetic components H, D, and Z.	133
4.7	Observed and theoretical longitude profiles at indicated times for Day 223, 1977. Profiles are referred to in text by the indicated label. Note that X, Y, and Z refer to magnetic components H, D, and Z.	138
4.8	Observed and theoretical latitude profiles at indicated times for Day 223, 1977. Profiles are referred to in text by the indicated label. Note that X, Y, and Z refer to magnetic components H, D, and Z.	139



## LIST OF FIGURES continued

- 4.9 Observed and theoretical longitude profiles at indicated times for Day 223, 1977. Profiles are referred to in text by the indicated label. Note that X , Y, and Z refer to magnetic components H, D, and Z. 140
- 4.10 Observed and theoretical latitude profiles at indicated times for Day 223, 1977. Profiles are referred to in text by the indicated label. Note that X , Y, and Z refer to magnetic components H, D, and Z. 141



## CHAPTER 1

### INTRODUCTION TO SUBSTORMS AND SURGES

#### 1.1 The Magnetosphere

Surface measurements show that the Earth's main magnetic field is nearly dipolar (Chapman and Bartels, 1940). However satellite measurements found that the outer field is far from dipolar. While the inner field co-rotates with the Earth, the outer field remains relatively stationary with respect to the Earth-Sun line with the sunward side compressed in comparison to a pure dipole and the anti-sunward side swept back in the fashion of a comet tail (see figure 1.1). It is the interaction of the solar wind with the Earth's field which causes this distortion.

In order to explain the anti-sunward orientation of comet tails, Biermann(1951) suggested that the Sun emitted a continuous stream of corpuscular radiation. Following this suggestion by Biermann, Parker(1958) suggested that the plasma of the Sun's corona was expanding radially. He named the effect the solar wind. His calculations, now experimentally verified, showed the solar wind to be supersonic and super-Alfvénic. The Alfvén velocity is the velocity of a magnetic disturbance in a plasma. The magnetic field lines of the Sun are "frozen" into the solar wind plasma and are drawn out in an Archimedean spiral because of the combination of the radial motion of the plasma and the





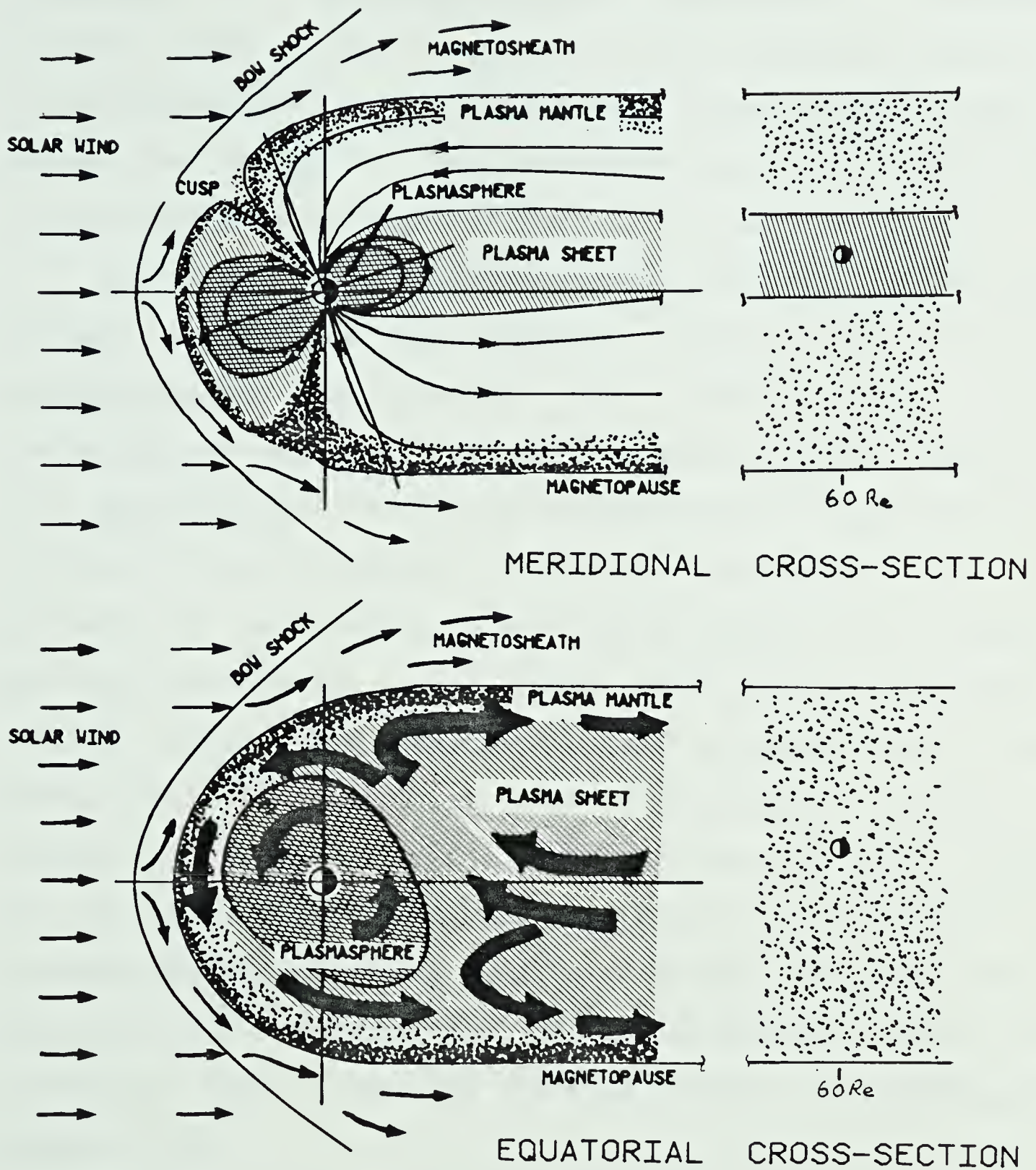


Figure 1.1  
 Plasma regions in the Earth's magnetosphere  
 (after Akasofu, 1977). Large arrows indicate  
 plasma flow (after Axford and Hines, 1961).



Sun's rotation. When this supersonic, super-Alfvénic, magnetized and collisionless plasma encounters a magnetic obstacle (the Earth's magnetic field) a standing magnetohydrodynamic shock is set up (Axford, 1962; Kellogg, 1962). Along the Earth-Sun line, the shock front stands about 14 Earth radii ( $R_E$ ) in front of the Earth (see figure 1.1).

As the solar wind plasma crosses the shock front it becomes thermalized and enters a region known as the magnetosheath. The plasma then flows around the magnetosphere separated from it by a sharp boundary known as the magnetopause. Axford and Hines (1961) suggested that this motion would result in a "viscous interaction" with the plasma near the boundary of the magnetosphere. The plasma and the associated field lines would then be drawn downstream. Dungey (1961) and others, have suggested that the solar wind interacts with the magnetosphere through a magnetic merging of the interplanetary magnetic field with the Earth's magnetic field. The field lines would then be carried downstream by the solar wind plasma. In either case, dayside field lines are seen to be compressed while the nightside field lines are extended to form the magnetotail (Ness, 1965).

The magnetotail has an approximately cylindrical cross-section, with an average radius of 20  $R_E$ . It consists of earthward directed field lines in the northern half of the tail and anti-earthward directed field lines in the southern half of the tail. The central separating plane is termed the





neutral sheet. The magnetotail has been observed at distances of 100 Re and has been detected by space probes extending beyond 1000 Re, although at this distance the characteristics are not so clearly defined. Near the Earth the magnetotail field lines become less extended and more dipolar in character.

The magnetosphere can also be characterized by distinct regions of plasma known as the plasma mantle, the plasma sheet and the plasmasphere (see figure 1.1). Before examining the nature of these plasma regions, we will briefly discuss some of the basic features of particle behaviour in a magnetized plasma.

In a homogeneous magnetic field a charged particle will gyrate around the field lines with positively charged particles moving clockwise and negatively charged particles moving counter-clockwise. If the particle's velocity has a component parallel to the field line then the particle will follow a helical path. If, in addition, there is a perturbing electric field acting normal to the magnetic field then the particle will drift with a velocity given by:

$$\vec{v}_d = (\vec{E} \times \vec{B}) / |\vec{B}|^2 \quad (1.1)$$

This drift velocity is perpendicular to both  $\vec{E}$  and  $\vec{B}$  and independent of the particle's charge. If, instead of an electric field, there is a magnetic field gradient present then the particles will also experience a drift. The drift is perpendicular to both the magnetic field and its gradient but its direction depends on the sign of the charge of the



particle. This is true for any charge-independent force acting normal to the magnetic field (see for example, Roederer (1970)).

The degree to which these individual particle motions are important in a plasma depends to a large extent on the collision frequency. With a high collision frequency the plasma is conductively isotropic and Ohm's law gives us the relation;

$$\vec{j} = \sigma (\vec{E} + (\vec{V} \times \vec{B})) \quad (1.2)$$

where we note that,  $\vec{V}$  is the plasma velocity and  $\sigma$  is the conductivity. If we let  $\vec{E}'$  be the electric field in the reference frame of a plasma moving with velocity  $\vec{V}$ , then;

$$\vec{E}' = \vec{E} + (\vec{V} \times \vec{B}) \quad (1.3)$$

and so,

$$\vec{j} = \sigma \vec{E}' \quad (1.4)$$

If the collision frequency is low enough then the individual particle motions become important and the conductivity of the plasma is anisotropic. The currents which flow in the plane perpendicular to the magnetic field are of specific interest. These are the Pederson current (parallel to the electric field,  $\vec{E}'$ ) and the Hall current (perpendicular to the electric field,  $\vec{E}'$ ). The conductivity is a tensor which has components given by;

$$\vec{j} = \sigma_p \vec{E}' + \sigma_h (\vec{B} \times \vec{E}') / |\vec{B}| \quad (1.5)$$

Here,  $\sigma_p$  is the Pederson conductivity and  $\sigma_h$  is the Hall conductivity. In the ionosphere the Hall and Pederson conductivities are height-dependent. In the F region (from





160 - 250 km.) the Pederson current will dominate while in the E region (from 85-160 km.) both Hall and Pederson currents are important. The Hall current is carried primarily by electrons while the Pederson current is carried primarily by the ions.

The primary source of magnetospheric plasma is the solar wind. Large scale convection patterns, possibly caused by the "viscous interaction" proposed by Axford and Hines (1961) or by the magnetic field merging proposed by Dungey (1961), provide a mechanism by which the inner regions of the magnetosphere could become populated with plasma. The exact way in which the solar wind plasma gains entry to the magnetosphere is not yet understood. However, it is generally felt that the anti-sunward flowing plasma (the plasma mantle and entry layer inside the tail magnetopause) eventually convects towards the center of the tail to form the plasma sheet.

The parameters of the plasma sheet are highly variable according to the state of the magnetosphere. An important characteristic is an electric field directed from dawn to dusk with a typical magnitude of  $\sim .2$  mv/m . A cross-tail current, flowing east to west in the plasma sheet, is also observed. On the average, the plasma sheet has a thickness of  $8 R_E$  being thinnest at the center of the magnetotail and flaring towards the edges. The average particle density is  $.5 \text{ cm}^{-3}$  with average electron energies of 1 Kev and proton energies of 6 Kev.



Unlike the plasma sheet the plasmasphere co-rotates with the Earth. Bounded at 3-5 Re by the plasmopause, it is populated mainly by particles with energies of  $\sim 1$  ev at a concentration of  $\sim 10^3$  cm $^{-3}$ . It also contains regions of trapped, high energy particles. These particles gyrate around the magnetic lines of force and bounce between mirror points in each hemisphere. Azimuthal drifts due to magnetic field line curvature and radial gradients, cause protons to drift westward and electrons to drift eastward. Just outside the plasmopause the conditions are such that this type of drift results in the formation of the ring current which may produce a significant magnetic effect at the Earth's surface during periods of strong magnetospheric activity.

## 1.2 The Magnetospheric Substorm

The magnetospheric substorm (or simply substorm) is an explosive process, the primary purpose of which is to release energy stored in the magnetotail. The process involves the energization of plasma sheet particles. Eventually these particles precipitate into the ionosphere, enhancing the horizontal conductivity and leading to the formation of large scale current systems. Much of the energy is dissipated through joule heating. The currents develop systematically, producing magnetic perturbations known as the polar magnetic substorm and , through the excitation of atmospheric constituents, optical effects (the auroral substorm ).



### 1.2.1 The Auroral Substorm

The aurora consists of either discrete forms or diffuse glow. The discrete forms constitute distinct arcs while the diffuse aurora are broad regions of luminosity (Snyder and Akasofu, 1974). The aurorae occur at heights of 100 to 200 km and generally lie within oval-shaped regions which sit eccentrically around the magnetic poles. These are known as the auroral ovals. Around the north pole, the oval is centered near  $78^\circ$  geomagnetic latitude on the dayside while at midnight, it is near  $68^\circ$ .

Davis (1972) has summarized the behaviour of the aurora. When the magnetic field imbedded in the solar wind, the Interplanetary Magnetic Field (IMF), is directed northward, the aurora is usually in a quiet phase. In this phase there are only a few weak forms and the auroral oval is contracted. With the turning of the IMF to a southward direction, a growth phase begins. As to whether this is a phase of the substorm or is independent of substorm activity, is still undecided. In any case, during this phase the auroral oval widens and expands equatorward. There is also an increased number of discrete arcs and the diffuse aurora intensifies. Auroral forms are observed to move westward in the evening sector, eastward in the morning sector and equatorward in both. This movement is presumably associated with convective processes in the magnetosphere.

The onset of an auroral substorm marks the beginning of the expansion phase as described by Akasofu (1964, 1968).





Figure 1.2 summarizes this development. At  $T=0$  (A in figure 1.2), there are only quiet arcs. Onset of the expansion phase is indicated by the brightening of one of the arcs or the formation of a new one ( $T=0-5$  min., B in figure 1.2). The expansion phase then continues to develop with the rapid poleward motion of the intensified arc, forming the "auroral bulge" ( $T=5-10$  min., C in figure 1.2). The bulge develops, expanding northward ( $T=10-30$  min., D in figure 1.2). On the westward edge, the expansion is marked by the propagation of a folded structure known as the westward travelling surge. Within the bulge patches form which drift eastward. The poleward border of the diffuse aurora often shows eastward drifting omega bands and westward drifting torches.

When expansion halts, the recovery phase begins and the bulge starts to contract ( $T=30$  min.-1 hr., E in figure 1.2). Auroral patches, loops and surges eventually degenerate and by the end of the recovery phase ( $T=1-2$  hr., F in figure 1.2) the situation is similar to  $T=0$ . Following the recovery phase the auroral oval will have contracted. If it is still expanded with respect to the quiet oval, further substorm cycles may occur. These may develop before the initial substorm has recovered.

### 1.2.2 The Polar Magnetic Substorm

As mentioned the ionosphere and the magnetosphere interact through large-scale current systems. During substorms we are concerned primarily with the nightside



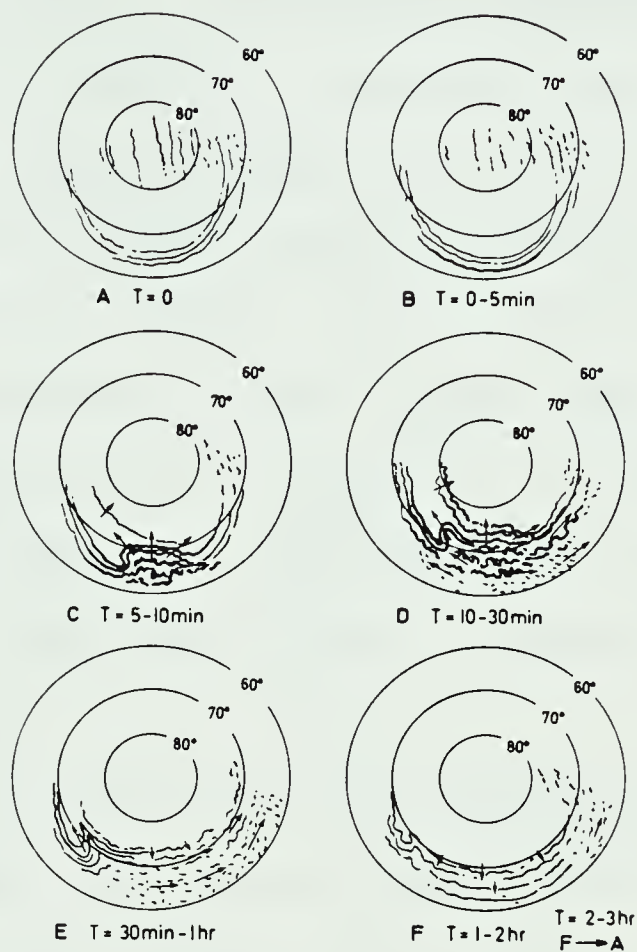


Figure 1.2  
 The development of the auroral substorm shown in sequential plots (after Akasofu, 1964).



current systems in auroral regions. On the evening side there exists an eastward ionospheric current known as the eastward electrojet. On the morning side there is a westward ionospheric current known as the westward electrojet. These electrojets overlap near midnight, separated by a region known as the Harang Discontinuity (see figure 1.3). They consist of a combination of Hall current (perpendicular to the ionospheric electric field) and a Pederson current (parallel to the ionospheric electric field). The relative magnitudes of these orthogonal currents at any point depend on the ratio of the Hall to Pederson height-integrated conductivities and the direction of the ionospheric electric field.

The ionospheric electrojets are connected to the particle source regions by field-aligned (or Birkeland) currents. On a large scale, the morning sector is characterized by downward field-aligned current in the poleward portion of the electrojet and upward current in the equatorward part. The evening sector, on the other hand, has upward current in the poleward portion and downward current in the equatorward part. In the midnight sector these systems intertwine as in figure 1.3. It seems likely that the poleward border currents map to regions deep in the plasma sheet while equatorward border currents map nearer to the Earth in more dipolar regions of the plasma sheet.

It is the development of the westward electrojet in the midnight and evening sectors whose magnetic perturbation





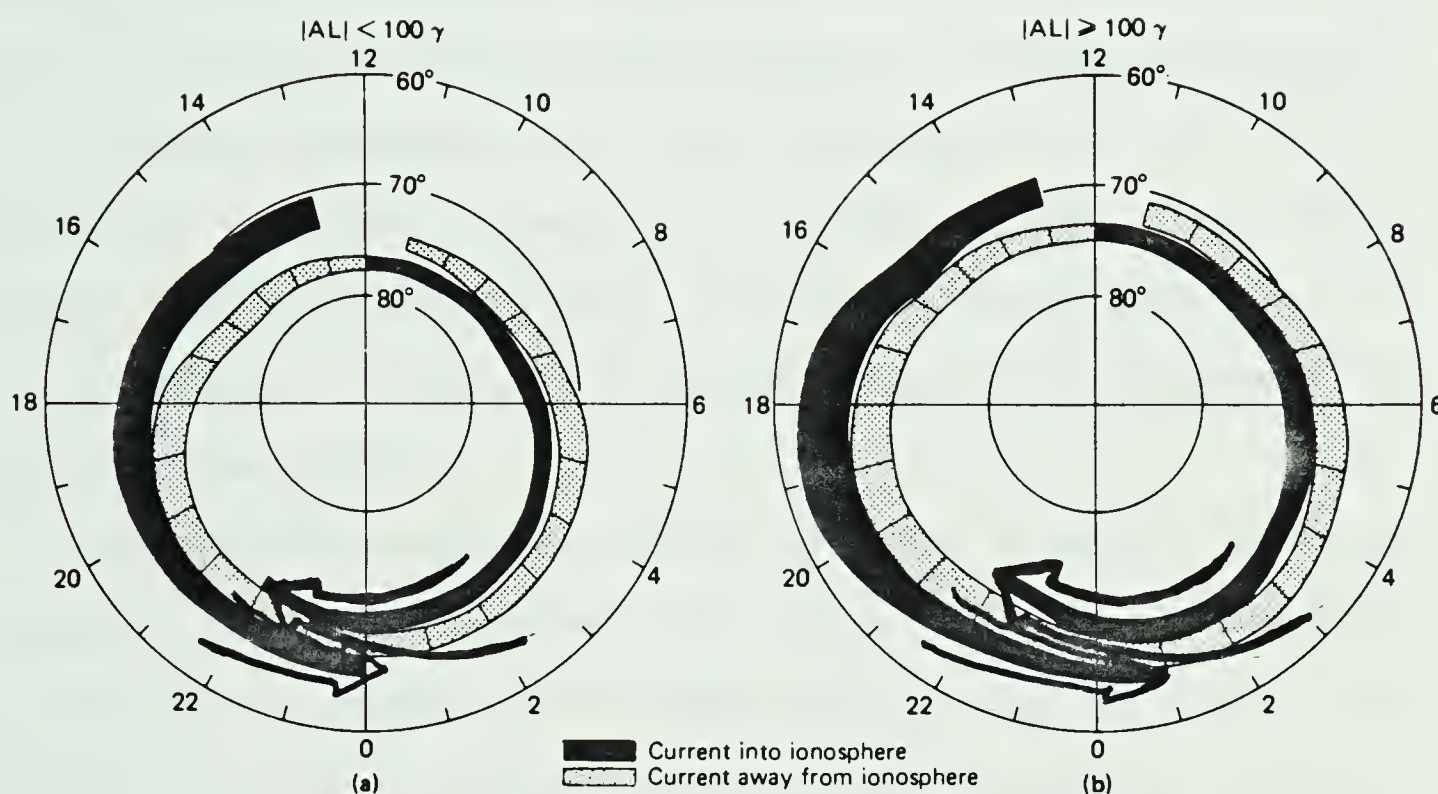


**Figure 1.3**  
 Location of eastward and westward electrojets. Region of overlap is known as the Harang Discontinuity. Location of field-aligned currents is also shown (after Iijima and Potemera, 1978).





constitutes the polar magnetic substorm. Since substorm related current systems generate large-scale magnetic deflections (several hundred nanoTeslas where  $1 \text{ nT} = 1 \text{ gamma} = 10^{-5} \text{ Gauss}$ ), it is generally through the interpretation of ground magnetic records that the description develops. The magnetic field is usually recorded in the orthogonal  $H'$ ,  $D'$ , and  $Z$  components of the local magnetic co-ordinate system. It is usually described in the orthogonal  $H$ ,  $D$ , and  $Z$  components of the geomagnetic dipole system. In these systems, the  $H'$  ( $H$ ) component is positive northward, the  $D'$  ( $D$ ) component is positive eastward and the  $Z$  component is positive downwards.

The observed magnetic effect depends strongly on the location of the observer. In order to get a complete picture, it is important to use data from a number of suitably placed stations. Using data primarily from a meridian line of stations Rostoker (1972) has summarized the morphology of an isolated polar magnetic substorm.

Prior to the expansion phase onset ( $T=0$  in the Akasofu model), there is often a slow growth of negative  $H$ , corresponding to a growth of the westward electrojet. This phase is not observed for all substorms and its role is not yet clear. It may indicate growth of steady convection prior to substorm onset or it may merely be the distant signature of a substorm to the east of the observer. The onset and first few minutes of the expansion phase is characterized by a very sudden growth of the southern border of the westward



electrojet and then rapid poleward motion of the entire system. The magnetic effects observed during the expansion phase depend to a great extent on the position of the observer. In sectors far from the source region the perturbations develop slowly and are usually quite smooth in their behaviour. In sectors near the source the perturbations develop suddenly and are normally quite sharp. In these sectors the major characteristic of the expansion phase is a large negative H perturbation. As the expansion phase continues, there are often "quasi-periodic" (every 5-15 minutes) intensifications of the magnetic field. Rostoker (1972) describes these as intensifications of the northern border. More recently, Wiens and Rostoker (1975) have described them in terms of a series of discrete jumps of the westward electrojet northward and westward into the evening sector (see figure 1.4). However, Pytte et al (1976) have suggested that the westward electrojet moves poleward in a smooth fashion. They describe its development in terms of a series of intensifications and the formation of multiple westward travelling surges.

Following the expansion phase the system decays and recovers ( the recovery phase ) over approximately one hour.

### 1.2.3 The Substorm Model

Many models of the magnetospheric substorm have been described (Akasofu (1977), Atkinson (1967), McPherron et al (1973), Rostoker (1974), Schindler (1974), Vasyliunas





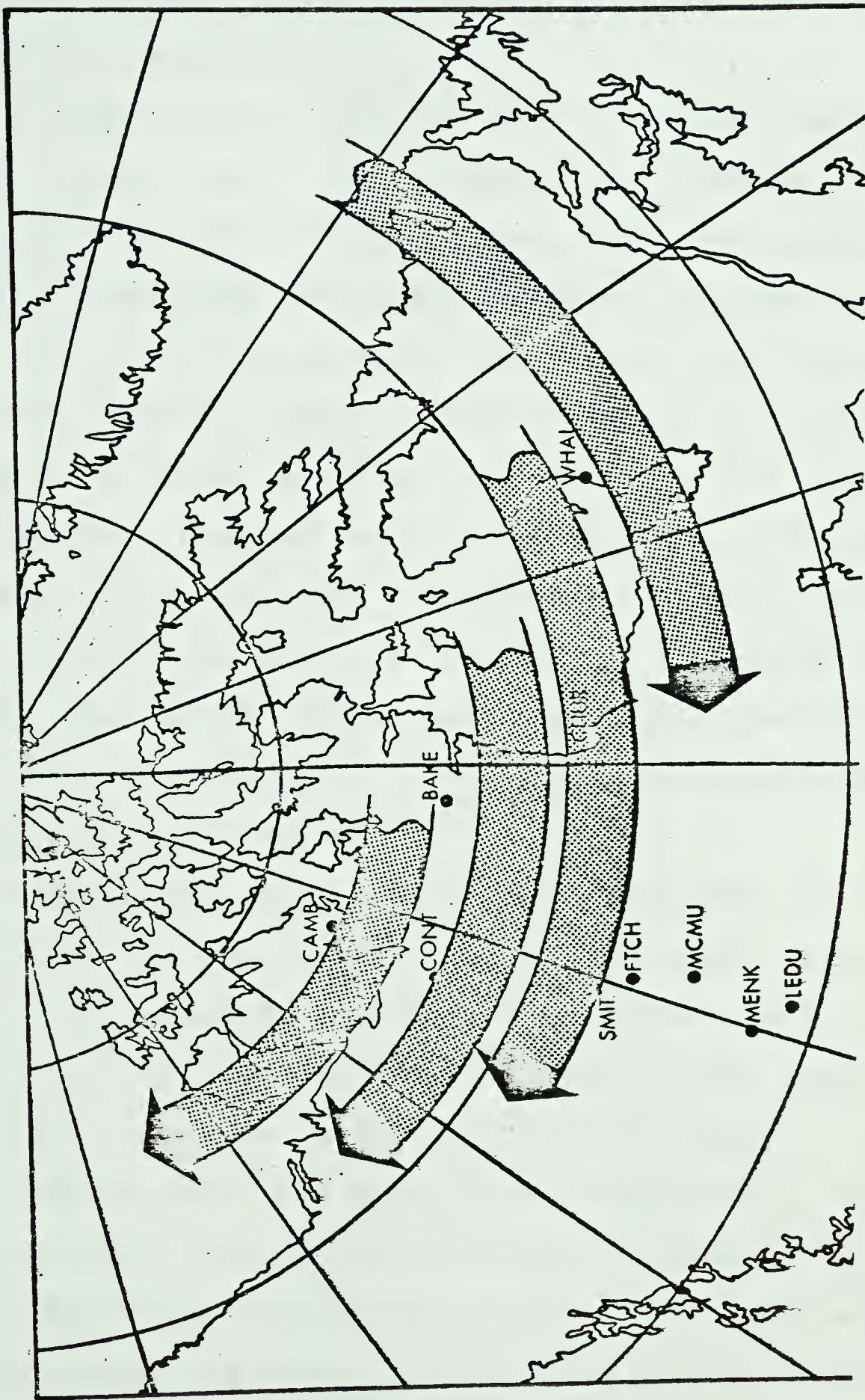


Figure 1.4  
 Wiens-Rostoker model for the expansion of the  
 westward electrojet showing stepping motion  
 (after Wiens and Rostoker, 1975).





(1970) ). While the models explain the major features of a substorm, they differ primarily in the description of magnetotail processes.

A rather widely accepted model is the reconnection model, shown in one form in figure 1.5. With the southward turning of the IMF, dayside reconnection is enhanced and dayside field lines are eroded and drawn back into the tail. The tail flux increases and the plasma sheet thins due to increased magnetic pressure. This continues to a point where there is a rapid increase in the rate of tail field reconnection (the tearing mode instability). A neutral line develops in the region of reconnection and the local plasma is energized through the associated cross-tail electric field. The plasma flows away from the neutral line eventually interacting with the ionosphere resulting in the substorm effects observed.

Recently Lui et al (1976) have argued that there is no indication of the formation of a near-Earth neutral line during the substorm. Furthermore, since there is no indication of energization of local plasma, they suggest that the reconnection model is not satisfactory.

Akasofu (1977) has described an alternative model in some detail. Basically, the onset is characterized by the sudden earthward displacement of plasma in the near-Earth plasma sheet. The result is a thinning of the plasma sheet. Within 15  $R_E$  the plasma flows earthward, beyond this it flows anti-earthward. An undefined plasma instability also



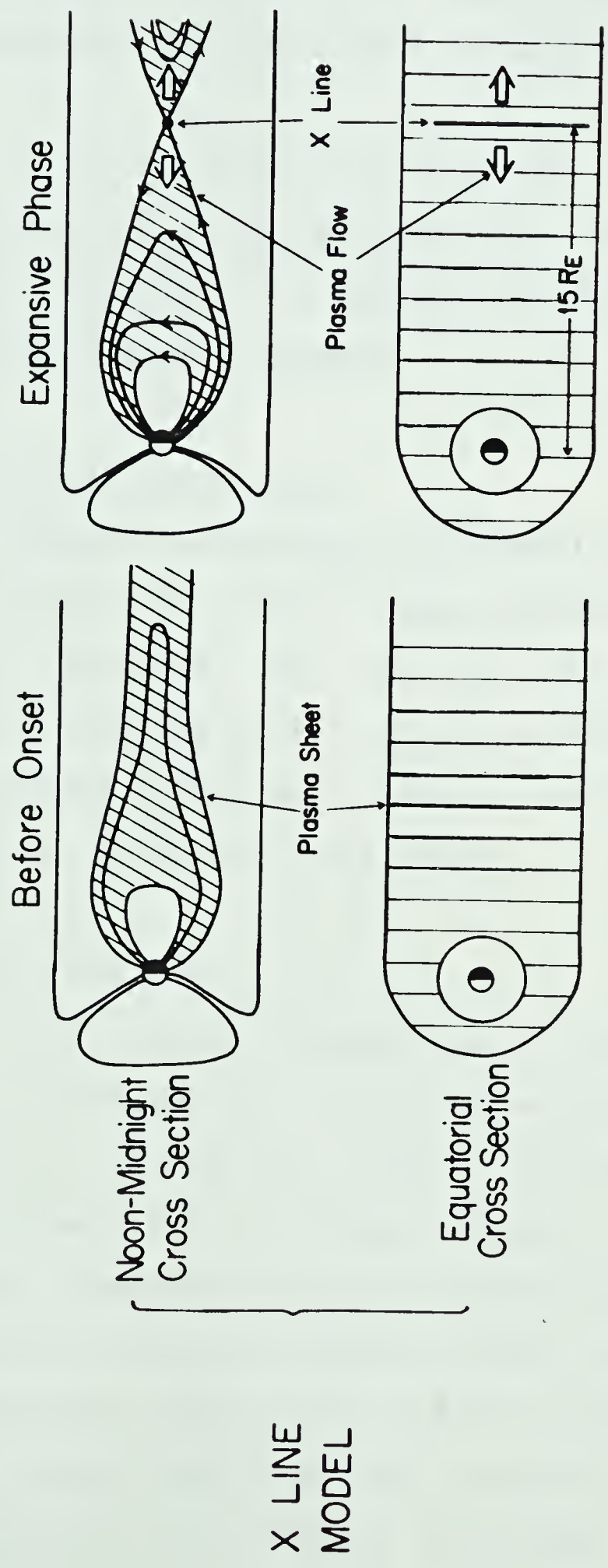


**Figure 1.5**  
Model for magnetospheric substorms involving reconnection of magnetic field lines in the magnetotail (after Akasofu, 1978).



occurs causing a diversion of the cross-tail current into the ionosphere (see figure 1.6). This disruption of the cross-tail current has been described earlier by Atkinson (1967).

Finally, a third model described by Heikkila and Pellinen (1977), stresses the importance of the induction field in the magnetotail to explain the energization and flow of the plasma during a substorm.

### 1.3 The Westward Travelling Surge

In a comprehensive examination of auroral forms using Defense Meteorological Satellite Program (DMSP) photographs, Akasofu (1974) described the surge as one of the most prominent auroral features during substorms. Akasofu (1964, 1968) and Fukunishi (1973) have examined the nature of the surge and its role in substorm development.

#### 1.3.1 The Auroral Behaviour

The surge is a large and intense auroral form. With an average width of about 800 km, it will often fill the entire field of view of an all-sky camera. It has an average velocity of  $1 \text{ km sec}^{-1}$  and an average lifetime of some 30 minutes. Surges, however, are quite variable and are often classified as weak, medium, or intense surges. Larger surges represent the westward edge of the expanding auroral bulge. Akasofu (1974) noted that it was not uncommon to observe a single or a series of wavy, folded structures travelling





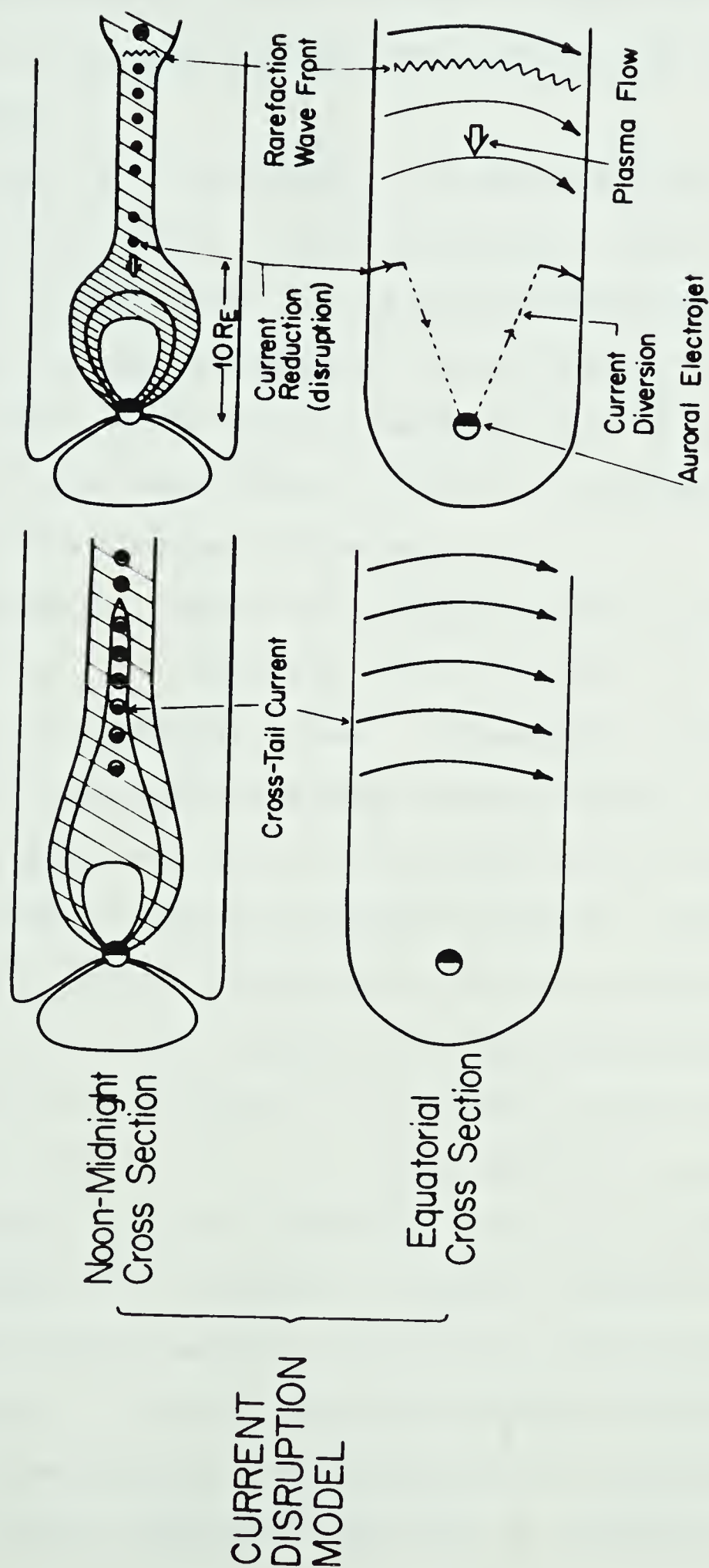


Figure 1.6  
Model for magnetospheric substorms involving disruption of cross-tail current in the magnetotail (after Akasofu, 1978).



westward along discrete arcs. These often occur prior to the passage of the surge. Though smaller in dimension, they are similar to the westward travelling surge and are classified as weak surges.

Just west of the surge a discrete arc will usually brighten. Akasofu (1964, 1968) considered this to be a preparatory state. That is, it is not a part of the surge but a region being influenced by it. The western and northern edges of the surge itself are made up of discrete arcs. Behind this surge front, within the expanding bulge, the aurora is diffuse and disturbed.

As mentioned, Wiens and Rostoker (1975) described the development of the substorm as a series of step-like expansions. Presumably, each expansion involves the generation of westward travelling surge. Although Pytte et al (1976) prefer to describe this behaviour as surge motion associated with an electrojet intensification, Akasofu (1977) has suggested that the existence of multiple surges, growing one on top of another, supports the Wiens-Rostoker approach. In any case, the development of the surge itself does not seem to be smooth. It is often observed to appear very suddenly rather than grow smoothly. While its basic shape remains stable, it generally becomes distorted, showing complicated internal motions and perhaps developing surges within surges or surges on top of surges. Initially, the surge may travel smoothly and rapidly but it generally slows or stops (often suddenly) followed by continued motion



and/or decay of the form. Lassen et al (1977) observed that during a particular substorm the westward travelling surge stopped for one or two minutes and then continued with its original velocity.

The particle precipitation associated with westward travelling surges has recently been studied by Meng et al, 1978. They observed that the bright arcs west of the surge are associated with an electron precipitation energy flux of  $\sim 5$  ergs/cm<sup>2</sup>sec.ster. and a peak energy of  $\sim 8$  Kev. Just inside the surge the energy flux was estimated to be  $\sim 10$  ergs/cm<sup>2</sup>sec.ster. . A dramatic feature in this region was a particularly hard, flat spectrum with a peak energy greater than 20 Kev as shown in figure 1.7.

Finally, since the surge is characterized by electron precipitation and since the curvature of the Earth's magnetic field will cause electrons to drift eastward, the westward motion, itself, is rather surprising. The motion is thought to be representative of a westward motion of the source region of the surge particles rather than of the particles themselves. The reason for this westward motion is not yet known.

### 1.3.2 The Magnetic Behaviour and the Surge Model

Although the surge is a large scale structure, its observed magnetic effect, like that of the substorm itself, will depend on the observer's position relative to it. It is important, then, to analyze the surge behaviour using a





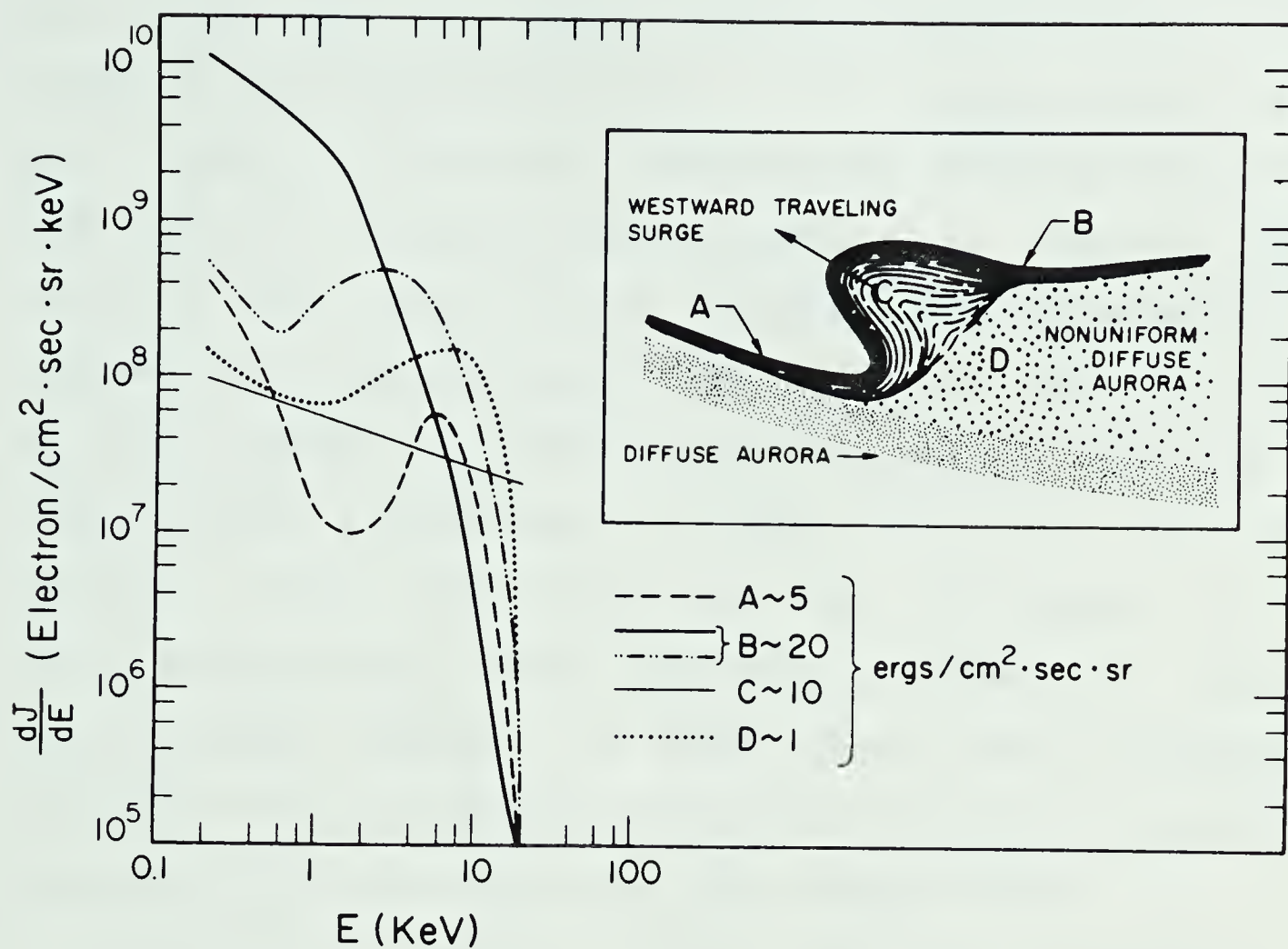


Figure 1.7  
Summary of electron precipitation within the westward travelling surge (after Meng et al, 1978).



properly arrayed grid of stations. With data from a meridional line of stations, Kisabeth and Rostoker (1973) have shown that an auroral surge is characterized by the following magnetic perturbation in the region under the form. There is a positive D perturbation centered under the form. South of the surge, the H component is positive and north of the surge it is negative. The Z component is observed to be positive north and south of the form but negative beneath it. Following the passage of the surge a large negative D deflection is often observed. Chen and Rostoker (1974) identified this with the passage of the Harang Discontinuity (which involves a region of upward field-aligned current). It would seem that the westward travelling surge represents the leading edge of the westward electrojet as it intrudes into the evening sector.

Kisabeth and Rostoker (1973) have also described a model current system for the surge. It is basically a three dimensional current loop with an equatorward ionospheric component, superimposed upon a north-south shear of the ionospheric current flow as shown in figure 1.8 .

Recently, Hughes (1978), in a comprehensive study of ionospheric-magnetospheric current systems, modelled the magnetic perturbations of a particular substorm. In this model, a portion of the westward electrojet was allowed to intensify and expand both poleward and westward. A region of the eastward electrojet was also seen to intensify but remained stationary. The surge, in this model, was treated



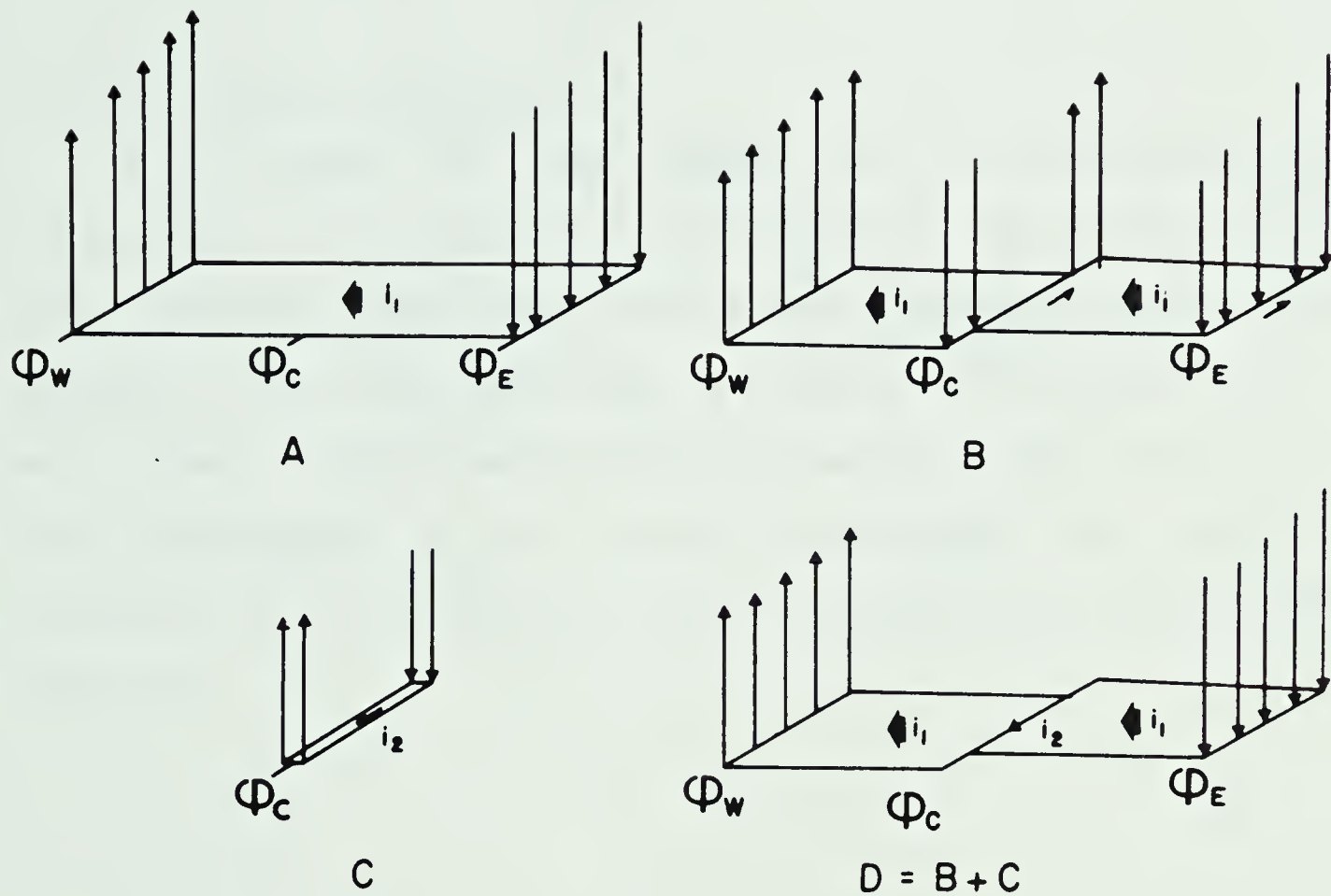


Figure 1.8  
Surge model showing north-south shear and superposed ionospheric current (after Kisabeth and Rostoker, 1973).





as a three dimensional current loop with an equatorward current flowing in the ionosphere. This system was superposed on the leading edge of the westward electrojet. The development of this current system is shown in figure 1.9.

#### 1.4 The Thesis Objectives

The purpose of this thesis is to investigate the development and evolution of the westward travelling surge and to model the associated current systems. Through the analysis of magnetic data from a meridian line and an east-west line of magnetometer stations and with the aid of all-sky photographs, we are able to identify the magnetic signature of the surge and follow its development within the substorm.



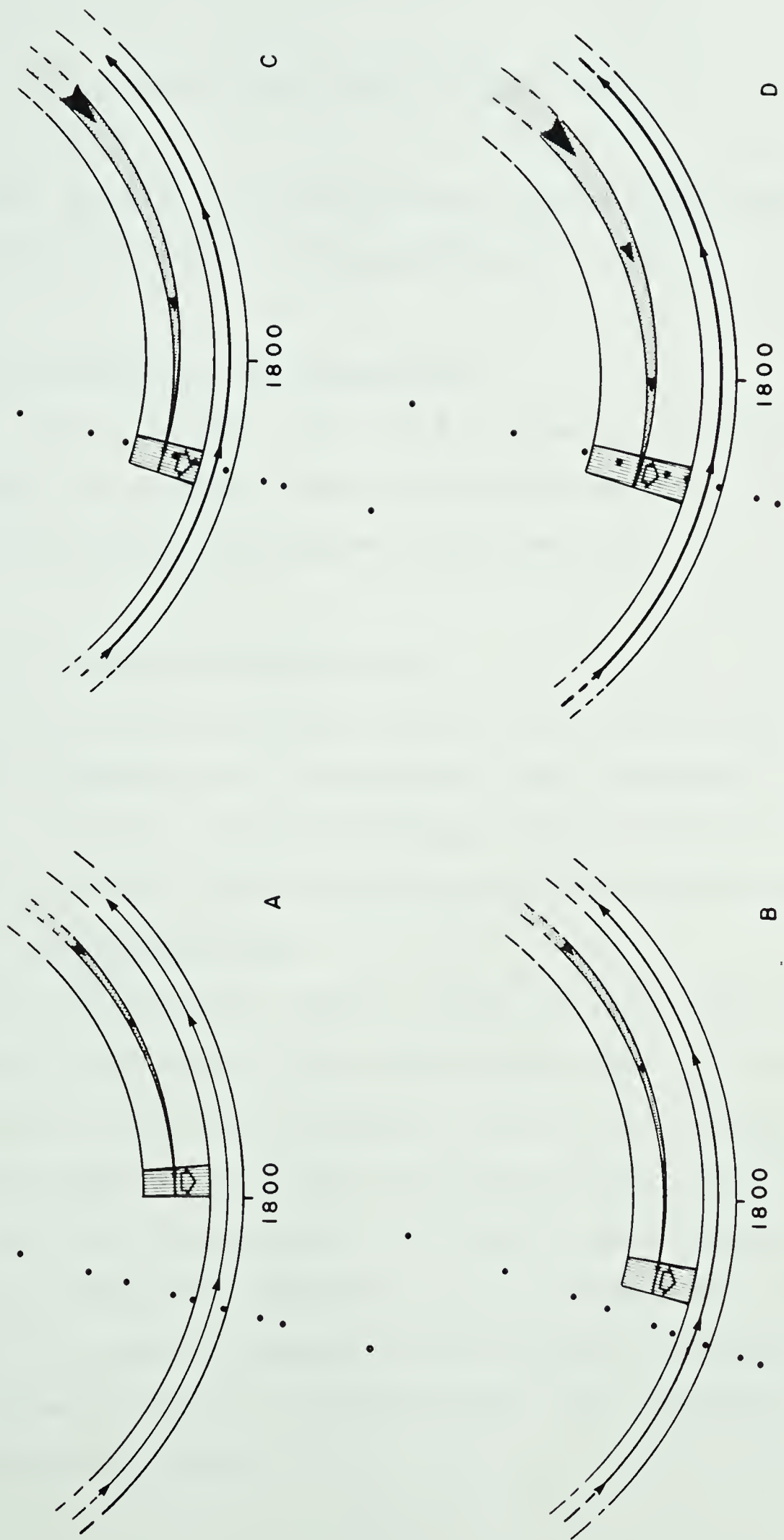


Figure 1.9  
Hughes model of westward electrojet development  
during a substorm including westward travelling  
surge (after Hughes, 1978).



## CHAPTER 2

### DATA COLLECTING AND HANDLING

This chapter is concerned with the methods involved in collecting, processing and presenting the data.

#### 2.1 Data Collection and Processing

In this section, we will briefly describe the monitoring equipment, the network of observation stations, and the processing techniques which are used.

##### 2.1.1 The Flux-Gate Magnetometer

The most important instrument used in this study is the fluxgate magnetometer. It measures each component of the Earth's magnetic field separately through three orthogonal sensing elements. These elements are located in the sensing head of the magnetometer.

The magnetometer system used in this study has been described by Kisabeth (1972). The system uses an analogue-to-digital converter yielding digital data which lends itself to computer handling and interpretation. The sensing head of the magnetometer is aligned with magnetic north (i.e. the east-west component,  $D$ , is nulled). The head is buried to reduce temperature variations. The magnetometer has a dynamic range of  $\pm 1000$  nT from the baseline and a resolution of  $\pm 1$  nT.





Of course, the purpose of the instrument is to monitor changes in the Earth's magnetic field. While the magnetometer can be calibrated to measure absolute values of the magnetic field, a measure of the variations from a fixed baseline for the three components of the magnetic field is usually all that is required. In any case, what is important is that the perturbations can be interpreted in terms of ionospheric current systems (Kisabeth and Kostoker, 1977).

### 2.1.2 The Riometer

The riometer (Relative Ionospheric Opacity Meter) is used to measure absorption of cosmic radio noise by the ionosphere. The riometer system used in this study is designed to detect cosmic noise at 30 MHz. The antenna system consists of two half-wave dipoles with an effective half power beamwidth of  $60^\circ$ . This gives a field of view with a scale size, at auroral heights, of about 100 km. The system is linear within the output voltage range of 0 to 5 volts. Calibration spikes are generated internally and are recorded every hour.

It is important to note that the intensity of cosmic noise is non-isotropic in space and time. As a result, the amount of noise is given, in decibels, with respect to a reference curve (a quiet day curve). The quiet day curve represents an average signal for the time period and station location under consideration. The riometer data presented in this thesis have had both the quiet day curve and the



calibration spikes removed.

The amount of absorption depends on the electron energy flux and collision frequency. Thus the characteristics of the absorption event are related to the character of the electron precipitation and, possibly, an associated auroral intensification, if any occurs. For example, the westward travelling surge involves a short-lived deflection with a sharp onset (Akasofu, 1968).

### 2.1.3 The All-Sky Camera

The all-sky camera is used to obtain a photograph having a full  $180^\circ$  angle of coverage. It consists of a spherical main mirror which reflects the image to a flat secondary mirror above it. This, in turn, reflects it back through the main mirror where it is focussed onto the film (figure 2.1). A centered cross-hair and the relevant time are recorded automatically onto the film. Over the period of observation during 1974 (see section 2.1.4), an all-sky camera (on loan from the University of Alaska) was operated at Fort Smith. Pictures were taken automatically every 30 seconds with alternating long and short exposure times.

The all-sky camera yields an important view of local auroral forms. Of course, it is sensitive to atmospheric conditions and, in particular, cloud-cover. Under clear sky conditions, it will give a horizontal field of view of 1000 km. The image, however, is highly compressed, particularly at the edges of the frame. This can be corrected for and



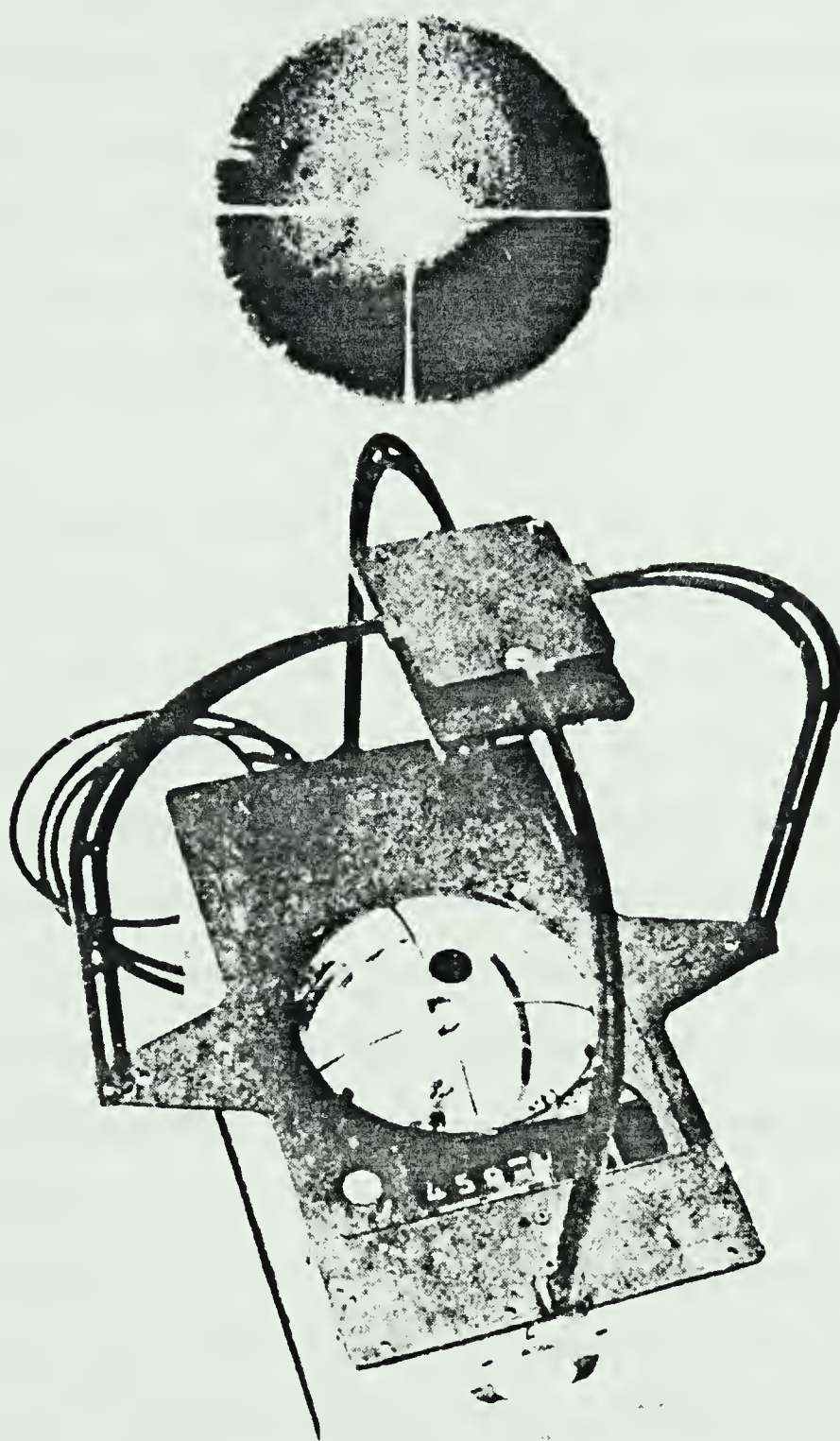


Figure 2.1  
Typical All-Sky camera and photograph (inset)  
(after Rostoker, 1975).







all-sky data presented in this thesis have been linearly mapped to permit proper interpretation. However, the technique requires some simplification and interpretation of the auroral forms. This process is often complicated by the location of the form as well as the picture quality. The use of all-sky photographs is mainly qualitative rather than quantitative (Rostoker, 1975).

#### 2.1.4 The Station Network

Data presented in this thesis were collected during two periods. From July to October in 1974, a system of magnetometer stations was operated by the University of Alberta. In particular, three stations (at Uranium City, Fort Smith, and Hay River) formed an east-west line. These are shown in figure 2.2 and the station co-ordinates are given in table 2.1. Each station included a three-component fluxgate magnetometer; as well an all-sky camera was located at Fort Smith.

In August of 1976, a network of seven stations was installed by the University of Alberta for use in the International Magnetospheric Study (IMS). This network, still in operation, consists of a meridian line and an east-west line of stations. The meridian line (Fort Smith, Fort Chipewyan, Fort McMurray, and Leduc) lies along  $300^{\circ}$  east longitude. The east-west line (Uranium City, Fort Smith, Hay River, and Fort Providence) lies along  $67^{\circ}$  north latitude. Fort Smith is common to both lines. The network is



Table 2.1  
Locations of Stations used in this Study

STATION NAME	CODE	GEOGRAPHIC		GEOMAGNETIC	
		NAME		CO-ORDINATES	
		LAT.	LONG.	LAT.	LONG.
		(°N)	(°E)	(°N)	(°E)
URANIUM CITY	URAN	59.6	251.5	67.4	304.3
FORT SMITH	SMIT	60.0	248.0	67.3	299.7
HAY RIVER	HAYR	60.8	244.2	67.3	294.1
FORT PROVIDENCE	PROV	61.3	242.4	67.5	292.0
FORT CHIPEWYAN	CHIP	58.8	248.9	66.3	302.1
FORT MCMURRAY	MCMU	56.6	248.8	64.2	303.2
LEDUC	LEDU	53.3	246.5	60.6	302.9
CAMBRIDGE BAY	CAMB	69.1	255.0	76.7	294.0
YELLOWKNIFE	YKNF	62.5	245.5	69.1	292.6
MEANOOK	MEAN	54.6	246.7	61.8	301.0
FORT CHURCHILL	CHUR	58.8	265.8	68.8	322.5
WHITESHELL		49.8	264.8	59.9	325.3
GREAT WHALE RIVER		55.3	282.2	66.8	347.2
VICTORIA		48.5	236.8	54.3	292.7
COLLEGE		64.9	212.2	64.6	256.5
SITKA		57.1	224.7	60.0	275.4
NEWPORT		48.3	242.9	55.1	300.0
BOULDER		40.1	254.8	49.0	316.5
HONOLULU		21.3	202.0	21.1	266.5





Figure 2.2  
Map indicating locations of most stations used  
in this study





shown in figure 2.2 and the station co-ordinates are given in table 2.1. Each station consists of a three component fluxgate magnetometer, a riometer and a digital recording system.

During both these observation periods, records were available from other magnetic observatories in Canada and the United States. The Canadian stations were operated by the Division of Geomagnetism of the Department of Energy, Mines and Resources. They supplied analogue records on microfilm, or, more recently, reconstituted analogue records produced from a digital sampling rate of 1 point/minute. The American observatories were operated by the United States Geological Service (USGS). Microfilmed analogue records were made available by the National Geophysical and Solar-Terrestrial Data Center. The co-ordinates of the stations are given in table 2.1 and most stations are shown in figure 2.2 .

The data from instruments operated by the University of Alberta were multiplexed and then put in digital form on a seven track tape at the site. In the 1974 period the three magnetic components (H,D,Z) were sampled every 1.92 seconds. During the IMS period the four signals (H,D,Z, and riometer) were sampled every 2.56 seconds. Approximately every 7.5 hours the data collection was interrupted for about 2 minutes while a WWVB time signal was received and recorded. When the station tapes were filled, they were sent to the university for further processing.



### 2.1.5 Data Processing

When the field tapes are received, they are read and the data transferred to a nine track tape. During this process, the WWVB timing blocks are read and the data blocks are labelled appropriately with the station name and the starting time. If the timing signal cannot be decoded by the computer, it is decoded by hand.

Once the data from each station are available for a specific time period (usually about 2 weeks), an event tape is produced. This simplifies data handling by gathering all the data for a particular event onto a single tape.

## 2.2 Data Presentation

Analysis of an event usually involves 1) reading the data from an event tape, 2) rotating it into geomagnetic dipole co-ordinate system and 3) further digitizing and filtering, if desired. The data can then be presented in the stacked magnetogram and/or the profile format.

### 2.2.1 The Stacked Magnetogram Format

In this format, the H, D, and Z components of the magnetic field data and, if available, the riometer data are plotted individually, station by station, as a function of time. From the top of the plot, the stations are arranged in order from east to west or from north to south. Hand digitized magnetograms can be included. The magnetic records are generally presented with the first point as the zero or



d.c. level. The riometer data, as mentioned, are given in decibels with respect to a quiet day level.

The purpose of this format is primarily to allow a qualitative interpretation of the longitudinal and latitudinal variations during the event. Using the techniques of Kisabeth(1972) the location of the electrojets and other current systems (Kisabeth and Rostoker, 1973) can usually be established. By studying the stacked magnetograms as a function of time, some indication of the behaviour of these systems can be obtained.

### 2.2.2 The Profile Format

An often superior format for the examination of the spatial and temporal variations of the magnetic field is the profile format. Here the magnetic data, at a particular point in time, are sampled from each station and then plotted as a function of station location. If the stations lie along a meridian line then we obtain a plot of the magnetic field as a function of latitude. This latitude profile, as it is termed, yields an instantaneous cross-section of the magnetic perturbation, showing clearly any latitudinal variations. Moreover, by taking profiles at different times, the changes in the profile will reflect the changes in the associated current system. The latitude profile has been used extensively in the analysis of current systems (Kisabeth, 1972 ; Kisabeth and Postoker, 1973, 1977 ; Hughes, 1978 ).





Since this study involves an investigation of the westward travelling surge, it was felt that a plot of the magnetic field as a function of longitude ( a longitude profile ) would give interesting information. Furthermore, with the availability of data from closely-spaced stations of nearly constant latitude, the longitude profile became a natural format with which to examine the longitudinal structure of the current associated with the surge.

The profile format is used to show the state of the magnetic field relative to some reference state. The reference state acts as a baseline for the profile. An important aspect of the profile format is the choice of the baseline. The baseline could be an absolute measure of the steady state or quiet-time magnetic field applicable to the time of the profile. More typically, the baseline is taken as the field value just prior to the onset of the event of interest. Profiles with this type of baseline have been termed differential profiles (Kisabeth, 1972).

The baseline for a differential profile is normally maintained for only a short period (a few minutes). After this time other current systems flowing in the magnetosphere and the ionosphere will have often changed significantly. The baseline must then be shifted in order to examine further developments of the current system of interest. It should be noted that propagation effects (for example, the westward travelling surge) complicate the choice of baseline for differential longitude profiles. For this reason, events



were selected which were preceded by quiet periods from which a baseline was taken. This baseline was maintained until the initial disturbance had passed and the profiles were relatively constant. The baseline could then be shifted and further events could be analyzed.

A difficulty exists in that many profiles used in this study consist of only four points and interpolation of the field between these points is rather restricted. Generally, the data points are joined smoothly as one would expect on physical grounds. The profile maxima and minima are normally restricted to data points. If, however, the neighbouring profiles indicate it, then peaks may be placed between the data points.

Finally, we note that the time values used to describe the events refer to Universal Time (UT). As mentioned in chapter 1 the symbols  $H'$ ,  $D'$  and  $Z$  refer to the unrotated data (as measured in the local magnetic co-ordinate system) while  $H$ ,  $D$ , and  $Z$  refer to the rotated data (in the geomagnetic dipole co-ordinate system). We also note that the symbols  $X$ ,  $Y$ , and  $Z$  used on all profiles refer to the  $H$ ,  $D$  and  $Z$  co-ordinates of the dipole system. The  $X$ ,  $Y$ , and  $Z$  symbols were chosen because they are centered by the plotter at the precise value of the perturbation.



## CHAPTER 3

### EVENT ANALYSIS

#### 3.1 Selection of the Events for Analysis

The substorm events presented in this thesis were selected as follows. Firstly, microfilmed magnetograms from key stations (particularly in or near the Alberta sector) were examined for possible surge activity during substorm events. Ninety-three events, primarily from the years 1976 and 1977, were chosen and the corresponding data from the Alberta array were then examined.

In terms of the magnetic behaviour, the events were chosen according to two main criteria. Firstly, the onset of the substorm should be characterized by a sharp, short-lived perturbation, representative of a westward travelling surge. Secondly, the activity prior to the onset in the Alberta sector should be reasonably quiet. This second criterion allows us to obtain a baseline from which the perturbations due to the surge can be analyzed. Furthermore, since we were primarily interested in the longitudinal variations associated with the westward travelling surge, events which were clearly detected by the east-west portion of the station network were chosen.

On the basis of these criteria, then, and also depending on the general quality of the data, 12 events were selected from the original 93 for analysis. Of these 12





events, three were considered reasonably representative and are presented in this chapter.

### 3.2 The Approach to the Analysis of the Events

In each event we shall first briefly examine the development of the electrojets during the substorm. This is done by examining the magnetic records in the Alberta and neighbouring sectors. Using the methods of Kisabeth (1972) and Kisabeth and Rostoker (1977), we can estimate a particular station's position with respect to the electrojets. Theoretical latitude profiles taken along various longitudes in the region of a  $20^\circ$  long and  $5^\circ$  wide westward current system are shown in figure 3.1. There are several features of these profiles which we can use to identify and position this current system. One of these is that the central latitude is characterized by a negative extremum in H and a transition point in the Z component. Another feature is that the equatorward border is marked by a negative extremum in the Z component. An H/Z ratio of  $+1$  is also indicative of a position near this border. An eastward current can be identified in a similar fashion. The important reason for using this method is to obtain consistent results at all stations. It is also important to recognize that variations in the nature of the electrojets require that the positions be regarded only as estimates. Indeed, as with most geophysical situations, it must be kept in mind that the solutions are non-unique.



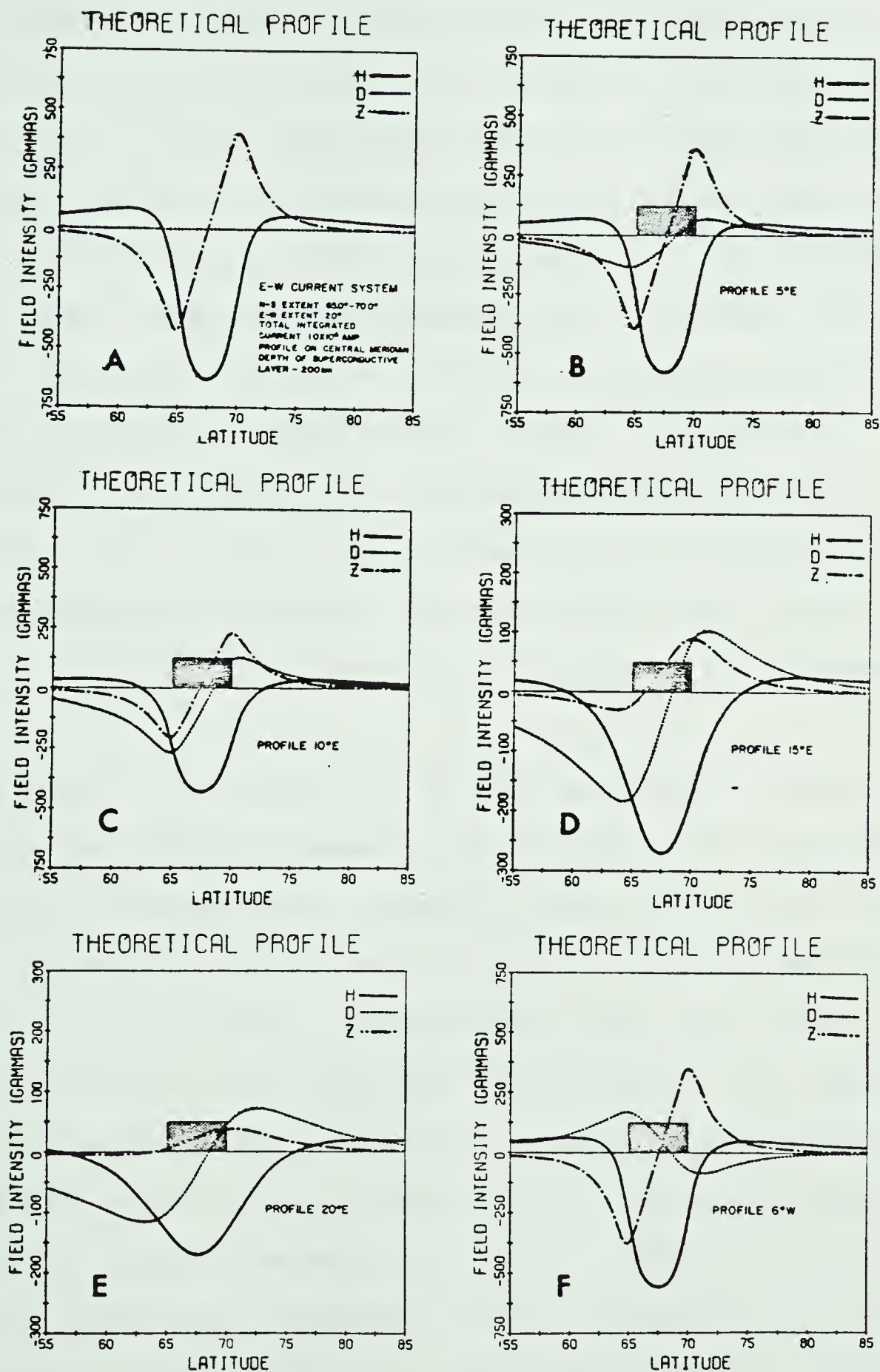


**Figure 3.1**  
Theoretical latitude profile at various positions beneath a westward electrojet (after Kisabeth, 1972).



The next step in the event analysis is to examine the surge development. This is done primarily through the use of longitude profiles and (with the exception of the the event on Day 214, 1974) latitude profiles. For the first event presented, the Day 214 event, all-sky photographs are also available. In this case, therefore, we can determine directly the relationships between the auroral and the magnetic features. Since the westward travelling surge is an auroral feature, establishing this relationship is particularly important. The other events (Day 307, 1976 and Day 223, 1977) are analyzed completely in terms of their magnetic behaviour. Through the analysis of these events we intend to define the magnetic signature of the auroral surge.

We hope, furthermore, to develop a realistic model of the causative current system and its subsequent development. As others have suggested (Hughes, 1978), much of the surge behaviour can be explained through a three dimensional current loop involving equatorward ionospheric current at its western edge. Such a current would produce an eastward magnetic perturbation (positive D perturbation) below the ionosphere. We have seen, however, that after the passage of the surge a sharp decrease in the D component may be observed (Chen and Rostoker, 1974). Although this may be explained in several ways, at least some events indicate that a region of poleward flowing current should be included behind the region of equatorward flowing current. Since the





surge represents the leading edge of an expanding westward electrojet, a westward current system is included in the model.

A simplified picture of the model current system is given in figure 3.2 . In this example the current density is 1 A/m everywhere, all ionospheric currents are at a height of 100 km and a superconductor is located at a depth of 200 km to simulate induction effects in the Earth. In order to see the magnetic behaviour of the model current configuration at different times during a substorm, a number of longitude and latitude profiles at various locations are shown in figure 3.3 . The locations of these profiles are indicated in figure 3.2 . There are many identifying features of these profiles. It is important to note that the magnitude of the observed perturbations will depend not only on the strength of the current but also very significantly on the relative location of the current systems.

All of the longitude profiles indicate that the leading part of the system is characterized by an extensive region of positive D while the trailing part displays an extensive negative D perturbation. The longitude profiles also show a positive Z regime in front of the leading edge of the system followed by an extensive negative Z region. This then recovers to a positive level except in regions south of the westward current (profile C). At locations where a negative extremum in Z is apparent there is a change in polarity of the D component. Finally, the H component of the longitude



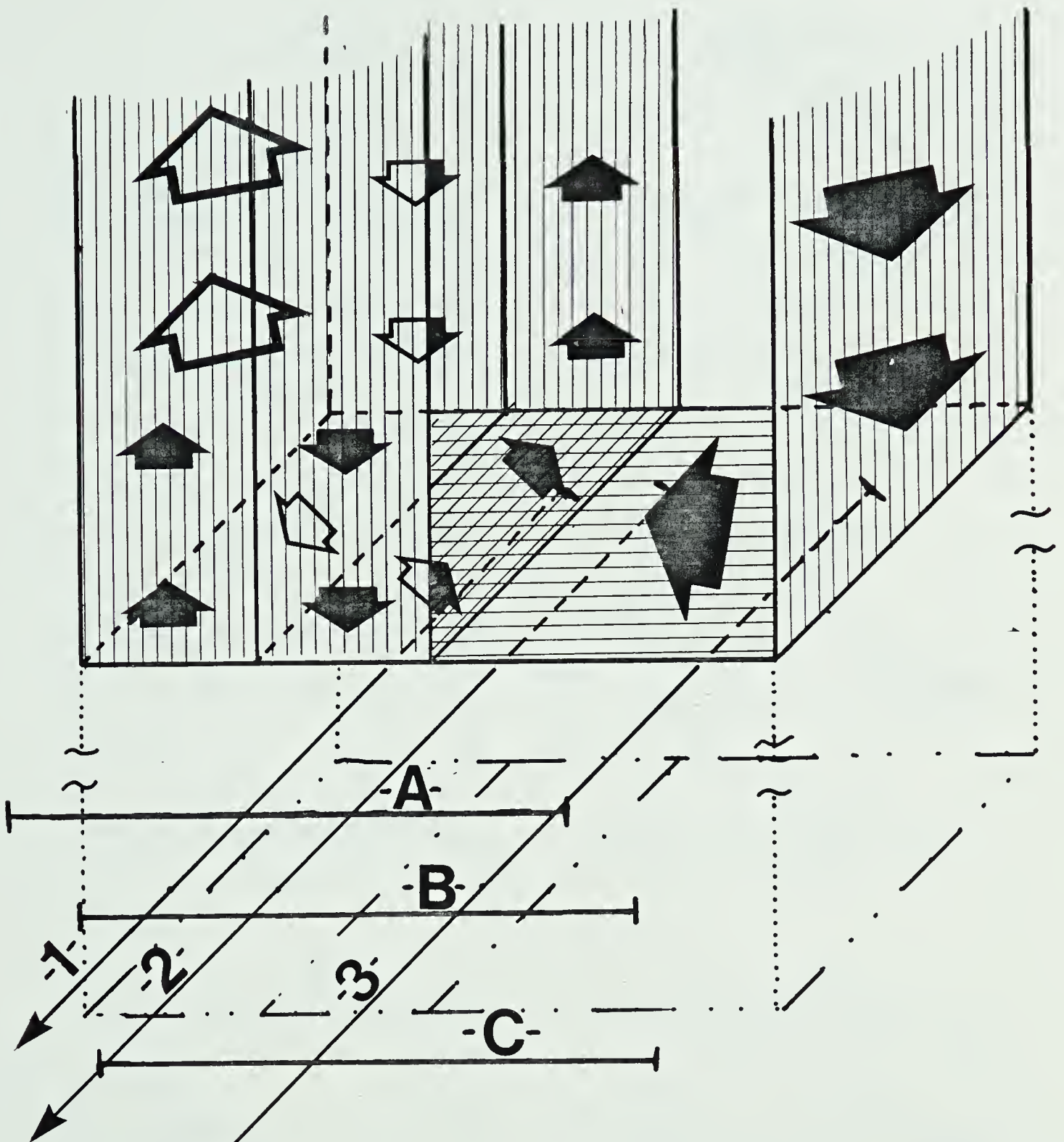
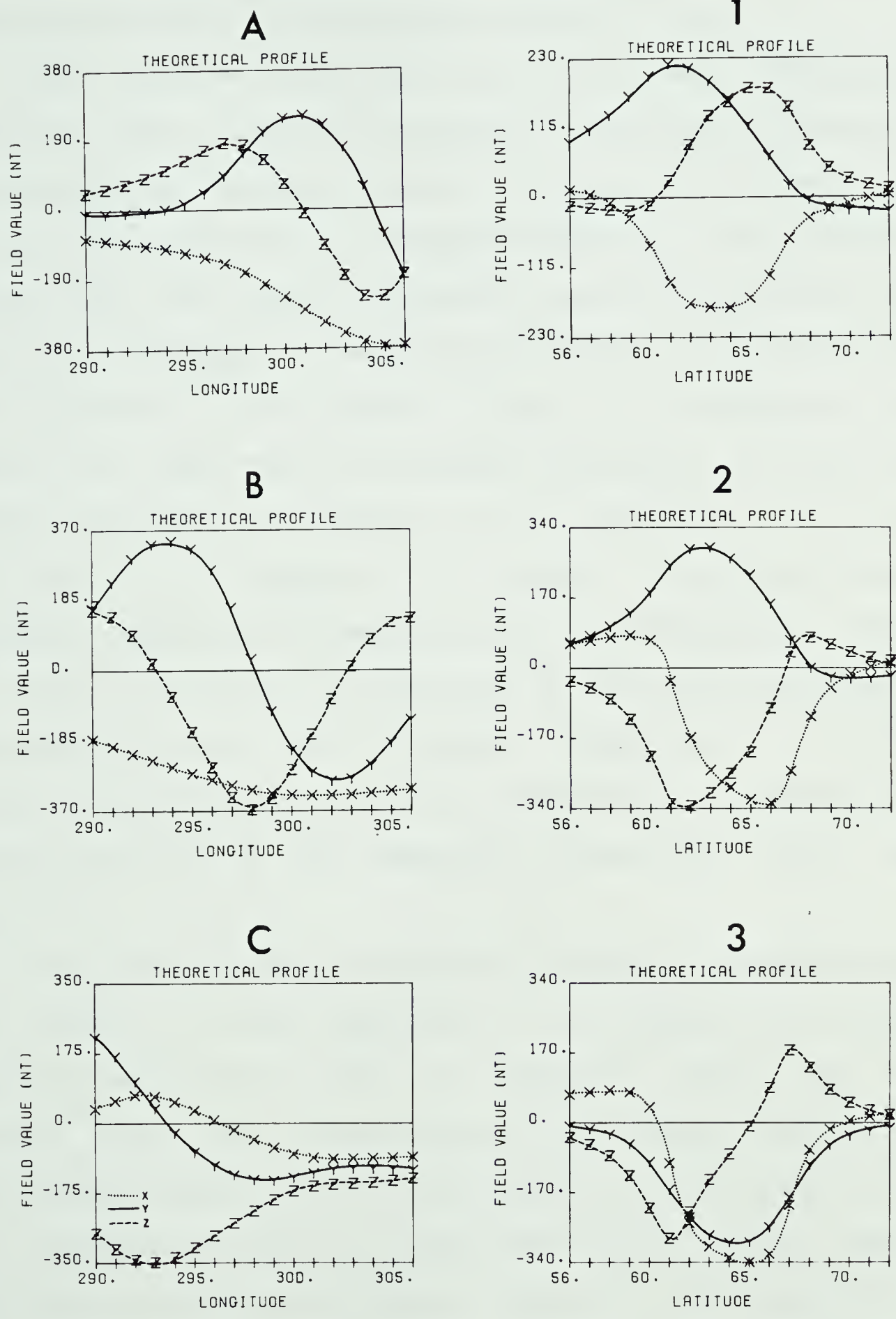


Figure 3.2

Diagram of surge model used in this study. The large arrows indicate a Birkeland current loop which is closed in the ionosphere with a westward current. The smaller arrows are used for loops with either equatorward or poleward ionospheric currents. White arrows are used in regions behind other current sheets. Dotted lines indicate a projection to the earth's surface where A, B, and C and 1, 2, and 3, indicate positions of longitude and latitude profiles shown in figure 3.3 .





**Figure 3.3**  
Longitude and latitude profiles at locations indicated in figure 3.2 . of surge model used in this study.





profiles is characterized primarily by the negative perturbation due to the westward current.

The latitude profiles also yield some identifying features. They show the positive and negative D regimes in the leading and trailing regions, respectively. Directly in front of the surge the Z component displays a large positive regime. This very quickly becomes a negative regime when the surge is overhead ( profile 2 of figure 3.3). Behind the surge (profile 3 ) the profile shows a Z component more typical of that due to a westward electrojet. As the surge passes overhead a transition from positive H at lower latitudes to negative H at higher latitudes becomes apparent. While this transition is not particularly strong in these profiles, it is enhanced by the intensification of eastward current at lower latitudes. Though such a current system is not shown here, it is included in the model if an intensification of the eastward electrojet has been indicated.

Other observations complicate the model. In particular, the surge is often observed to be preceded by a small negative deflection in the D component. There are many sources which may contribute to this effect. Firstly, the north-south system itself could produce it. We have seen in the profiles of figure 3.3 that west of the leading edge of the north-south current system, prior to the positive D regime, there is a weak negative D regime. Secondly, we have also seen in the earlier latitude profiles of figure 3.1



that if the stations are in the south-west portion of a westward current, then this effect will be felt. Thirdly, if a portion of the westward electrojet is tilted to the north-west a negative D will be observed in the vicinity of that electrojet.

Aside from the current configuration used to represent the surge, this model differs from others by allowing the possibility of current systems being tilted with respect to the observer. More details of the model and its variations associated with the events which follow will be given in chapter 4.

### 3.3 Event Analysis ... Day 214, 1974

#### 3.3.1 Introduction

The stations in the Alberta sector detect the onset of substorm activity at 0630 on Day 214 (August 2), 1974. The H', D', and Z component behaviour is given, in stacked format, in figures 3.4, 3.5, and 3.6. Times of interest are indicated on these figures and will be referred to in the analysis.

An inspection of the Alberta sector magnetograms shows that the activity here prior to onset was weak. The Kp index (an index of the average global magnetic activity) has a three-hour average value of 1 prior to the substorm onset. This indicates that the global activity was also at a low level.



# H' COMPONENT: DAY 214, 1974

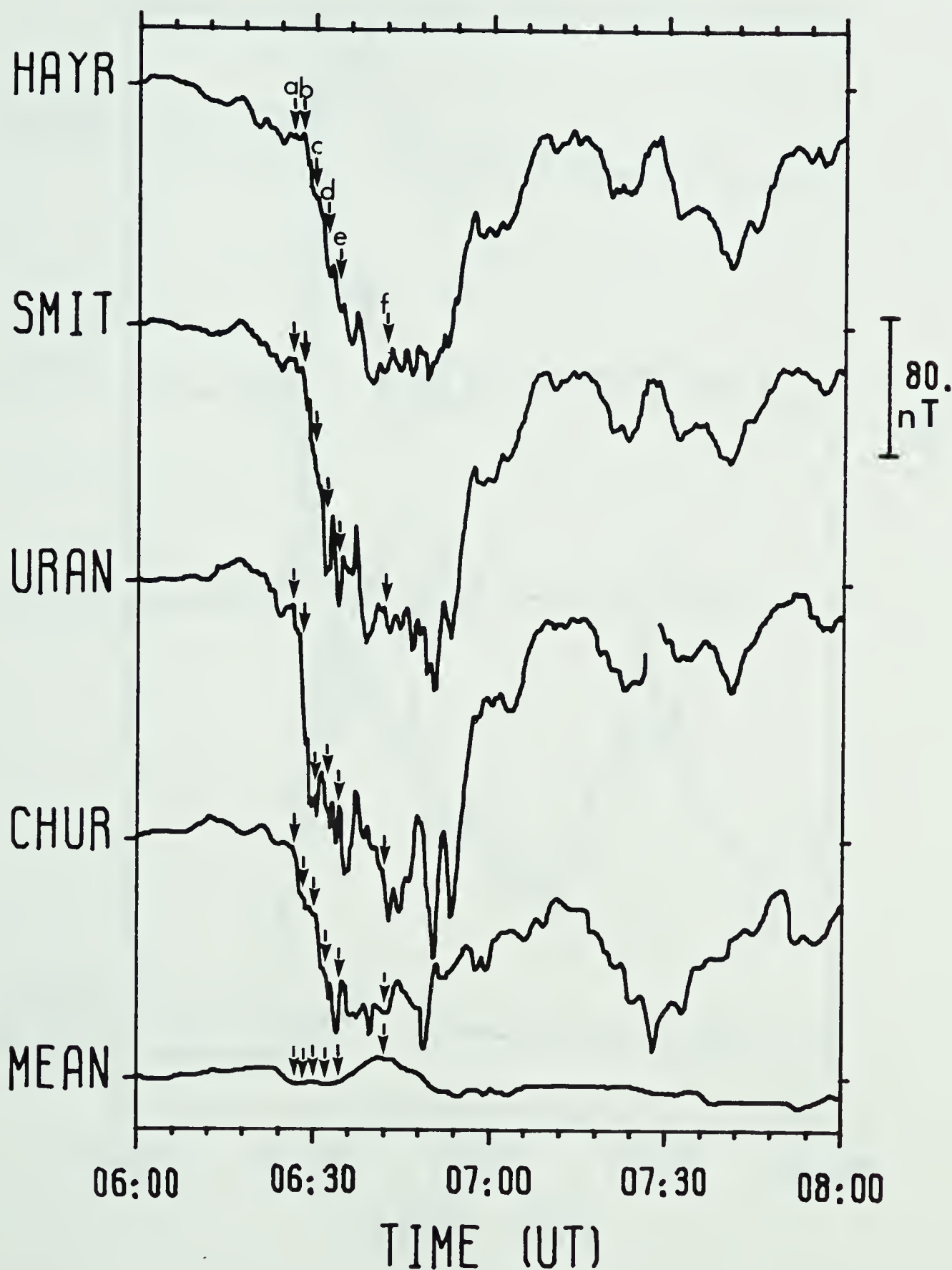


Figure 3.4  
 Stacked magnetograms: H' component for Day 214, 1974. Arrows indicate times of interest referred to in text.





## D' COMPONENT: DAY 214, 1974

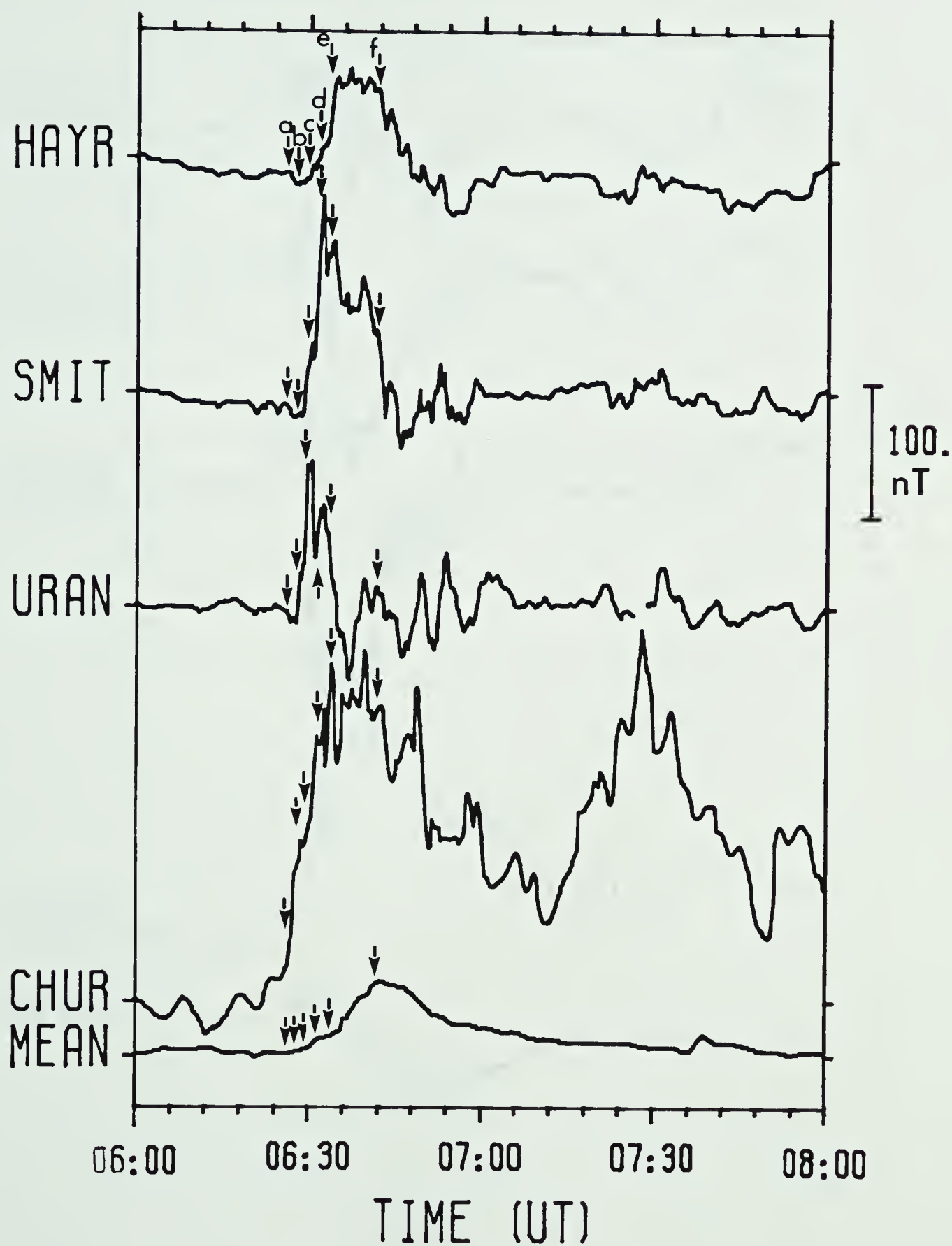


Figure 3.5

Stacked magnetograms: D' component for Day 214, 1974. Arrows indicate times of interest referred to in text.



# Z COMPONENT: DAY 214, 1974

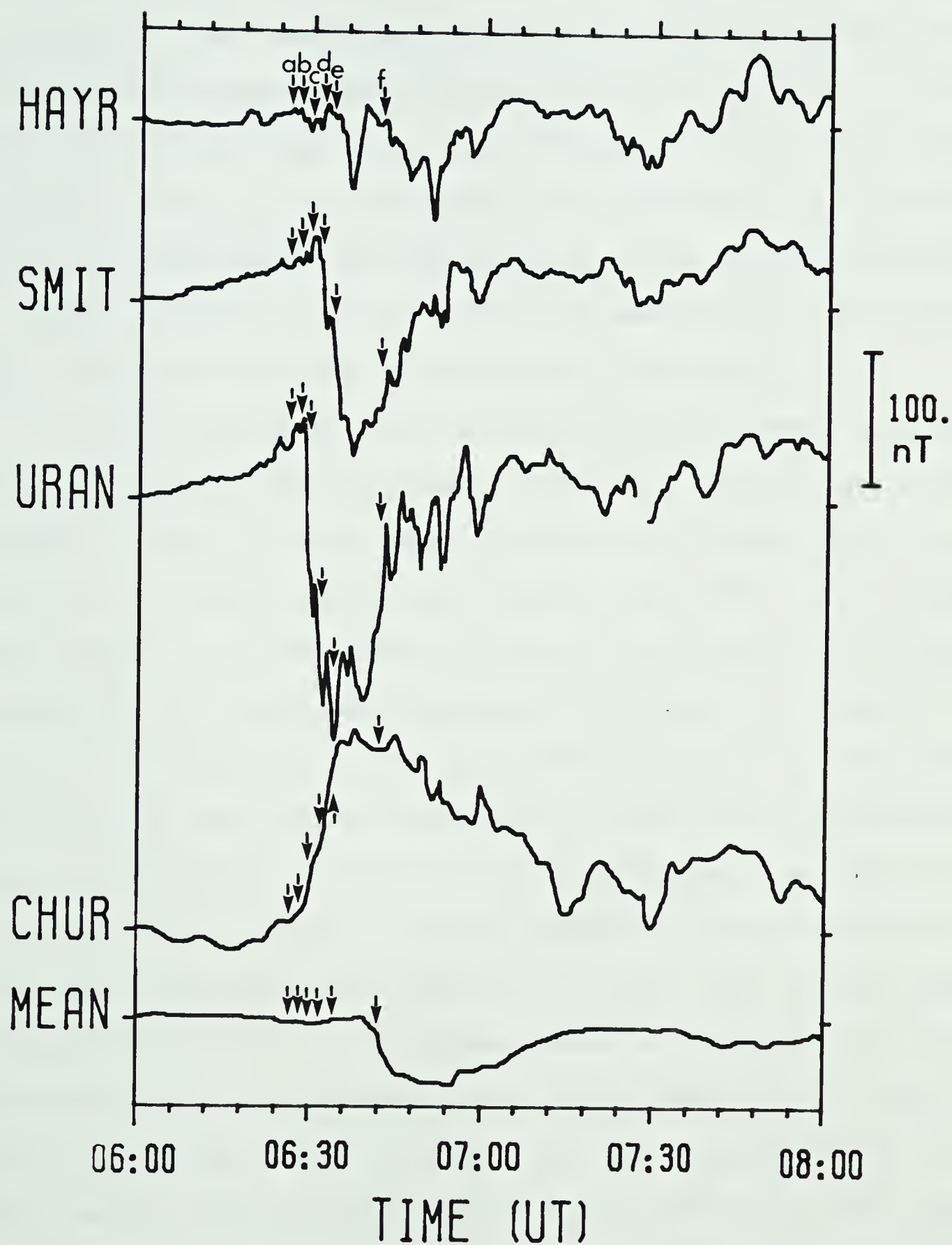


Figure 3.6

Stacked magnetograms: Z component for Day 214, 1974. Arrows indicate times of interest referred to in text.



The substorm seems to be isolated and localized. It is seen only as a distant effect at Great Whale River (magnetogram is not shown). At Fort Churchill the westward electrojet is established by 0628. The  $H'/Z$  ratio is  $-.75$  indicating that Churchill is positioned very near the poleward border of the electrojet. The station at Meanook detects a positive  $D'$  perturbation at 0630. This represents a distant effect of upward field-aligned current associated with the western edge of the westward electrojet.

In the Alberta sector, Uranium City, Fort Smith and Hay River lie along a common line of latitude ( $67.3^\circ$  N). The all-sky camera at Fort Smith provides the auroral data. The baseline for the analysis was chosen at 0625. The surge development as indicated by both the corrected all-sky images and the associated longitude profiles is shown in figures 3.7 and 3.8. As mentioned, prior to 0625 the activity was weak and in particular, there was no indication of a growth phase. At 0626 an arc brightening is observed and at this moment, a small negative  $D'$  perturbation is observed at all stations along the line. The north-south aligned arc seen at this time (panel A in figure 3.7), is suggestive of an approaching surge form. The leading edge of this form is about 10-15 degrees east of Uranium City. We have seen, in longitude profile A of figure 3.3, that just east of a north-south current system there is a positive  $Z$  regime and a weak negative  $D$  regime. The magnetic behaviour at Uranium City (panel A of figure 3.7) can, therefore, be

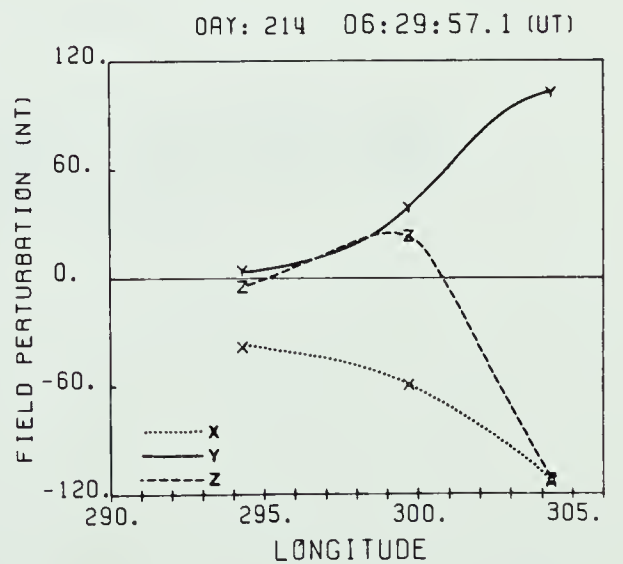
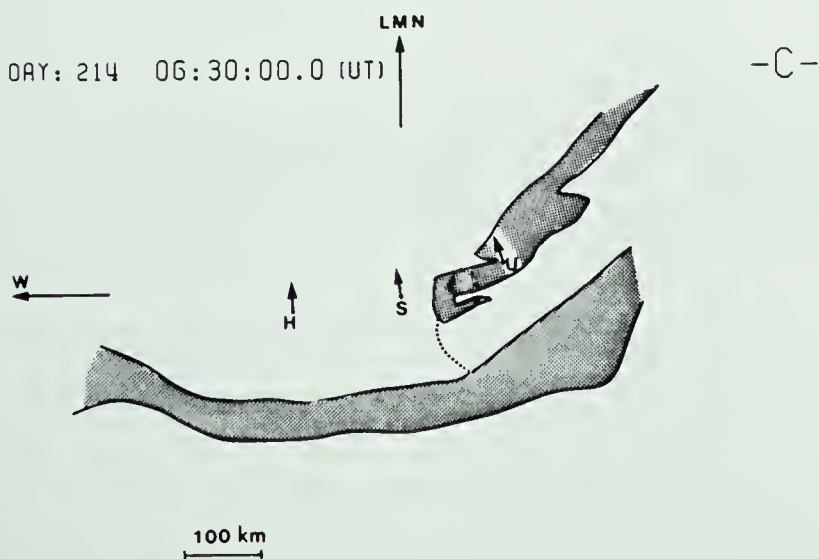
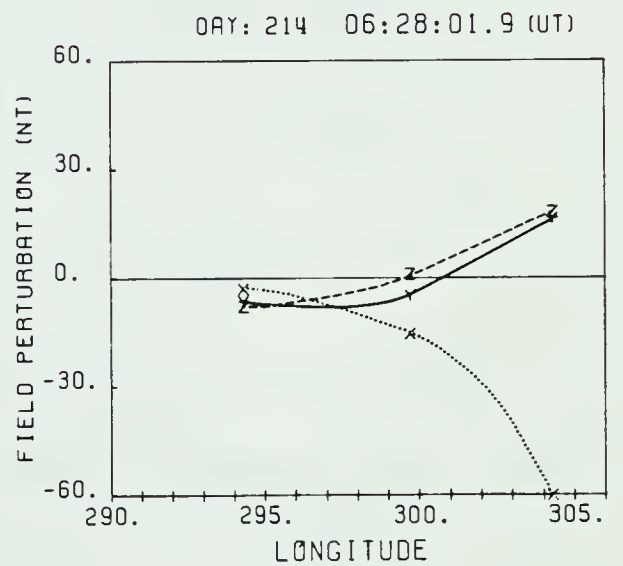
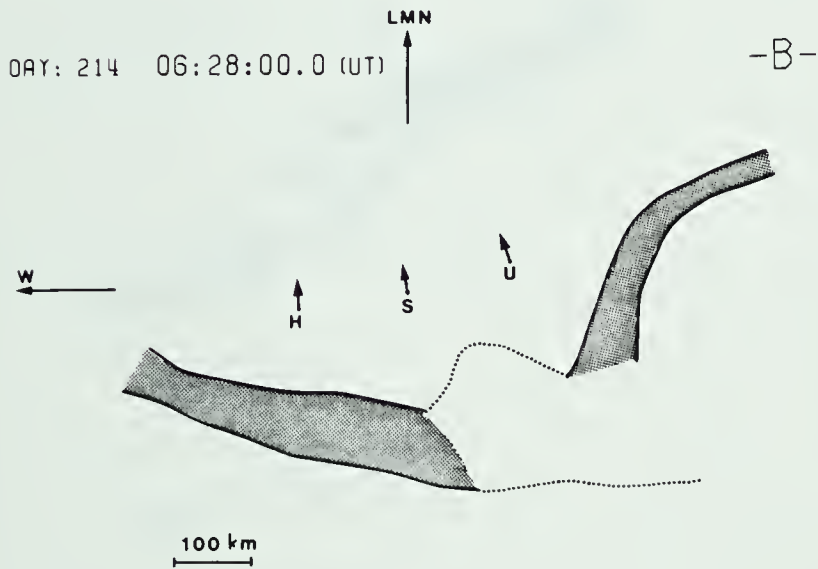
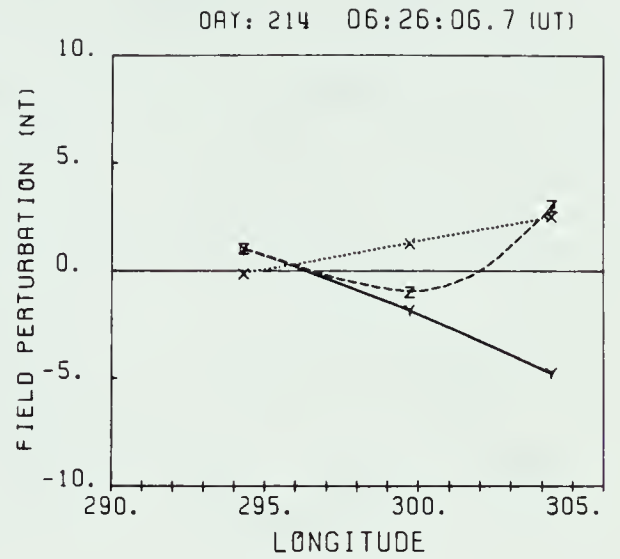
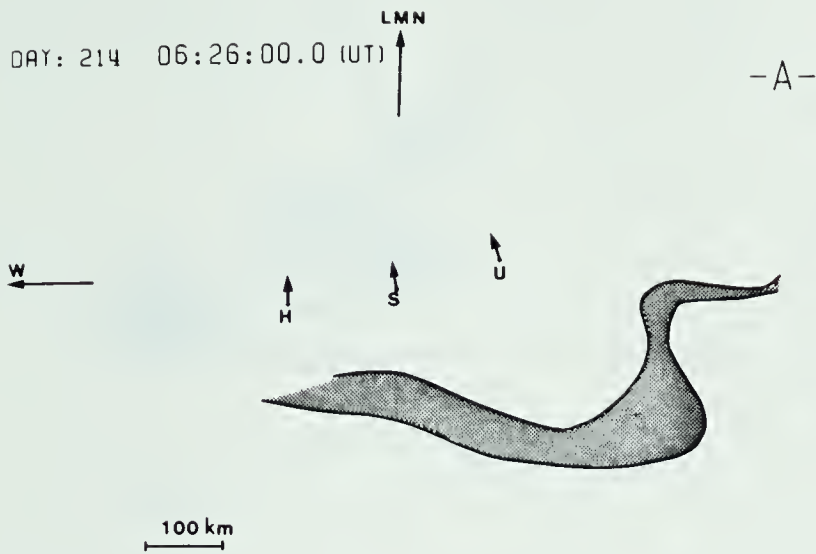




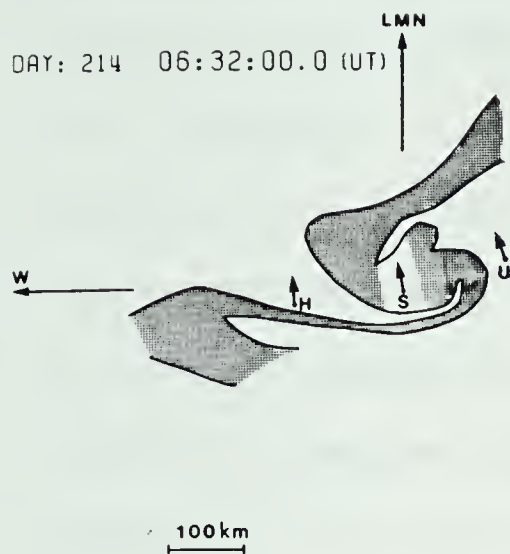


Figure 3.7

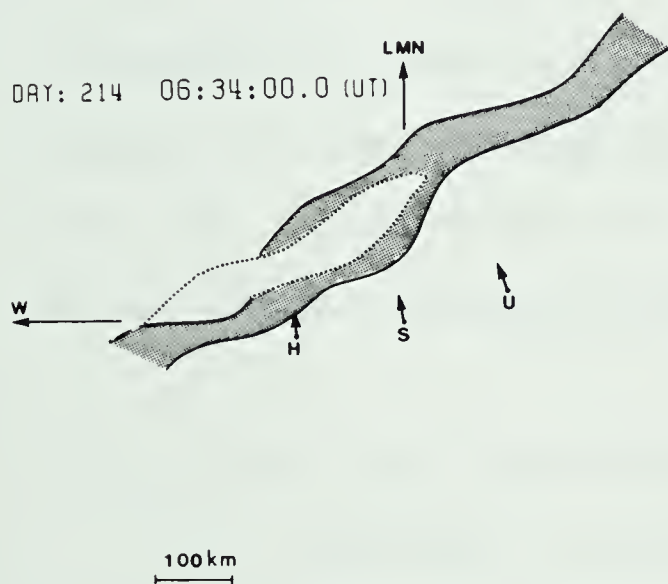
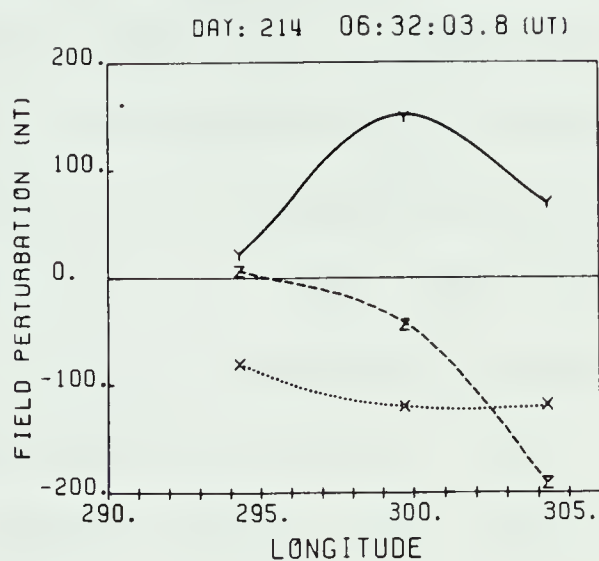
Corrected All-Sky camera images and associated longitude profiles at indicated times on Day 214, 1974. H, S, U refer to stations at Hay River, Fort Smith and Uranium City respectively. Arrows at the stations indicate geomagnetic north. LMN refers to Local Magnetic North. X, Y, Z refer to magnetic components H, D, Z, respectively.







-D-



-E-

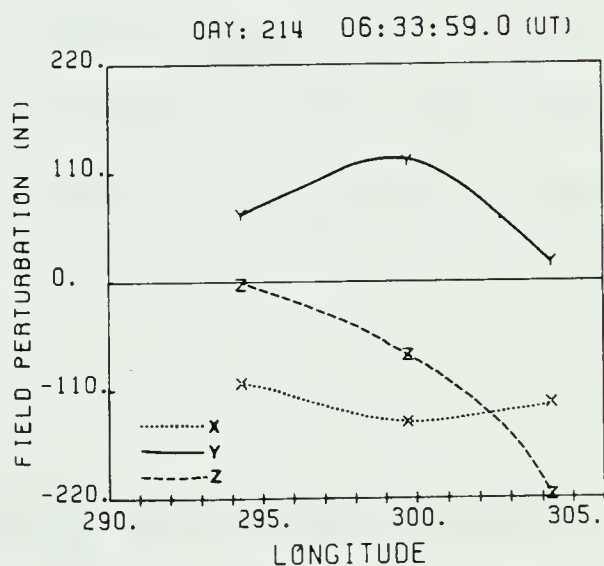


Figure 3.8  
Corrected All-Sky camera images and associated longitude profiles at indicated times on Day 214, 1974. Symbols as in figure 3.7 .





understood in terms of an approaching surge form. This is supported by the all-sky photograph at this time . There is also, however, an east-west aligned arc located south of the station line. This may be associated with westward current and, since it seems to be at an angle to the line of constant geomagnetic latitude, it could contribute to the observed negative D behaviour. The positive trend in the Z component of the profile also supports such a tilt. The H component, however, is positive and a westward current system would produce a negative H deflection. This discrepancy is most likely due to the effect of field-aligned currents associated with the surge and it indicates that the contribution of any westward current to the perturbation is probably small.

### 3.3.2 Surge Onset and Development

The appearance of the surge over the station array is characterized by the sharp changes in each component of the magnetograms with the effect being most clearly seen in the D' component. At 0628 Uranium City experiences a sharp positive D' excursion. Fort Smith does not detect this onset until 0629. Hay River does not seem to detect this initial sharp onset at all responding in a rather slow manner typical of being distant from the source. The auroral forms seen in panel B of figure 3.7 show that at 0628 a north-south aligned structure is approaching Uranium City but is still several degrees to the east. As the profile at this



time indicates, a positive D and a positive Z inflection precede the arrival of the surge form. Furthermore, we can see in the negative trend in the H component of this profile that the magnetic effects of a westward current are beginning to dominate at Uranium City.

The D' component at Uranium City undergoes a second intensification at 0629 which peaks approximately one minute later. This intensification is again delayed at Fort Smith. It starts at 0630:30 and does not peak until 0632. Again Hay River detects a relatively slowly changing perturbation. The all-sky image (panel C in figure 3.7) shows that at 0630 the surge is now centered over Uranium City. As the related profile indicates, a positive peak in the D component is not well defined but the region of positive D has certainly moved westward with the surge form. As mentioned earlier, the source of the positive D is likely a local north-south current system. The Z component of the profile shows the development of a negative regime. We have seen that a profile of this type is expected near the westward edge of a north-south system. The profile, however, is undoubtedly complicated by the approaching westward electrojet, the existence of which is indicated by the negative trend in the H component.

The positive D peak does not reach Fort Smith until 0632. At this time (panel D in figure 3.8) the surge has moved west and is now overhead at Fort Smith. The profile at this time shows a clear peak in the D component at Fort



Smith. The negative Z region has also moved westward. The H component has flattened somewhat, indicating a more uniform westward electrojet across the station line.

From 0626 to 0631 the all-sky pictures show a reasonably smooth westward motion of the surge. From 0631 to 0632:30, however, the surge seems to remain stationary, retaining its basic form. By 0633 the surge has shifted its position dramatically, with its western edge now to the west of Hay River. It is not clear whether the surge has jumped to or formed at this new position. Nevertheless, the D component at Hay River marks this change with a sharp positive increase at 0633. Following this the surge apparently regains its original velocity and, by 0634 the head of the surge is no longer detectable. An important observation, however, is that at this time the D component remains positive at all stations. This is apparently because, following the passage of the surge, the stations are left in the south-eastern region of a westward electrojet. We will see in the next chapter that such an arrangement can yield the observed effects. It is interesting that while there is no surge associated with the profile at this time, the latter is remarkably similar to that at 0632 which is associated directly with the surge.

We have seen that the westward movement of the surge is clear in both the all-sky photographs and in the D component profiles. One would expect to find that the motion of the surge would be reflected in the motion of the magnetic





signature recorded on the ground. In particular, if we assume that the behaviour of the D component is caused by surge-related currents then we would expect that the position of the D component cross-over point would be related to the position of the surge. In the plot in figure 3.9 we compare the location of the leading edge of the surge form (as indicated by the all-sky pictures) and the position of the D component cross-over point. The general features of their behaviour are seen to correspond. Both show the uniform motion of the surge and ,at ~0631, both level off indicating that the motion has stopped. Although the number of data points is limited, there is an indication that at 0633 the surge regains its motion at a new location about 15° further west and at its previous velocity. For the reasons which we have discussed, the position of the D component cross-over remains stationary.

While the basic features correspond, the magnitude of  $V_s$ , the velocity of the surge, which is found to be  $1.87 \pm .15$  km sec.<sup>-1</sup>, differs slightly from the magnitude of  $V_d$ , the velocity of the D component cross-over point, which is found to be  $2.30 \pm .24$  km sec.<sup>-1</sup>. A number of points must be considered in order to interpret this result.

One reason that we might expect to find  $V_d$  greater than  $V_s$  is that  $V_d$  is related to  $V_s$  by the relation;

$$V_d = V_s / \cos(\theta) \quad (3.1)$$

where  $\theta$  is the tilt of the surge with respect to a line of constant geomagnetic latitude. In figure 3.10 we show a

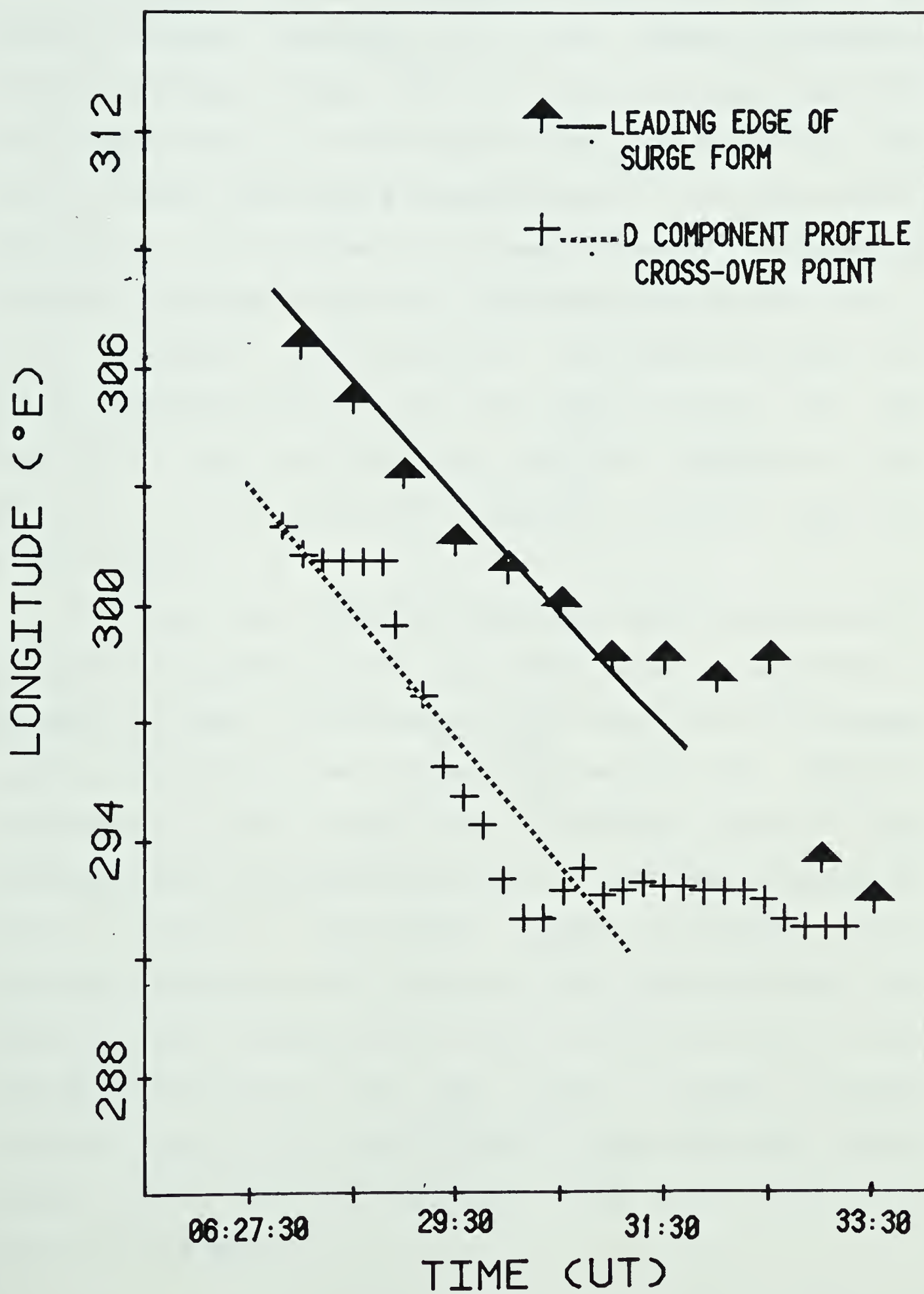




Figure 3.9

Graph of position versus time showing the motion of both the leading edge of the surge form and the D component cross-over point.

## POSITION vs TIME







contour plot of the D component perturbation due to a simplified model current system for the surge. This model includes only a current loop which is closed by equatorward flowing current followed by a loop which is closed by poleward flowing current, both of which have been tilted  $20^\circ$  to the north-west. In this figure we can see that the zero level contour lies nearly perpendicular to the direction of propagation. As this contour crosses a line of stations of constant geomagnetic latitude, the detected velocity will be given according to equation 3.1. The surge velocity,  $V_s$ , can be determined if the tilt angle can be found. For this particular event no significant tilt was detected but even with a tilt of  $10^\circ$   $V_d$  is only decreased by  $.05 \text{ km sec}^{-1}$  to  $2.25 \text{ km sec}^{-1}$ .

We also note that the process of determining the position of the edge of the surge form could contribute a systematic error in determining the velocity of the surge. The key feature of this process is to correct the original, distorted, all-sky image with a correcting template. Once corrected, the location of the edge of the form is estimated and its position is determined through a scaling factor found by calibrating the template. While care was taken, the error in the scaling factor was 5% giving an error in the velocity measurement of 5%. This yields a surge velocity value of  $1.87 \pm .24 \text{ km sec}^{-1}$  which is now consistent, within error, with the D component cross-over velocity of  $2.21 \pm .27 \text{ km sec}^{-1}$ .



## D COMP. CONTOUR

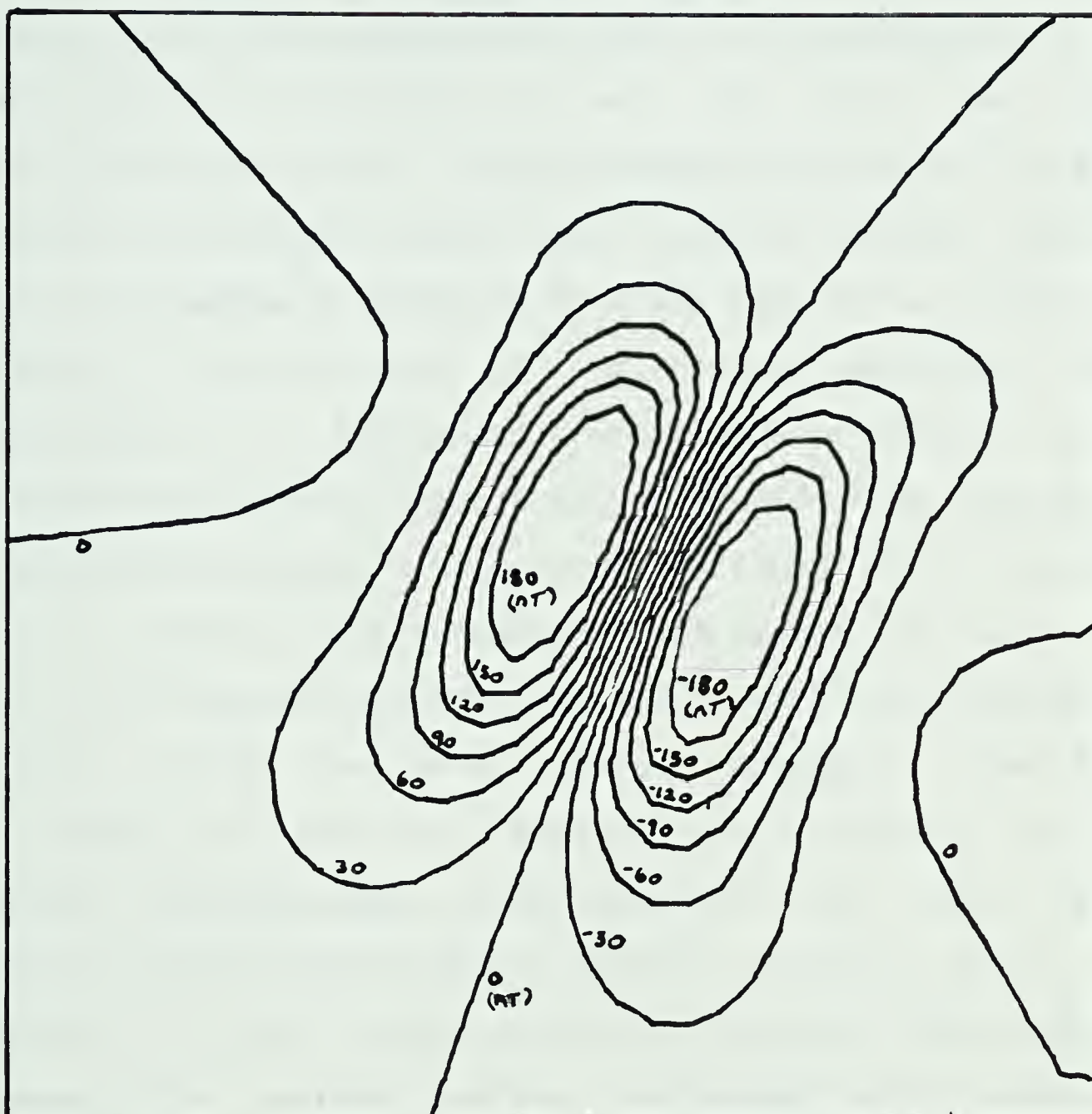


Figure 3.10  
Contour plot of D component perturbation due to  
a simplified model for the surge.



### 3.3.3 Following the Passage of the Surge

Following the passage of the surge, the westward electrojet remains relatively steady. At 0642, however, (position f on the magnetograms) there is an indication of a change with the  $D'$  component at both Hay River and Fort Smith beginning to drop. As the latitude profiles in figure 3.1 show, the southern portion of a westward current system there is a region of positive  $D$  to the west and a region of negative  $D$  to the east of its central meridian. The observation of a decreasing  $D$  would seem to indicate that the region of westward current has moved west. The behaviour at Meanook also supports this movement. Since this station is well south of the ionospheric electrojet, the magnetic effects are governed primarily by the distant field-aligned currents. Prior to 0642, Meanook detects a positive perturbation in the  $D'$  component and little or no  $Z$  component perturbations. This suggests that there is a region of upward field-aligned current directly north of Meanook. In terms of the westward electrojet, this region represents its western portion. Following 0642, Meanook detects a decreasing  $D'$  and a rather sharp onset of negative  $Z$ . This indicates that Meanook is now south of the westward electrojet, with upward field-aligned current to the west and downward field aligned current to the east. From its position prior to 0642 to its position after 0642, the westward electrojet has apparently expanded westward. The suddenness of the shift is suggestive of the stepping motion





inherent in the Wiens-Rostoker model of the substorm.

### 3.3.4 Summary for Day 214, 1974

We can now list the more important features of this event.

1.) There is a negative D perturbation prior to the onset of the surge. This seems to be an effect caused by the approaching surge.

2.) The magnetic variations, in longitude, due to the surge are characterized by:

a) A positive D region, peaking beneath the forward portion of the surge form. We note that there was no negative D region seen behind this surge form.

b) A positive to negative transition of the Z component with a cross-over prior to the peak in D. There was no clearly defined negative peak and the negative region was of a larger magnitude than the positive region. These may represent electrojet influences.

3.) The surge does not propagate smoothly. Initially, it moves smoothly westward at a speed of  $2.0 \text{ km sec}^{-1}$  into the Alberta sector. It then stops for about 2 minutes and then either jumps to or re-forms at a point  $15^\circ$  further west, proceeding at its original velocity (at least while it is in the camera's field of view).

4.) The western edge of the substorm disturbed region experiences a sudden shift, possibly a discrete step, to the west toward the end of the event.



### 3.4 Event Analysis ... Day 307, 1976

#### 3.4.1 Introduction

At 0625 on Day 307 (November 2) 1976 magnetic activity was detected in the Alberta sector. Figures 3.11, 3.12, and 3.13 show the behaviour, along an east-west line, of the H', D', and Z components, respectively. Figures 3.14, 3.15, and 3.16 show this behaviour along a south-north line. Figure 3.17 shows the behaviour of the available riometer signals. Five periods of interest (A, B, C, D and E) are indicated and will be referred to in the analysis.

The three hour averaged value of Kp prior to 0600 is 3-. This implies that this period is globally quite active. Although activity is initially seen at 0625 in the Alberta sector, we will see that this initial action is very localized. The station at Fort Churchill detects only a slowly increasing Z component at this time giving no indication of substorm activity. It is not until 0655 that a sharp negative H and positive Z signify the occurrence of a substorm. In a sector west of Alberta, at College, Alaska (not shown), there is also no indication of substorm activity until 0655. It would seem that the major onset of activity occurs at 0655. The activity in the Alberta sector prior to this onset may or may not be related to the following substorm. Nevertheless, it does contain a sequence of surge-like events which warrant further analysis.



## H' COMPONENT: DAY 307, 1976

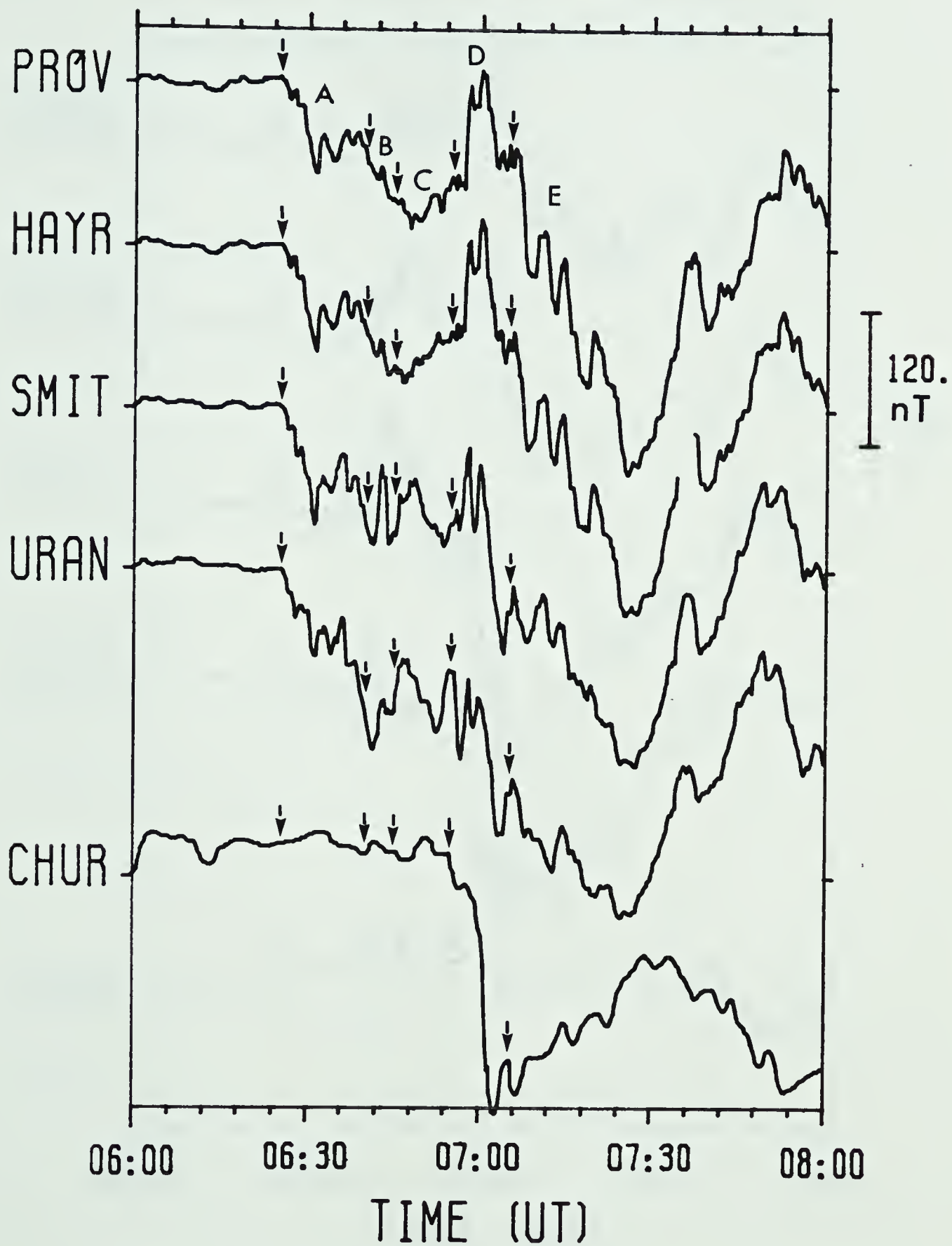


Figure 3.11  
 Stacked magnetograms along east-west station chain: H' component for Day 307, 1976. Regions of interest referred to in text are indicated.





## D' COMPONENT: DAY 307, 1976

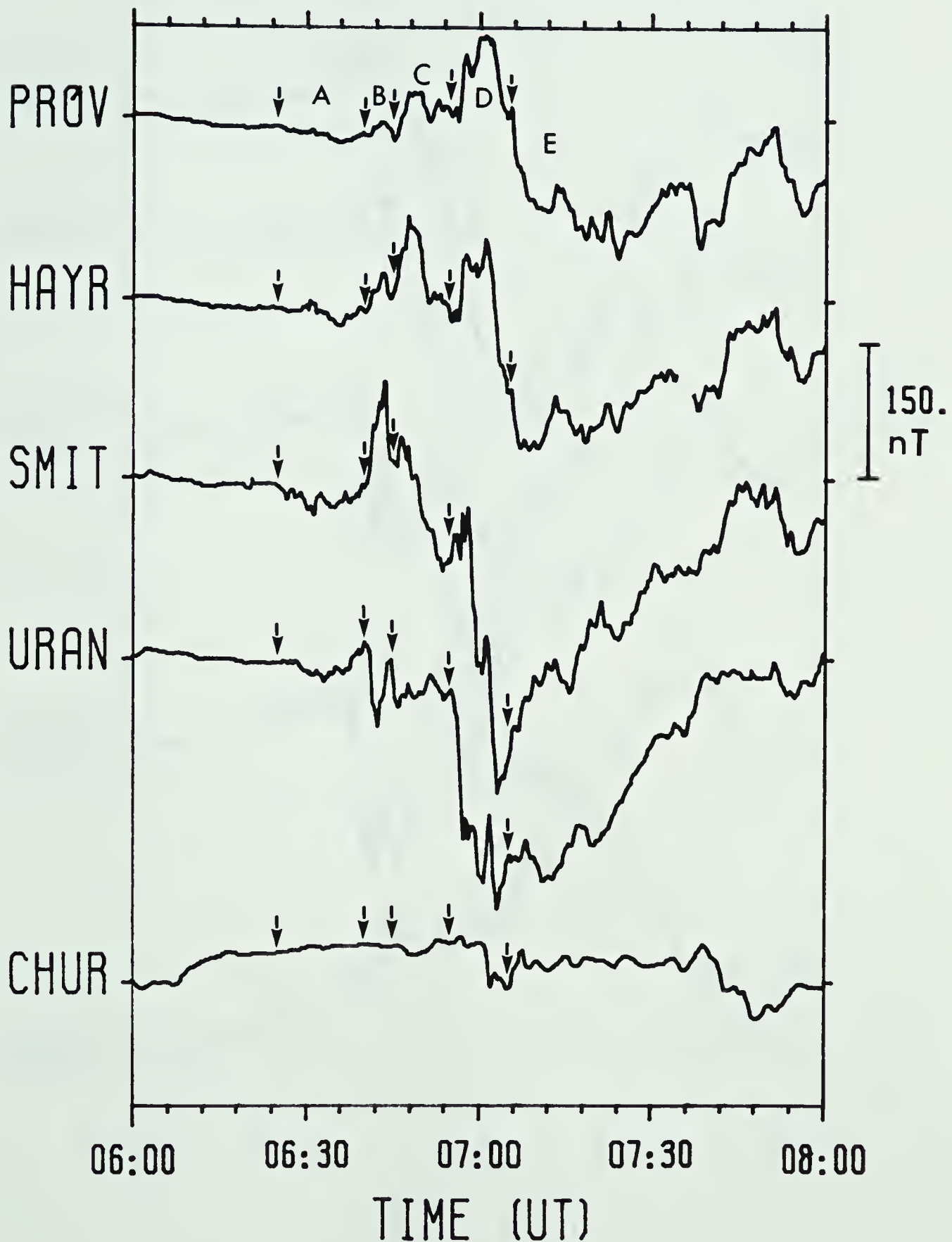


Figure 3.12  
 Stacked magnetograms along east-west station chain: D' component for Day 307, 1976. Regions of interest referred to in text are indicated.



# Z COMPONENT: DAY 307, 1976

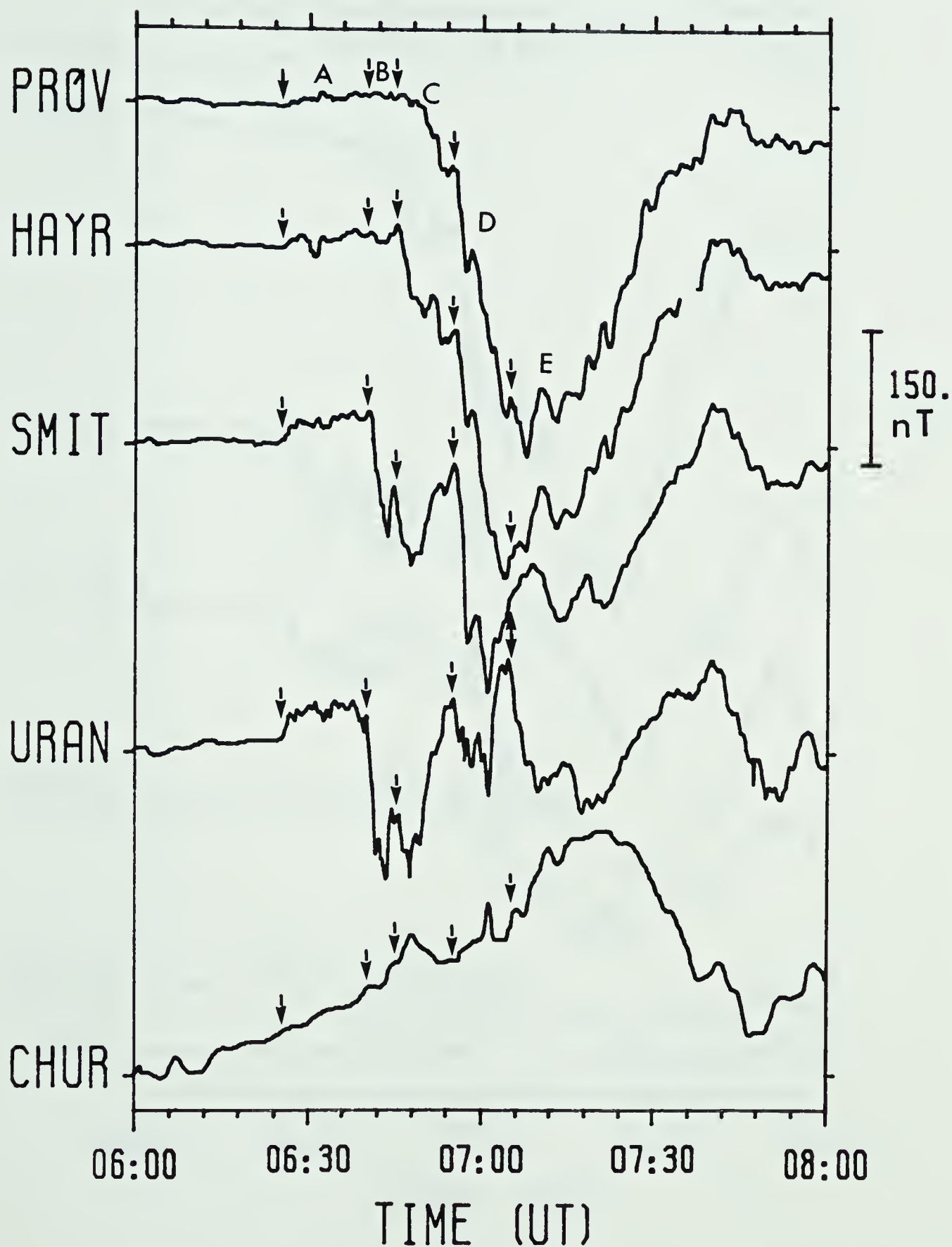


Figure 3.13

Stacked magnetograms along east-west station chain: Z component for Day 307, 1976. Regions of interest referred to in text are indicated.



# H' COMPONENT: DAY 307, 1976

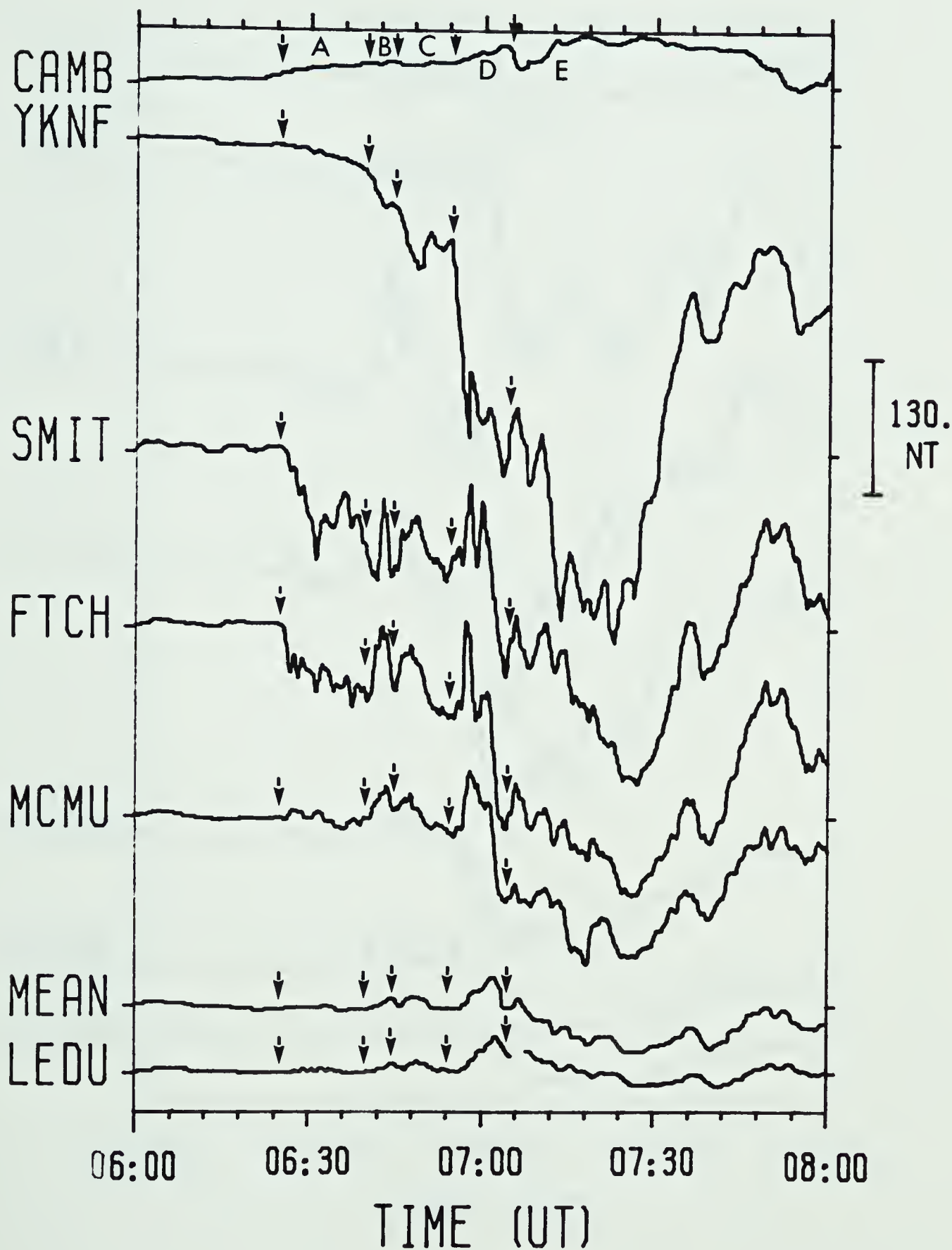


Figure 3.14  
Stacked magnetograms along south-north station chain: H' component for Day 307, 1976. Regions of interest referred to in text are indicated.





## D' COMPONENT: DAY 307, 1976

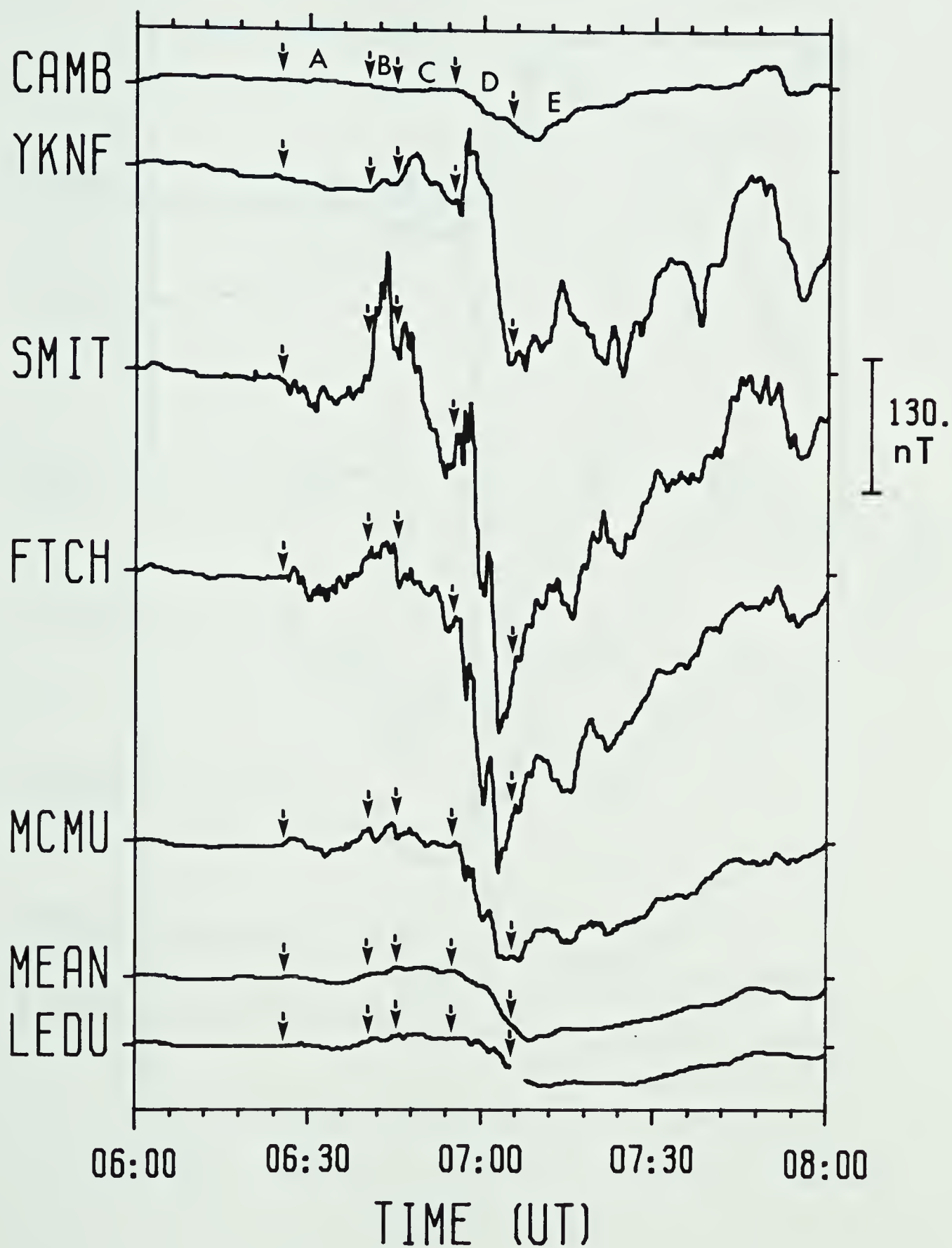


Figure 3.15

Stacked magnetograms along south-north station chain: D' component for Day 307, 1976. Regions of interest referred to in text are indicated.



# Z COMPONENT: DAY 307, 1976

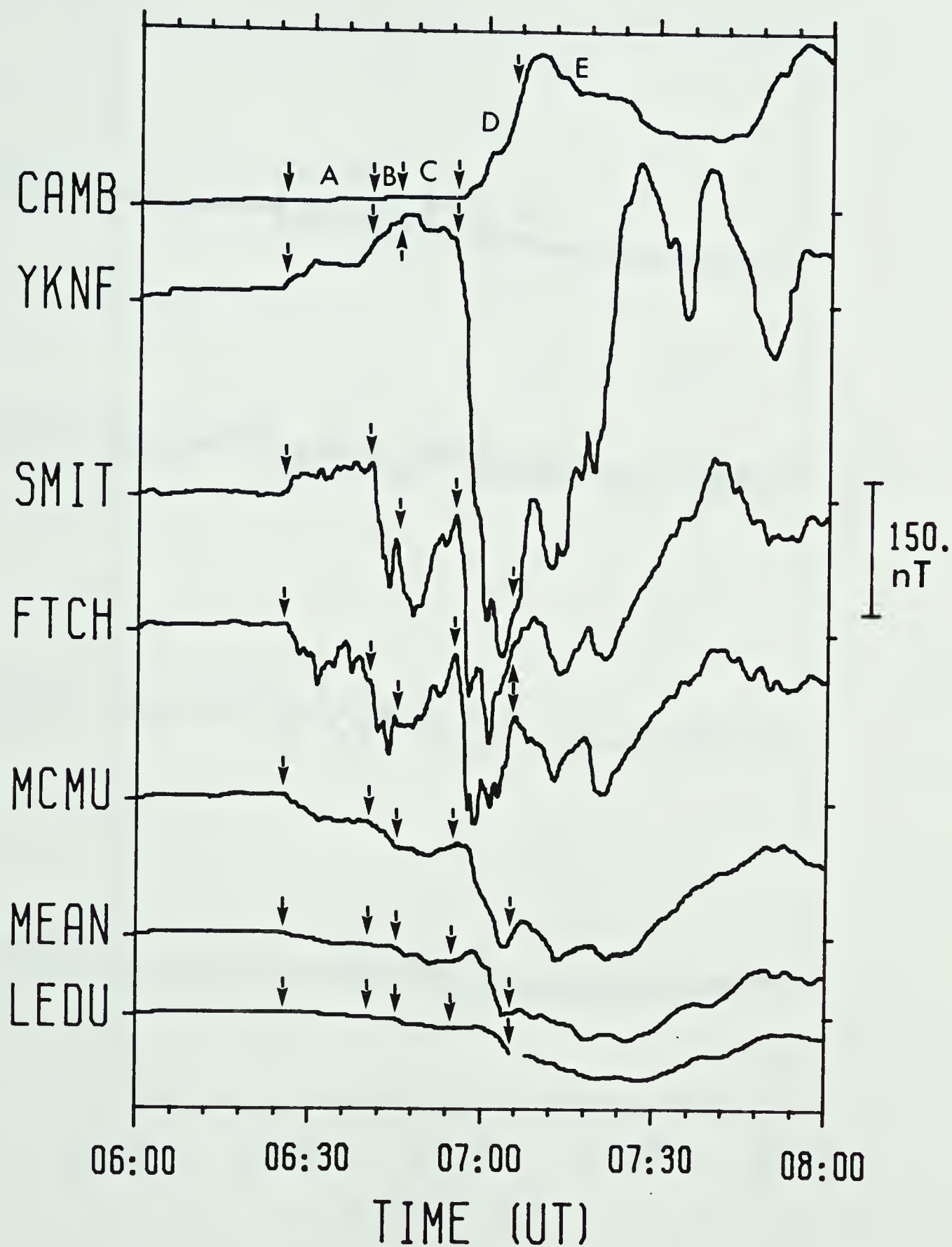


Figure 3.16

Stacked magnetograms along south-north station chain: Z component for Day 307, 1976. Regions of interest referred to in text are indicated.



# RIOMETER : DAY 307, 1976

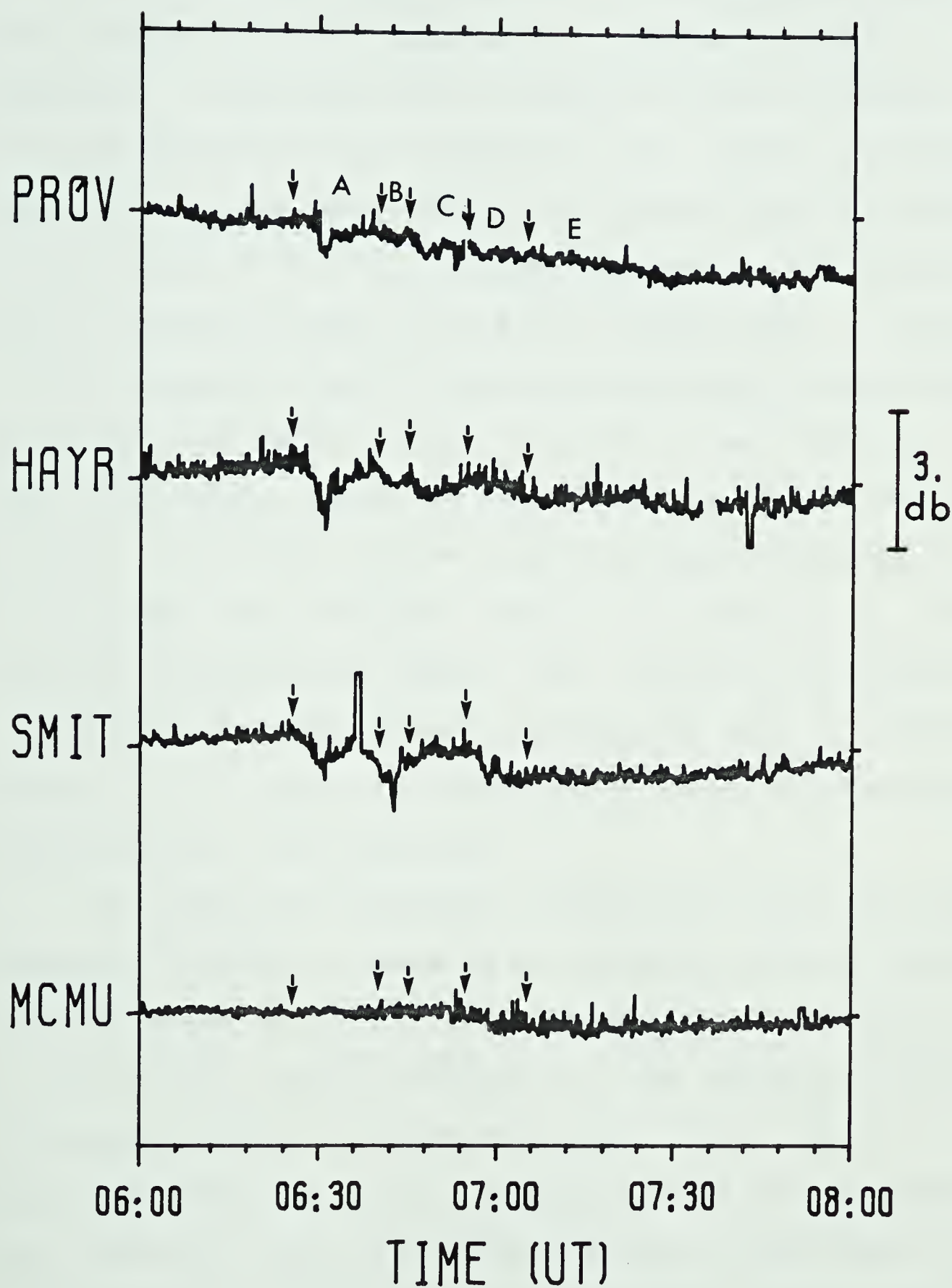


Figure 3.17  
 Stacked riometer signals at available stations for Day 307, 1976. Regions of interest referred to in text are indicated.





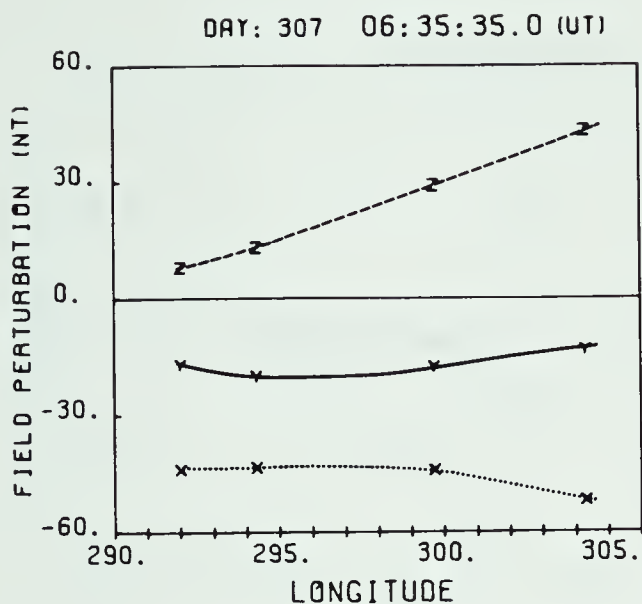
### 3.4.2 Surge Onset and Development

From 0625 to 0640 (period A) profiles along the east-west station line show relatively uniform negative H and negative D components. The Z component shows a linear trend being considerably more positive to the east, at Uranium City, than to the west, at Fort Providence (see for example, A in figure 3.18). All of these deflections are relatively weak. A current system which might produce such a magnetic effect would be a weak 'westward' electrojet tilted towards the north-west. Uranium City would be to the north of and Fort Providence would be nearly at the center of such a current. A latitude profile during this period (A, in figure 3.19) shows a well defined region of negative H. The Z component transition places the center of the current at  $67^{\circ}$  N latitude. The negative extremum of the Z component allows us to place the equatorward border of the westward electrojet at  $65^{\circ}$  N latitude.

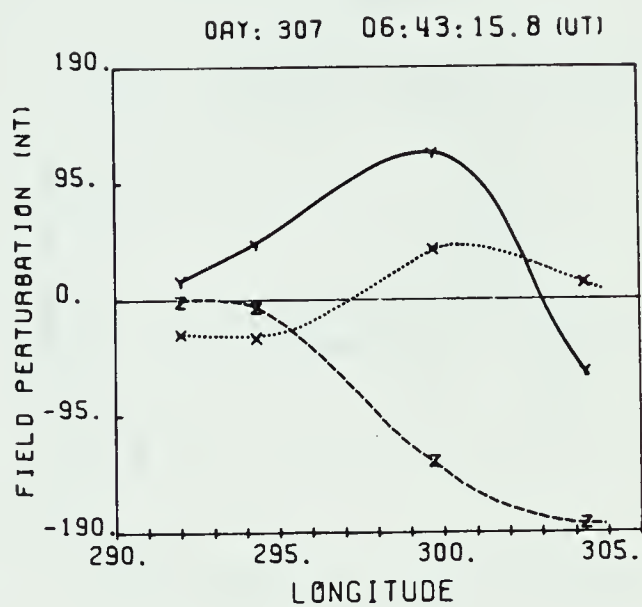
Now, under the simplifying assumptions that the H and D component values are produced by a uniform westward current, the tilt angle (given by the  $\arctan\{D/H\}$ ) can be determined. By selecting typical profiles over the period of interest, an average value of the D/H ratio and, thus, of the tilt angle was obtained. Though systematic errors may be present, the error on the tilt consists solely of the error in the value of the D/H ratio. Using this approach we can estimate the tilt of the westward electrojet at this time to be  $15^{\circ} \pm 5^{\circ}$  to the north-west.



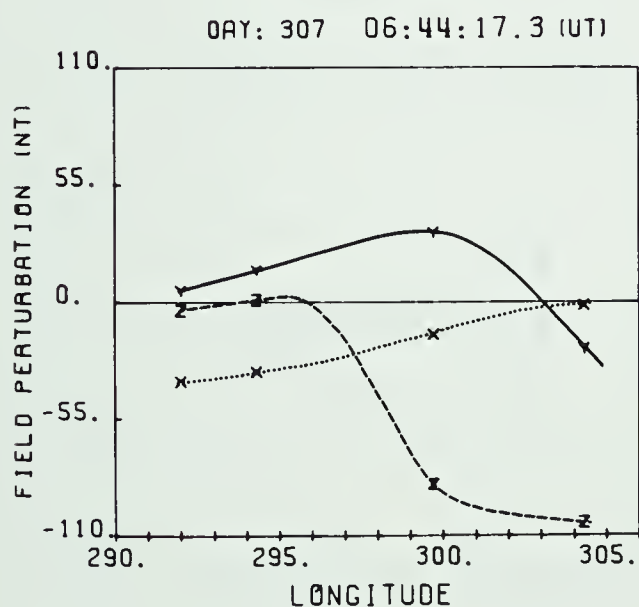
-A-



-B1-



-B2-



-C-

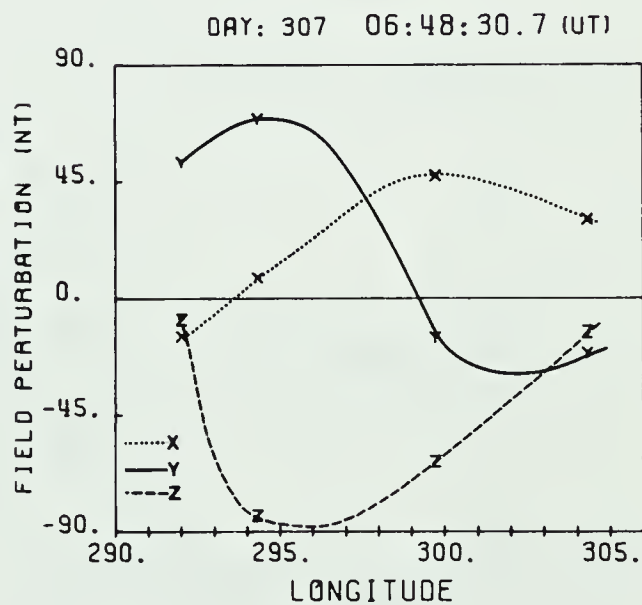
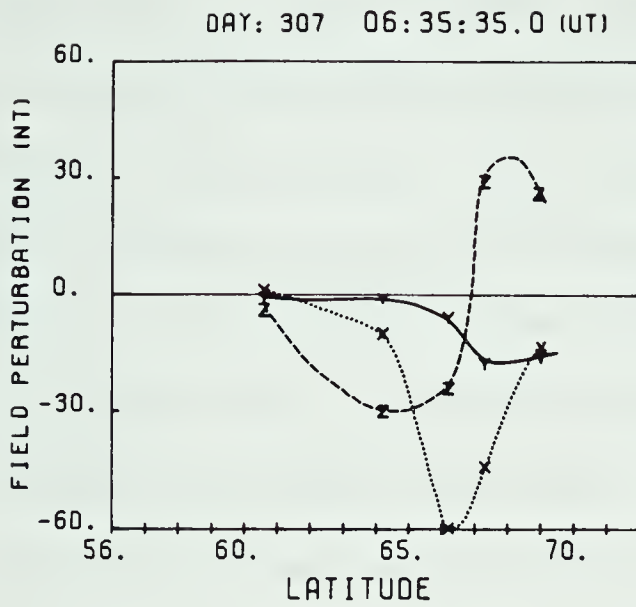


Figure 3.18

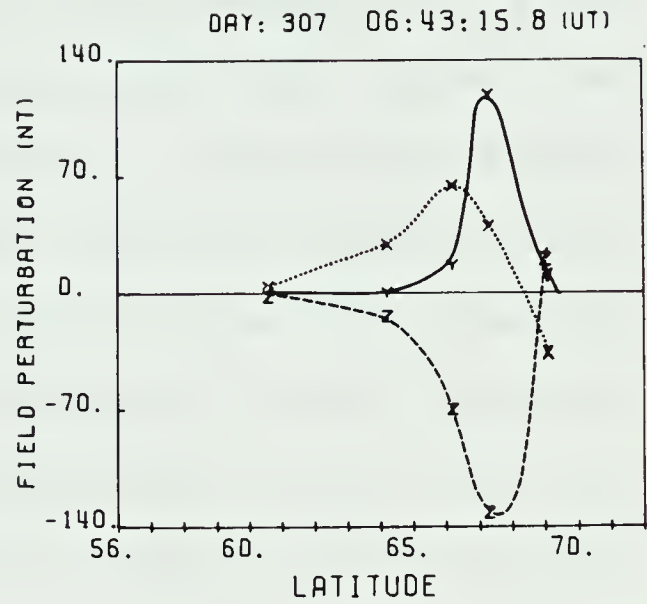
Longitude profiles at indicated times for Day 307, 1976. Profiles are referred to in text by the indicated label. Note that X, Y, and Z refer to magnetic components H, D, and Z.



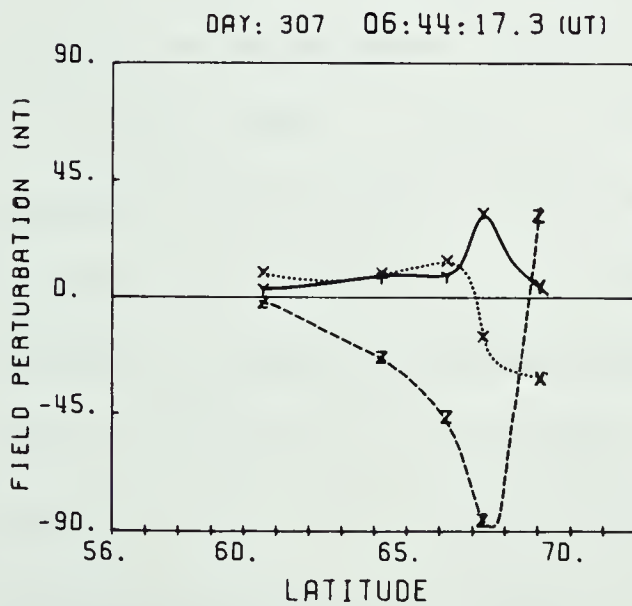
-A-



-B1-



-B2-



-C-

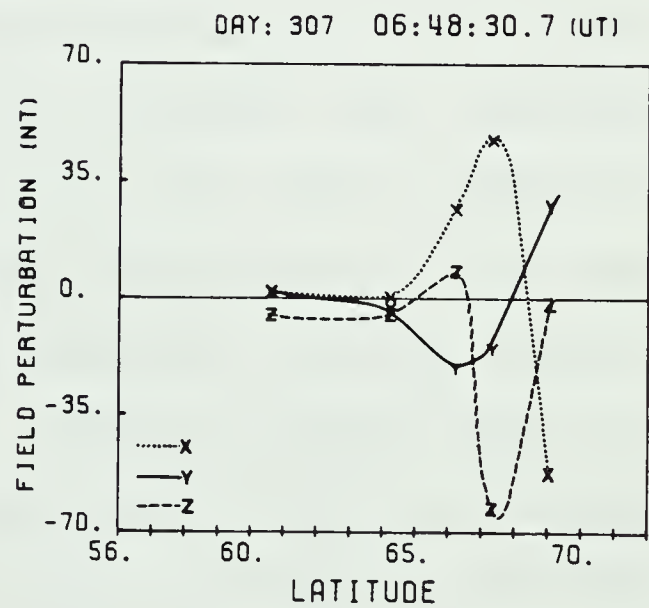


Figure 3.19

Latitude profiles at indicated times for Day 307, 1976. Profiles are referred to in text by the indicated label. Note that X, Y, and Z refer to magnetic components H, D, and Z.



From 0640 to 0645 (period B) a new event is observed. In particular, a very localized positive  $D'$  perturbation is detected at Fort Smith. There is a weak positive  $D'$  at Hay River and a negative  $D'$  at Uranium City. To the north and south, Yellowknife and Fort McMurray respectively detect very little perturbation while Fort Chipewyan (which is very close to Fort Smith) also detects the positive  $D'$  clearly. Associated with this  $D'$  component behaviour at Fort Smith is a small but sharp positive  $H'$  perturbation. At the same time there is a major decrease in the  $Z$  component, particularly at Fort Smith, Fort Chipewyan, and Uranium City. Yellowknife, on the other hand, shows a positive increase in the  $Z$  component.

The longitude profile at this time (B-1 in figure 3.18) shows the signature for this event. The baseline was chosen at 0640. The  $D$  and  $Z$  profiles resemble the profiles associated with the surge on Day 214, 1974. The  $D$  component reaches a positive peak at  $299^\circ$  E longitude. It then goes through a transition at  $304^\circ$  E, entering a negative regime. The  $Z$  component indicates the negative regime which we expect to find beneath a surge form with the negative extremum being positioned very near to the  $D$  component transition. We have previously noted this as a characteristic of the magnetic signature of the surge. However, as the Day 214 event showed, not all positive  $D$  deflections represent surges. The appropriate effects can be produced near the edge of a westward current, although, one





would expect to observe a negative H perturbation under such circumstances. The occurrence of a positive H perturbation throughout suggests that these effects are probably surge related. It has been observed that there is a positive H region south of the surge and a negative H region to the north (Kisabeth and Rostoker, 1973). A latitude profile at this time (B1 in figure 3.19) shows that the H component undergoes a transition at  $68^{\circ}$  N latitude. Since the longitude profiles do not show any significant westward current to be present at this time, we can infer that this transition in H occurs near the center of the surge form. The baseline for this profile was taken at 0640, as it was with the longitude profile.

The form of the profiles (both longitude and latitude) remains relatively constant throughout period B (see profile B2 of figure 3.18 and B2 of figure 3.19). The peak amplitude of the D component perturbation does, however, decrease considerably in magnitude from B1 to B2. The causative current system has apparently decayed while having remained relatively stationary. While it does not display any significant motion the current system does seem to produce a profile similar to that which we have associated with the westward travelling surge (see figure 3.3).

From 0645 to 0650, period C, another perturbation is observed. Longitude profile C in figure 3.18 and latitude profile C in figure 3.19 show the magnetic variations during this period. The baseline used for these profiles was taken



at 0645. From the D' component magnetograms (figure 3.12), Hay River detects the positive D' deflection most clearly, while Fort Providence detects a similar but weaker effect. Fort Smith detects an initial, short-lived positive D' which is followed by a sharp negative D' deflection. Just north of Hay River, at Yellowknife (see figure 3.15) the positive D' perturbation is apparent but much weaker. The D and Z components of the longitude profile show the characteristics of a surge-related profile. The positive H component suggests that the stations are in the southern region of the surge form and under the influence of little or no westward current. The latitude profile shows a transition in the H component across  $69^{\circ}$  N latitude. As we have previously noted, this transition is probably near the center of the surge. The profiles are similar in form to those of period B. As before, it would seem as though the causative current system is similar to one associated with the westward travelling surge. The position of this new form, however, is slightly further to the north and to the west. As with the event during period B the profiles (not shown here) maintain their form while the level of the perturbation decreases in magnitude. There is no indication of any significant motion associated with this current system during the period of decay.

The next period of activity (period D) marks the onset of the major current systems of this substorm, as can be seen from the magnetograms. By 0656 all the stations show a



significant drop in the Z component. At the same time, the D and H components at Fort Smith and Fort Chipewyan begin to rise and the D and H components at Uranium City begin to fall. At Fort Providence and Hay River both of these components remain quite flat. The baseline was chosen at 0655 where the magnetic behaviour is relatively unchanged from that occurring several minutes earlier. The variations which have developed by 0656 are shown in the longitude profile (D1 in figure 3.20) and the latitude profile (D1 in figure 3.21). The behaviour of the Z component does not seem indicative of an approaching surge form. The slow response seems more likely to correspond to an intruding westward electrojet, north of the station line. The positive D response at Fort Smith and Fort Chipewyan could be generated by upward field-aligned currents near the western edge of such an electrojet.

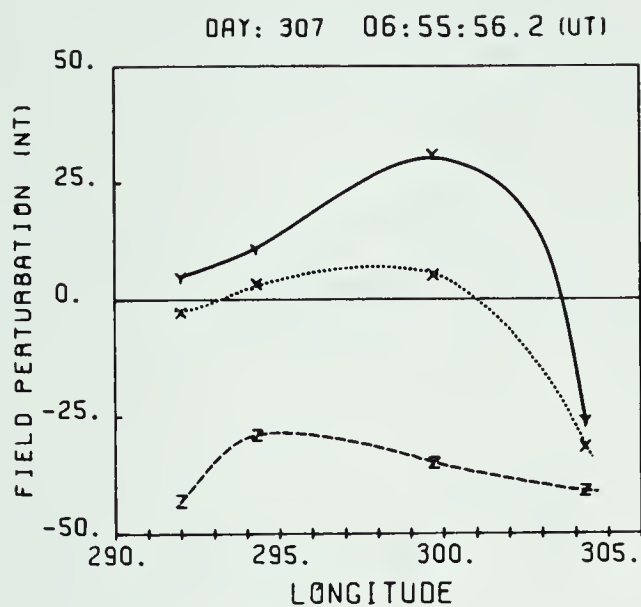
Just prior to 0656:30, the D component at Fort Smith drops some 30 nT in about 15 seconds. In the same period, the Z component at Uranium City increases, positively, about 20 nT. This may signify an approaching or growing surge structure. Indeed, at 0656:40 the D component at Fort Smith, Hay River, Yellowknife, and Fort Providence jumps very sharply, signifying the onset of the surge. The longitude profile (D2 in figure 3.20) shows the signature. The peak in D, corresponding to the center of a north-south system, lies between Hay River and Fort Smith. Unlike the event on Day 214, 1974, the surge has apparently formed within the sector



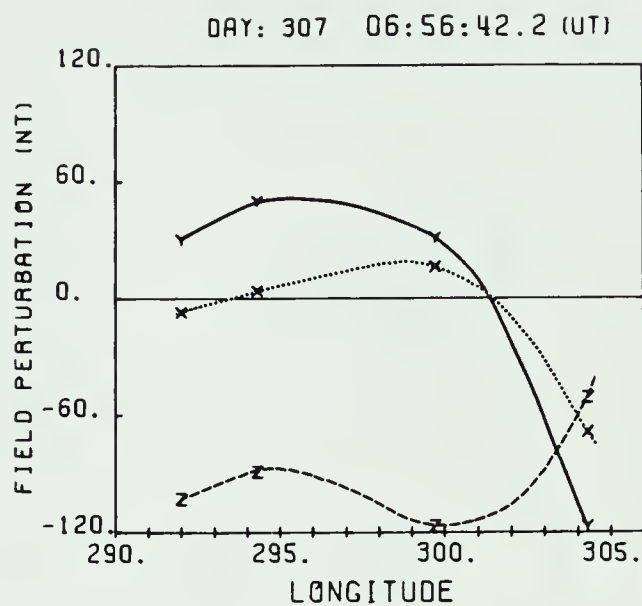




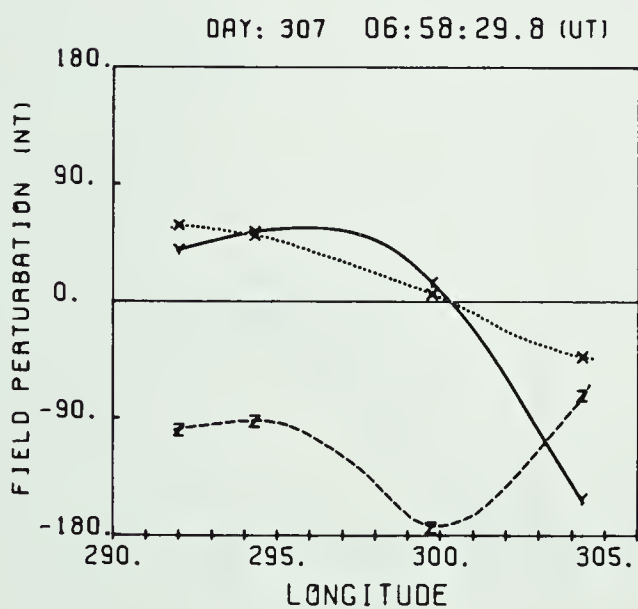
-D1-



-D2-



-D3-



-D4-

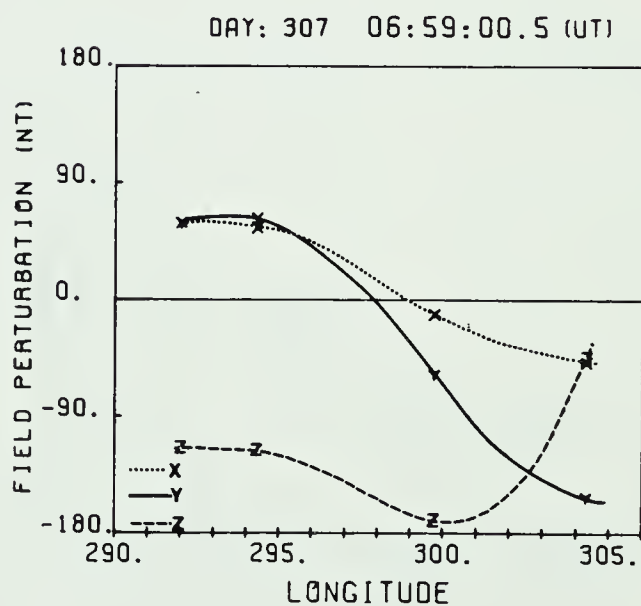
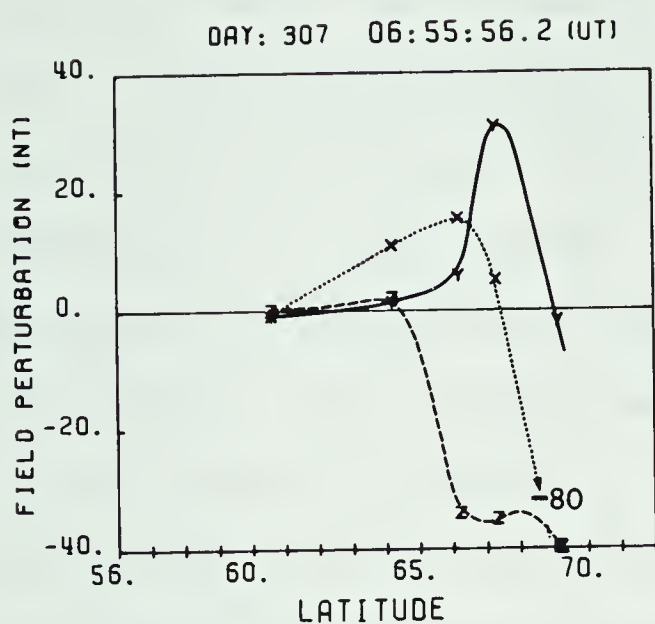


Figure 3.20

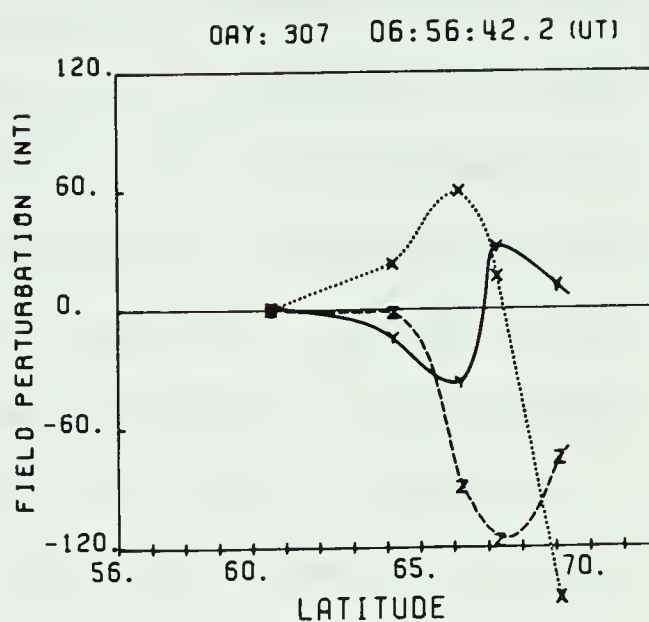
Longitude profiles at indicated times for Day 307, 1976. Profiles are referred to in text by the indicated label. Note that X, Y, and Z refer to magnetic components H, D, and Z.



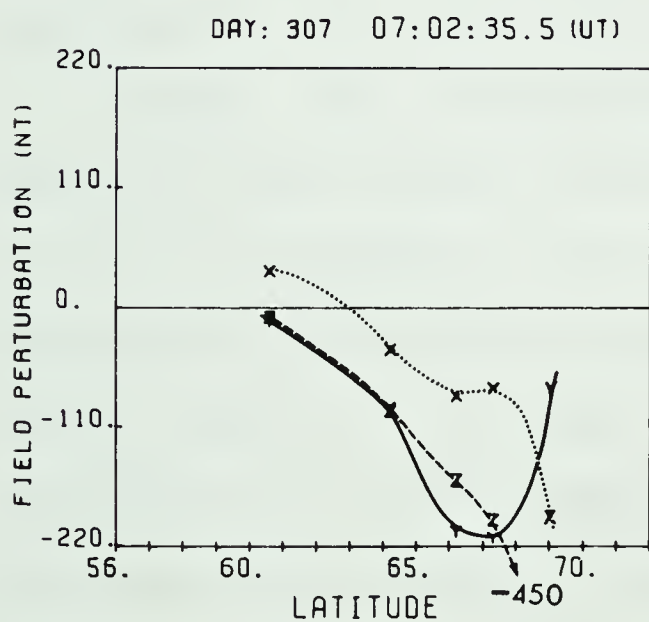
-D1-



-D2-



-D6-



-E-

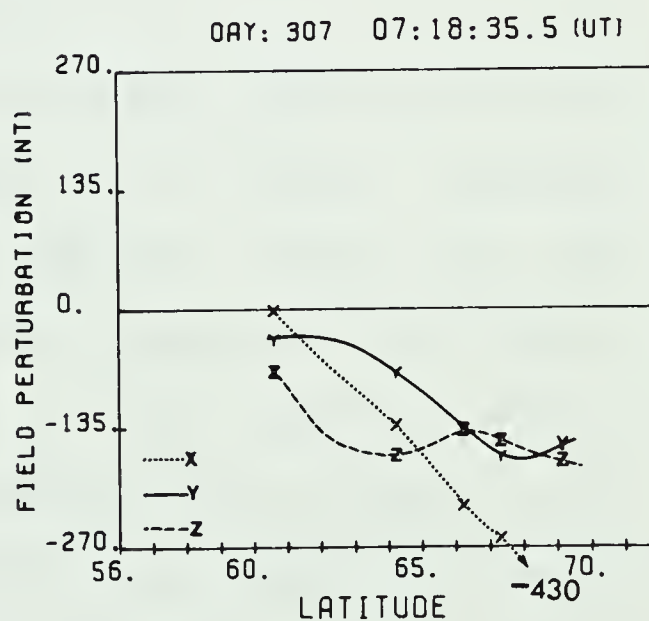


Figure 3.21

Latitude profiles at indicated times for Day 307, 1976. Profiles are referred to in text by the indicated label. Note that X, Y, and Z refer to magnetic components H, D, and Z.



and not travelled into it. The Z profile shows the negative extremum near the cross-over point in D which is expected from a surge-related current system. It is, however, biased negatively, presumably because of the effect of the westward electrojet to the north. The magnitude of the negative D component at Uranium City, however, cannot be explained by the effects of a tilted westward electrojet or the north-south system. A possible source of this negative D deflection is a region of poleward flowing current positioned behind the equatorward system. The latitude profile at this time, D2 in figure 3.21, shows the extensive positive H region which (from the interpolated cross-over point) positions the center of the surge slightly to the north of the east-west station line.

During the two minutes following the appearance of the surge over the station array, there is an overall increase in the magnitude of the perturbations. There is some decrease in the magnitude of the H component at Uranium City, however, the basic form of the profile remains unchanged. At 0658:30 (longitude profile D3 of figure 3.21) the point of cross-over from positive D to negative D begins to shift westward. This motion, however, ceases shortly afterward at 0659 (profile D4, figure 3.21). At this point the magnetograms show that a peak similar to the initial surge-related perturbation has begun to develop. It is most clearly defined in the H component at Fort Smith, but is also apparent in the D component. At Hay River and Fort





Providence there is a second positive D inflection while Fort Smith and Uranium City both detect an increased negative D perturbation. As profile D5 in figure 3.22 shows, this second perturbation grows in magnitude, while remaining otherwise stable, until 0701. In the following three minutes the positive D region is seen to move smoothly westward (see profile D6, figure 3.22). The latitude profile at this time (D6 of figure 3.21) shows a large region of negative D, particularly in the northern portion. This indicates that the head of the surge is now west of the line. The large negative H and Z suggest an intensified portion of the westward electrojet centered well to the north of the line. The H/Z ratio at Cambridge Bay is .4 indicating that the center of the westward electrojet is some 6 or 7 degrees to the south at  $71^{\circ}$  N latitude. By 0704 (D7 in figure 3.22) we are left entirely with negative D. The velocity of the motion can be determined from the change in the position of the D cross-over point over time. The value obtained is  $1.2 \pm .1 \text{ km sec}^{-1}$ .

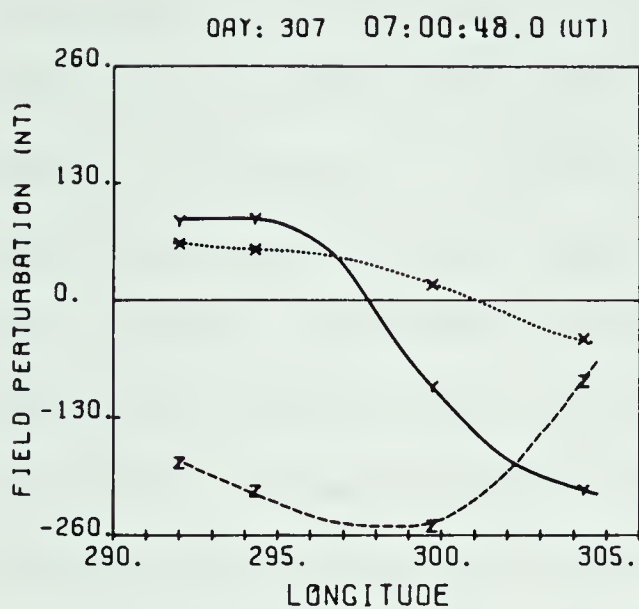
If we assume that this observed magnetic behaviour is due to a surge travelling westward and tilted at the angle of the westward electrojet then according to equation 3.1 the surge velocity is  $1.1 \text{ km sec}^{-1}$ . However, without supporting evidence, for example all-sky camera photographs, such an interpretation must be carefully examined.

In theory, if the current system magnitude were to change while the spatial location remains the same, the

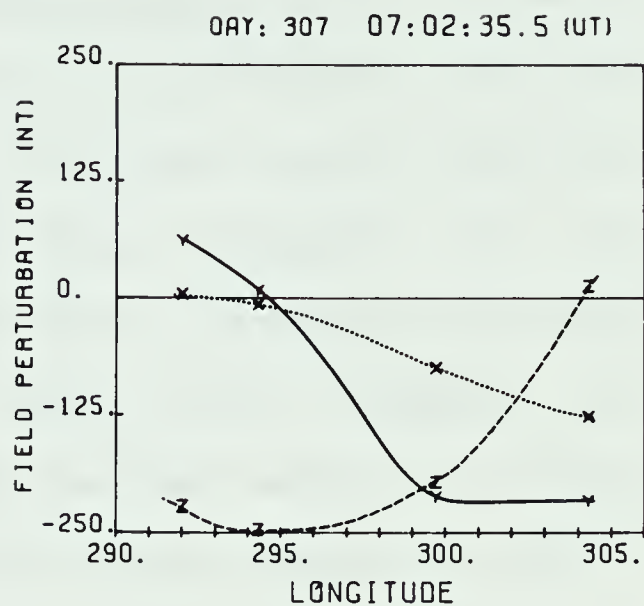




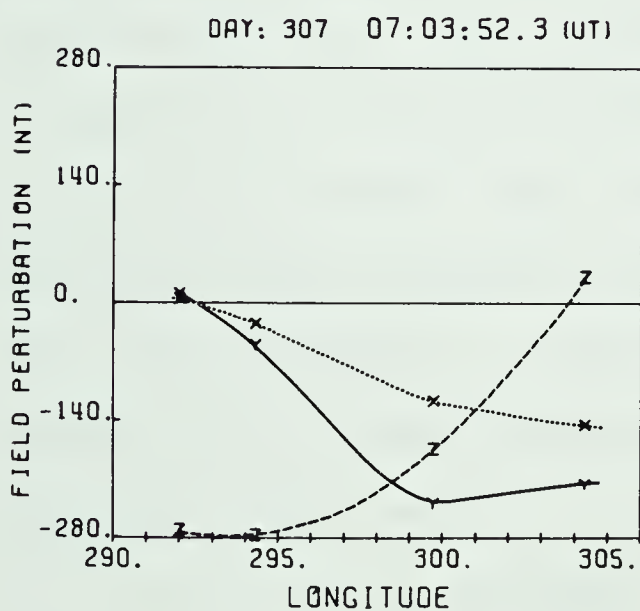
-D5-



-D6-



-D7-



-E-

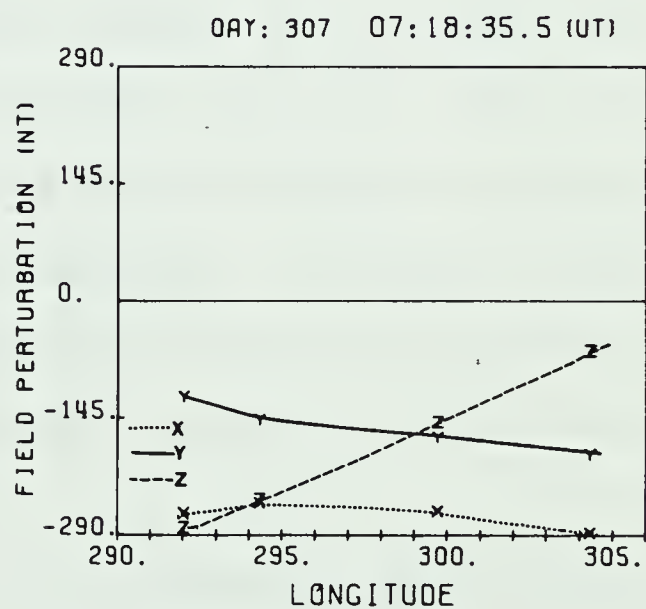


Figure 3.22  
 Longitude profiles at indicated times for Day 307, 1976. Profiles are referred to in text by the indicated label. Note that X, Y, and Z refer to magnetic components H, D, and Z.



magnitude of the perturbation would alter while the form of the profile would remain unchanged. In particular, the zero-point (the cross-over) would remain fixed. However, when one system decays, a different, previously less important (perhaps non-existent) system may become dominant. If this new system produces a magnetic effect comparable with the decaying system then such a decay could produce the signature of motion. For example, in this case if the surge form is not moving but is, instead, merely decaying then a new system must have developed which is capable of generating profile D7 of figure 3.22. The only other system which seems relevant is the intensified westward electrojet which has developed to the north of the station line. If this electrojet has a tilt which places Uranium City near its central latitude and Fort Providence to the south of central latitude, then the Z component behaviour would be observed. The behaviour of the D component, however, could only be produced in the south-eastern portion of such an electrojet. It would seem unusual that such a development could have occurred.

It is also possible that the changes in the profiles could be caused by a change in the boundaries of the surge system. Again, in theory, any such changes would be reflected in the shape of the profile. If the current system became wider, for example, then the region of positive D in the profile would become broader and the cross-over points would occur further from the peak. In the case under



consideration, the profile shows the eastern side of the surge. An expanding surge would cause the D cross-over on this side to move eastward and not westward. A decaying surge could produce the westward shift, however, the magnitude of the perturbations is increasing and this is not suggestive of a decaying form.

Finally, the surge which forms at the leading edge of an expanding westward electrojet (as does the one under consideration) is known to travel westward with its form remaining quite stable. Therefore in this case, we feel that the westward movement of the profile form can be interpreted as westward movement of the surge form. Nevertheless, the possibility of complications because of a combination of temporal and spatial effects must always be considered.

The riometer behaviour during this event is shown in figure 3.17. Significant absorption is seen to occur along the east-west line during period A. The analysis has indicated that a westward current system existed near the line at this time. This absorption reflects enhanced particle precipitation associated with this current system and suggests that a brightening of the auroral arcs may be occurring. During period B only Fort Smith detects any significant absorption. The analysis has indicated that there was a surge form near Fort Smith at this time. The absorption, therefore, reflects the localized particle precipitation associated with this surge. Finally, during periods C, D and E there is no strong absorption detected.





This is because the activity is centered several degrees to the north of these stations and beyond the range of the riometer.

#### 3.4.3 Following the Passage of the Surge

Following the passage of the surge, the substorm continues to develop. A longitude profile taken at 0725 (E in figure 3.22) and a latitude profile (E in figure 3.21) suggest the existence of a dominating westward electrojet. The longitude profile shows the negative H characteristic of a westward electrojet. The negative trends in the D and Z component indicate that the electrojet is to the north of the station line and tilted north-westerly with respect to it. We recall that the weaker electrojet which was seen prior to onset was also tilted. With an H/Z ratio at Cambridge Bay equal to .4 we can estimate the mid-point of the electrojet to be at  $71^{\circ}$  N and  $300^{\circ}$  E.

Prior to the onset, an estimate of the tilt was  $15^{\circ} \pm 5^{\circ}$ . Now as we enter the recovery phase (profile E), we can estimate the tilt to be  $20^{\circ} \pm 5^{\circ}$ , so that we can see that the orientation has remained reasonably constant throughout the course of this substorm event.

#### 3.4.4 Summary for Day 307, 1976

We can now list the more important features of this event.



1.) Activity was seen to precede the onset of the major substorm perturbation. Stations east and west of the Alberta sector do not detect this activity which seems to be localized to the Alberta sector. The activity appears to represent a weak westward current system which is restricted to the Alberta sector.

2.) Within the activity prior to onset there are a series of magnetic perturbations. These are seen to develop in highly localized regions. There is no indication of movement from these locations and the effects decay within about 5 minutes. While these initial events do not propagate the longitude profiles are suggestive of surge-related current systems (see below).

3.) Magnetic deflections, related to an intruding westward electrojet, are seen prior to the onset of the surge. The westward travelling surge is not seen to propagate into the sector. Instead it appears to develop within the sector at a point north and west of the station line.

An intensification of the surge signature occurs shortly after onset. In terms of the longitude profile, the surge displays the following signature:

a) a positive D region near the head of the surge followed by a negative D region. The negative D region suggests a region of poleward flowing current behind the surge front.

b) A positive to negative Z transition. The peak of the negative Z region corresponds with the cross-over point in



the D component.

The head of the current system associated with the surge travels with a speed of  $1.1 \text{ km sec.}^{-1}$ . This is indicated by the westward motion of the associated signature of the longitude profile.

4.) The westward electrojet, which is dominant after the surge has passed, is centered much further north than the weaker electrojet detected prior to the substorm. Both are, however, apparently tilted at approximately the same angle with respect to the east-west line.

### 3.5 Event Analysis ... Day 223 1977

#### 3.5.1 Introduction

At 0325 on Day 223 (August 11) 1977, substorm activity was detected in the Alberta sector. Figure 3.23, 3.24 and 3.25 show the behaviour of the H', D', and Z components along a line from east to west. Figures 3.26, 3.27 and 3.28 show this behaviour along a line from north to south. Figure 3.29 shows the behaviour of the available riometer signals.

This event has some distinctive characteristics. Firstly, the magnitude of both the substorm electrojet (peak negative H) and the surge-related D perturbation are key features. The surge related effects (from 0328 to 0333) seem quite easily distinguishable from the effects due to the westward electrojet. Secondly, the time of onset is rather unusual, occurring about 4 hours prior to local midnight.





# H' COMPONENT: DAY 223, 1977

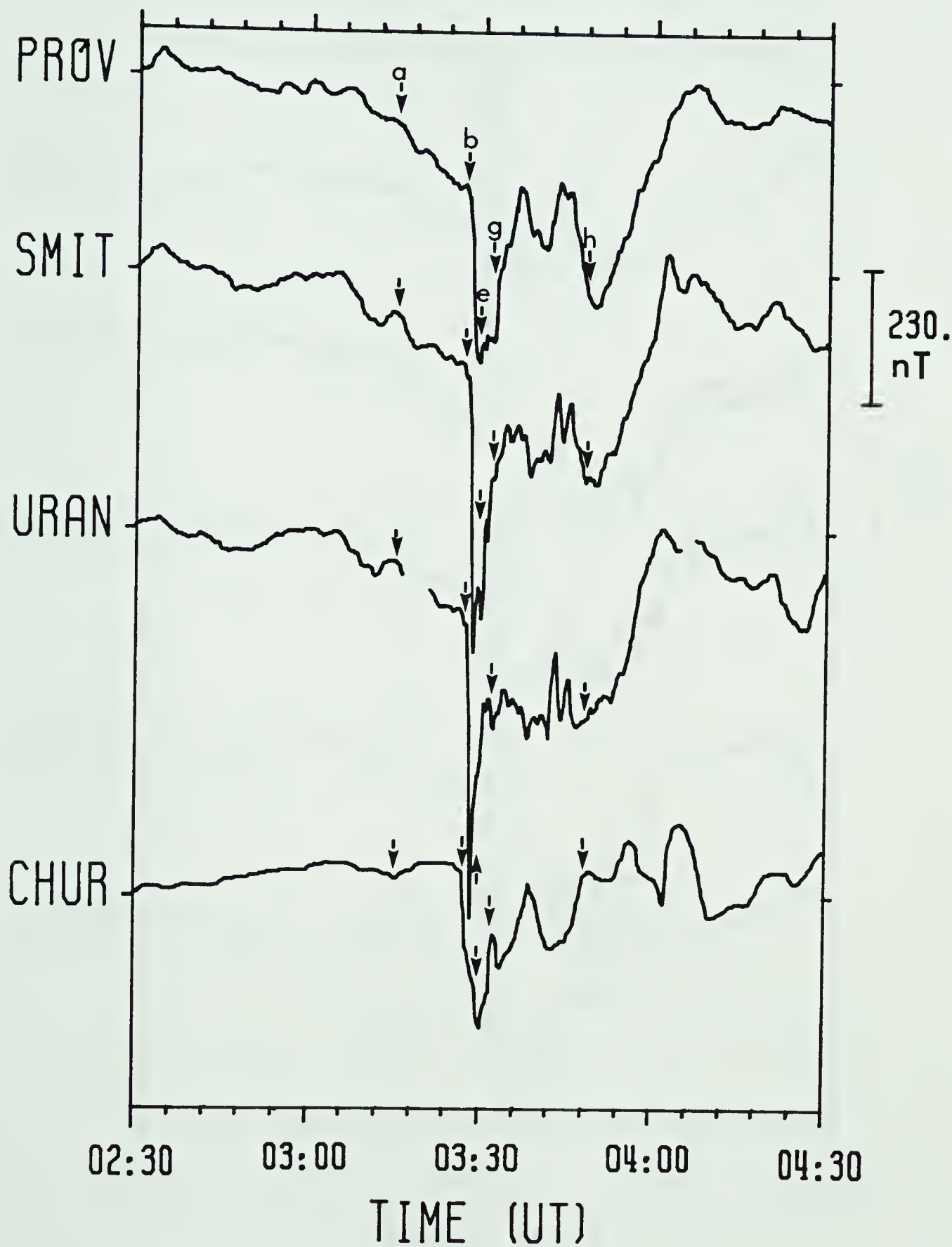


Figure 3.23

Stacked magnetograms along east-west station chain: H' component for Day 223, 1977. Regions of interest referred to in text are indicated.





## D' COMPONENT: DAY 223, 1977

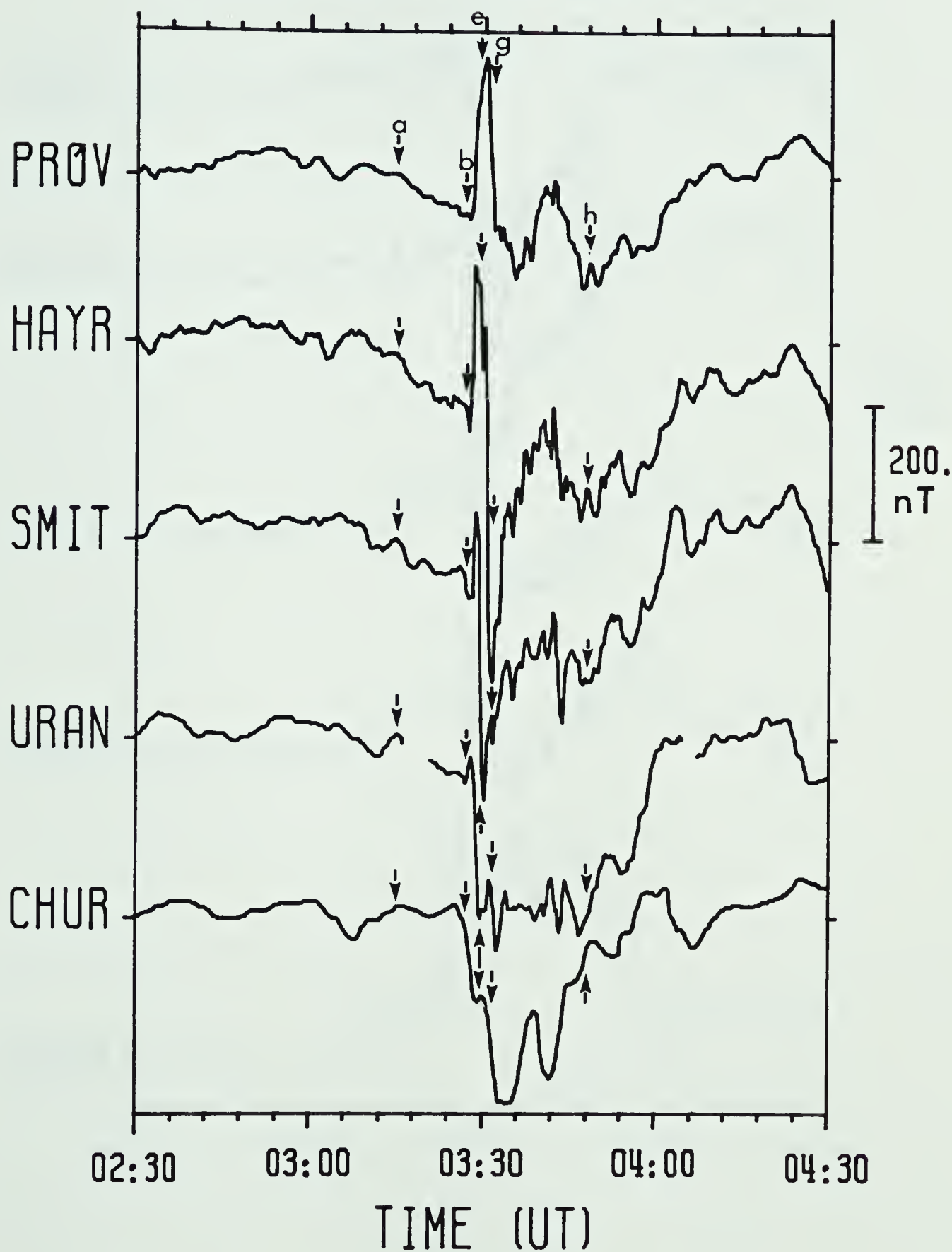


Figure 3.24

Stacked magnetograms along east-west station chain: D' component for Day 223, 1977. Regions of interest referred to in text are indicated.



## Z COMPONENT: DAY 223, 1977

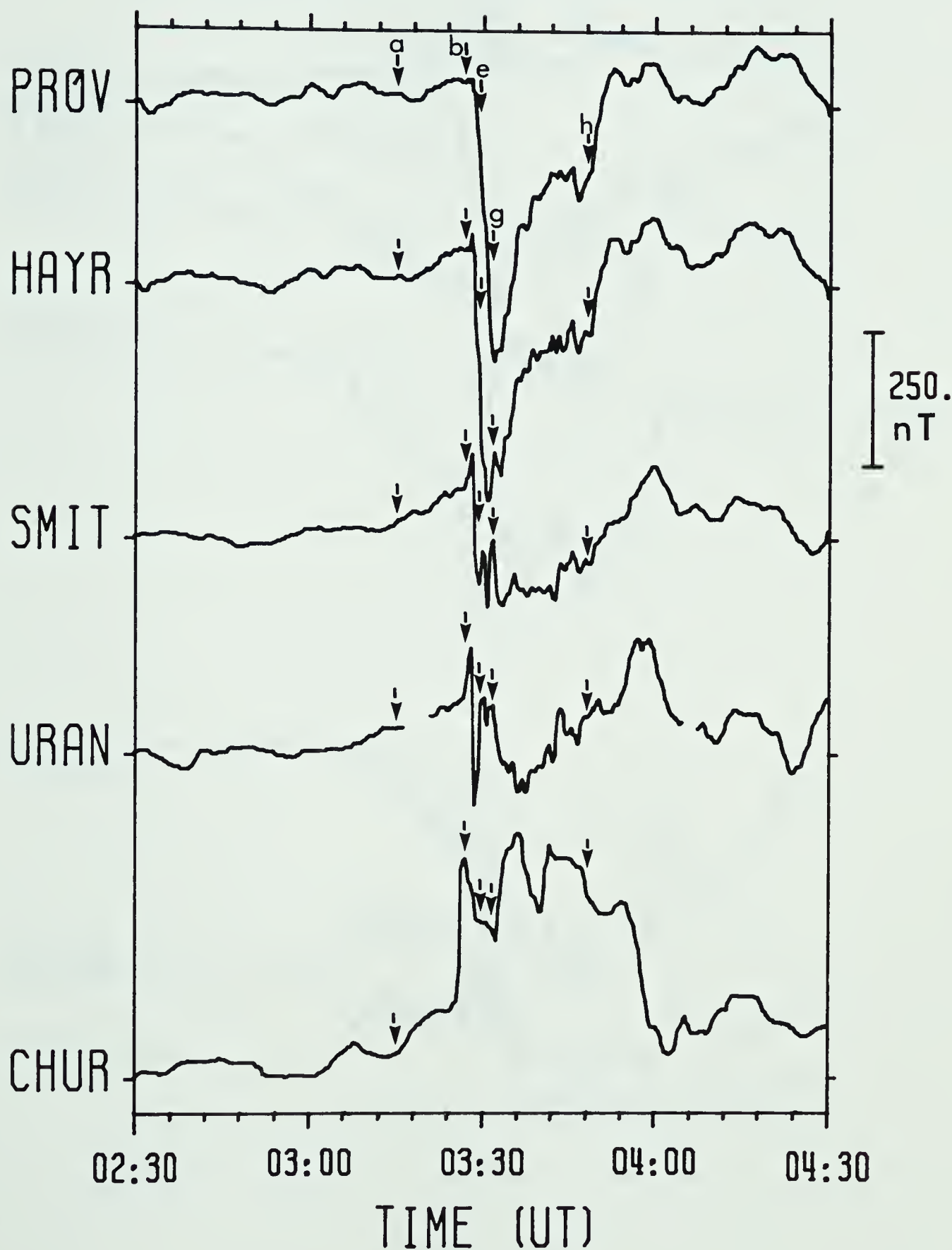


Figure 3.25

Stacked magnetograms along east-west station chain: Z component for Day 223, 1977. Regions of interest referred to in text are indicated.



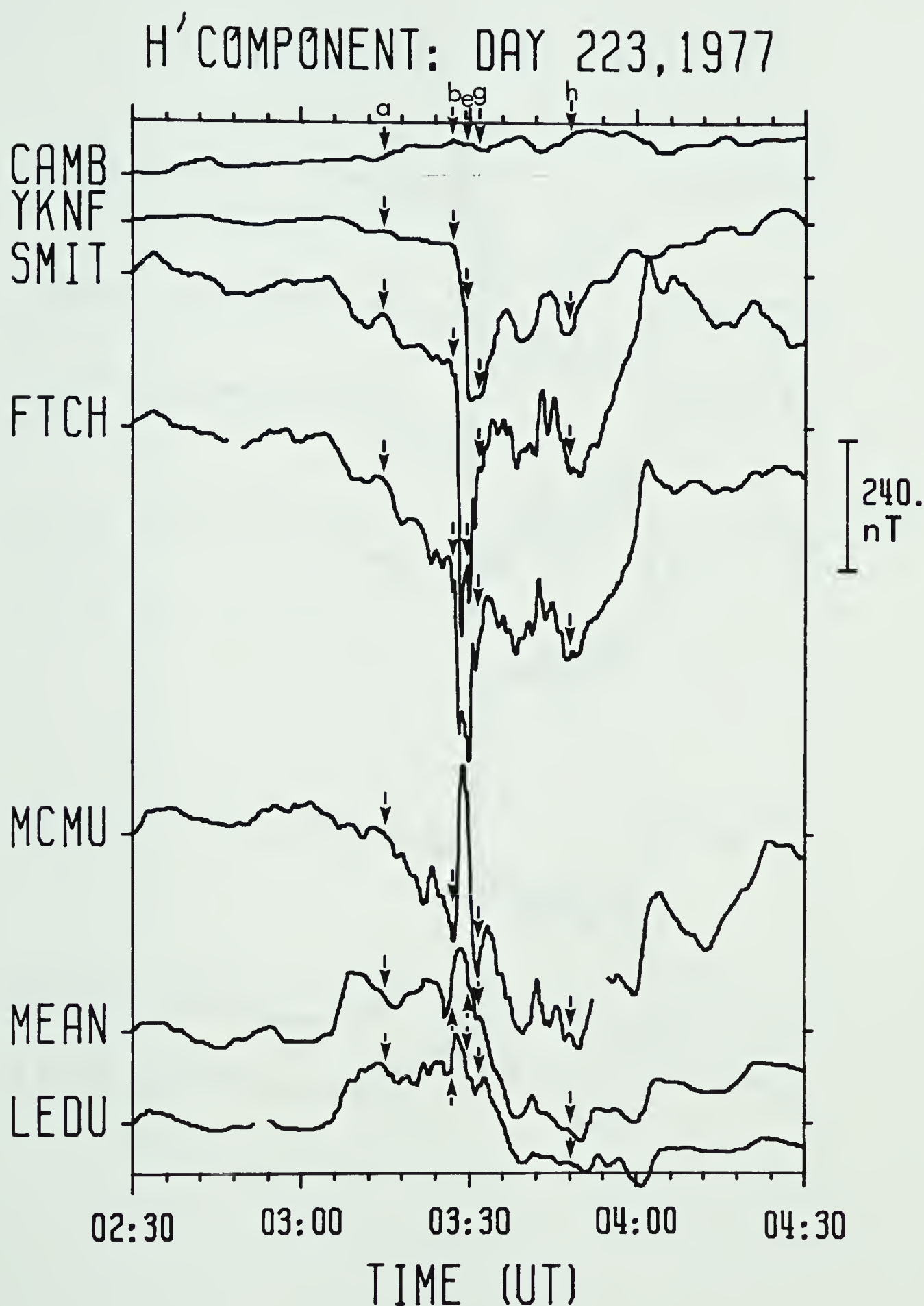


Figure 3.26  
Stacked magnetograms along south-north station chain: H' component for Day 223, 1977. Regions of interest referred to in text are indicated.





## D' COMPONENT: DAY 223, 1977

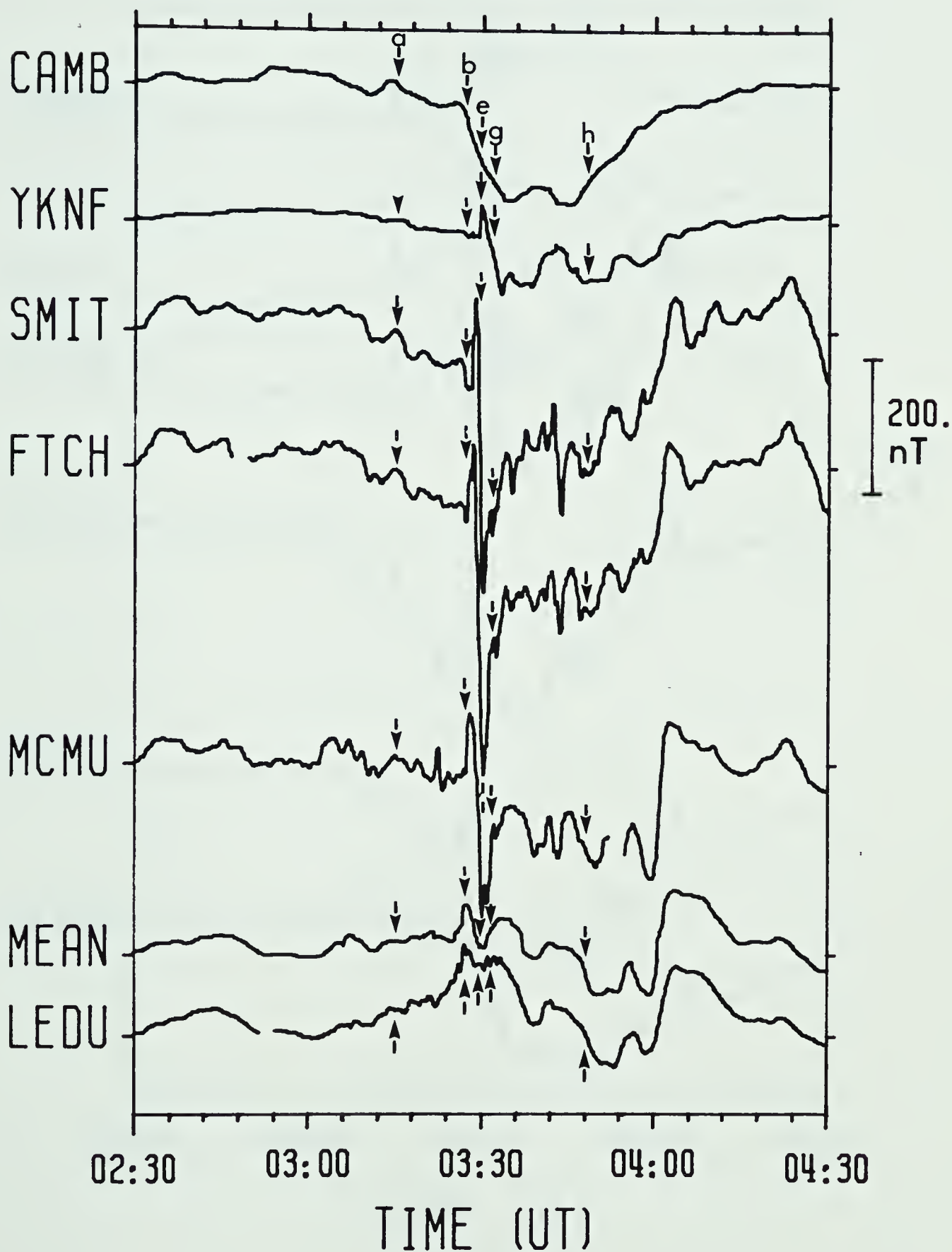


Figure 3.27

Stacked magnetograms along south-north station chain: D' component for Day 223, 1977. Regions of interest referred to in text are indicated.



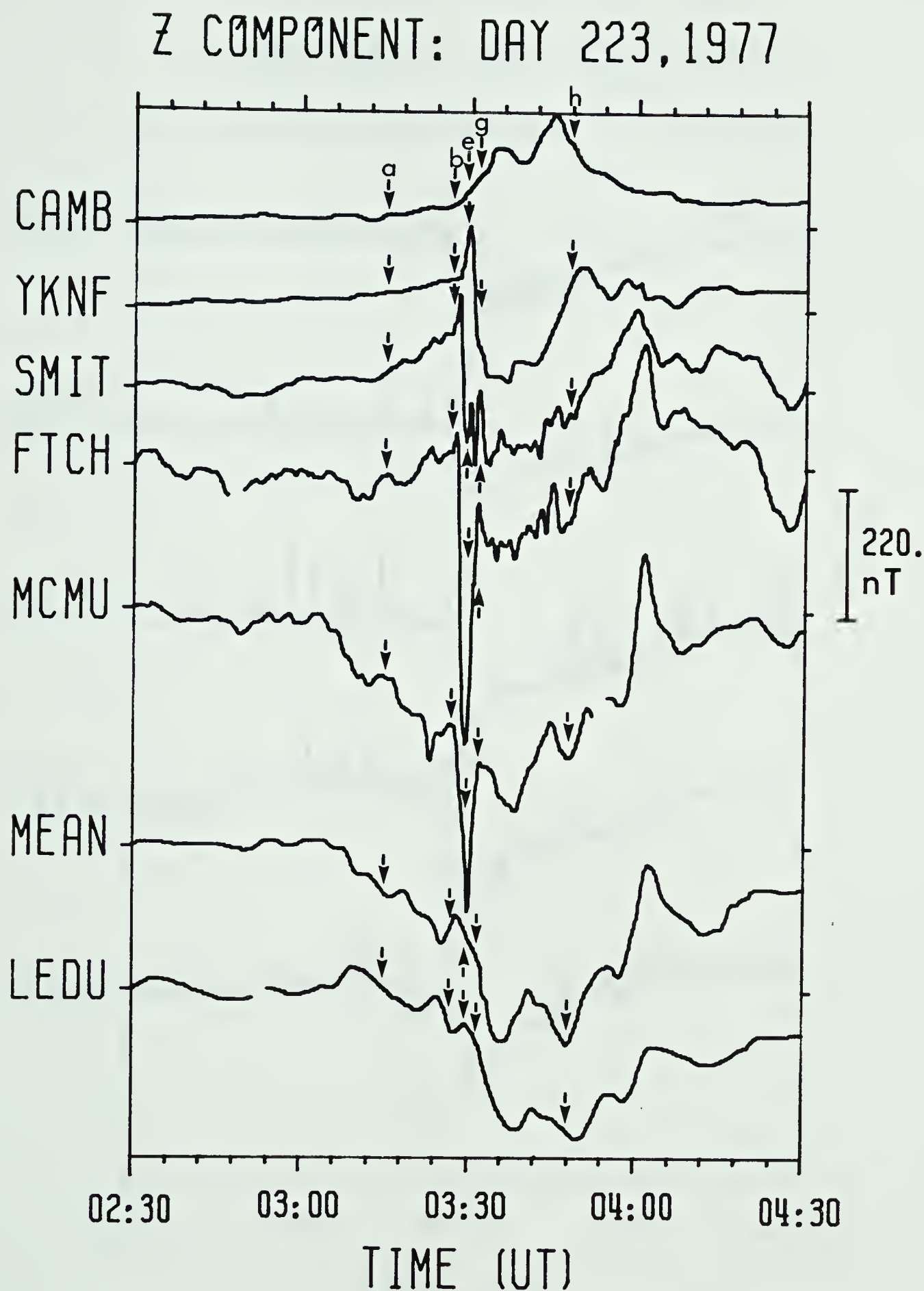


Figure 3.28

Stacked magnetograms along south-north station chain: Z component for Day 223, 1977. Regions of interest referred to in text are indicated.



# RIOMETER : DAY 223, 1977

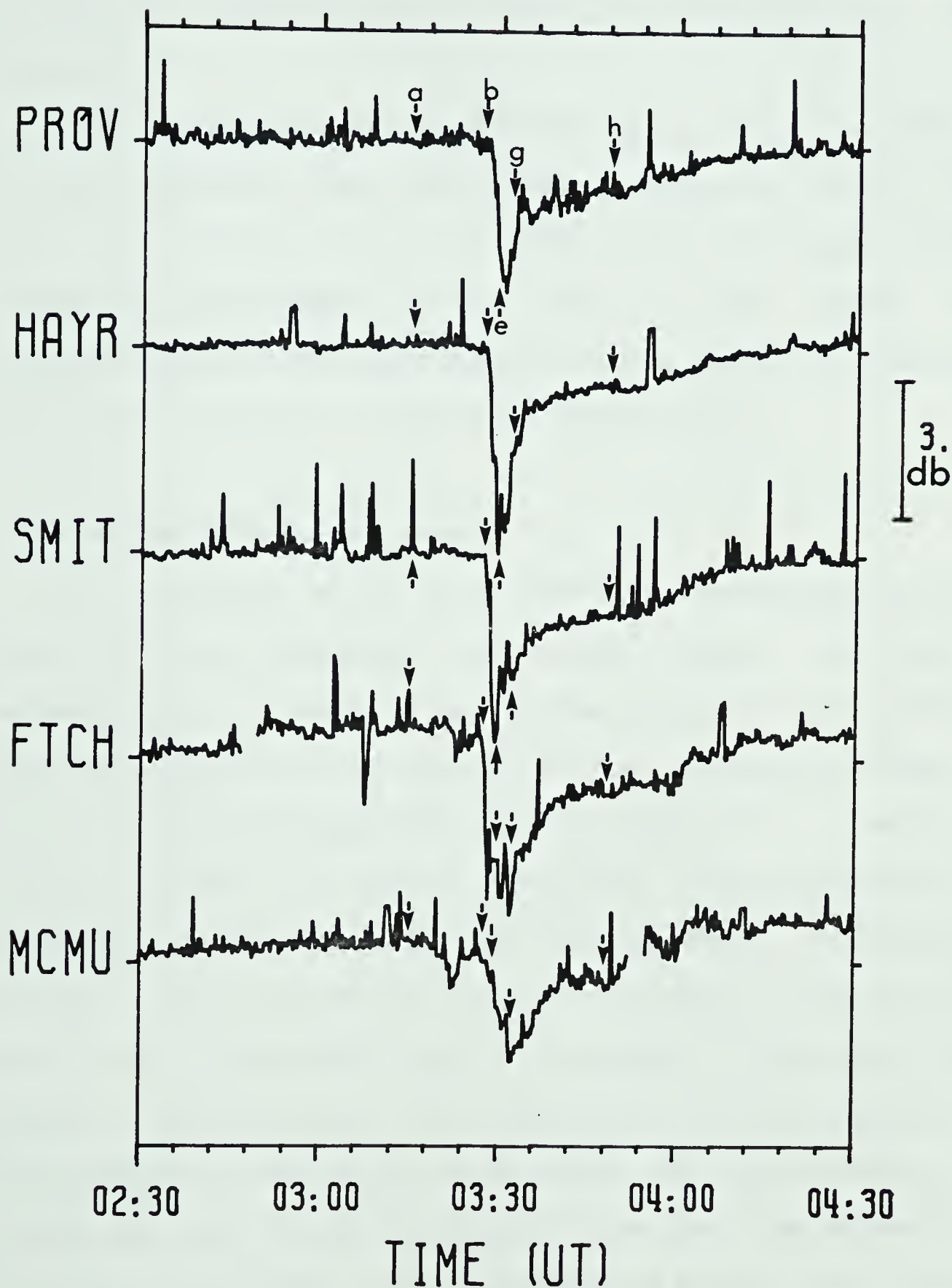


Figure 3.29  
 Stacked riometer signals at available stations  
 for Day 223, 1977. Regions of interest referred  
 to in text are indicated .





Finally, the substorm recovery phase (starting at about 0400) seems quite sudden and short-lived. This is particularly true at the more southerly stations (e.g. Fort McMurray).

The three-hour averaged value of  $K_p$ , prior to 0300, is 3+. This indicates that the global activity is fairly high prior to onset. We can see that there is some activity present in the Alberta sector prior to the onset. This activity is also seen at stations to the east. It would seem to set the stage for the further developments.

### 3.5.2 Activity Prior to Onset

In figure 3.30, the magnetic behaviour at Fort Churchill and Whiteshell is shown. These stations are respectively in northern and southern regions of the sector about one time zone to the east of the Alberta stations. The only activity at Churchill prior to onset is a weak but positive trend in the Z component. This indicates that Churchill is far north of the source region. Whiteshell, however, shows a distinct onset of activity at 0312 in both the  $H'$  and Z components. The  $D'$  component is somewhat more obscure. Nevertheless, the negative  $H'$  and negative Z perturbations yield an  $H'$  to Z ratio of approximately 1, indicating that Whiteshell is near the equatorward border of a westward electrojet. The magnitude of the  $H'$  bay is of the order of 200 nT, which is quite sizeable. Stations further east, Great Whale River and Ottawa, (not shown) detect very





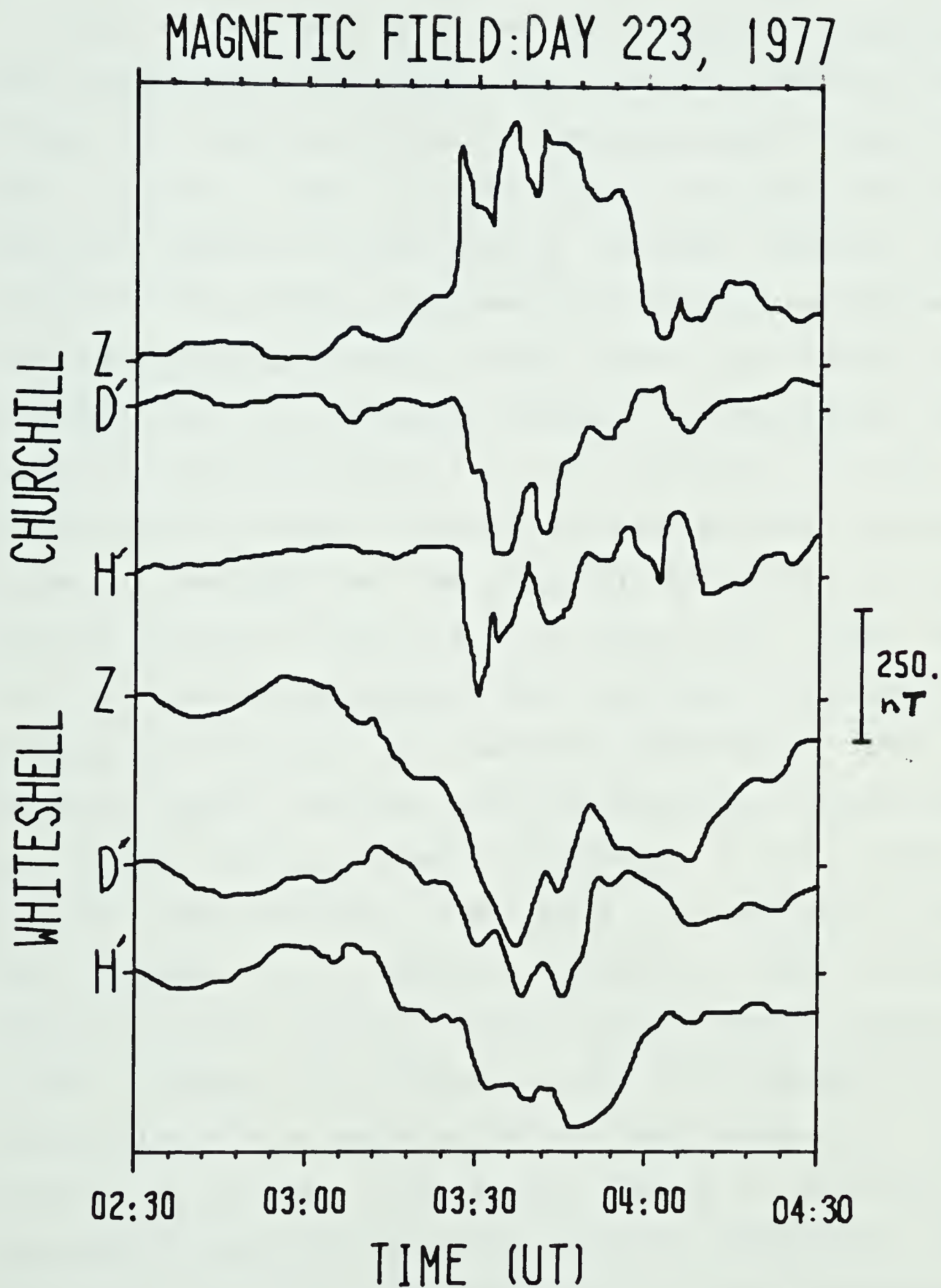


Figure 3.30  
Magnetograms from Churchill and Whiteshell for  
Day 223, 1977.



erratic behaviour signifying extensive substorm activity.

From a baseline taken at 0300, during a relatively quiet period, both longitude and latitude profiles were studied. The profiles at 0315 are representative of the pre-onset activity. The longitude profile (A in figure 3.31) displays a negative H indicative of westward current. The transition in Z from being negative at Fort Providence and Hay River to being positive at Fort Smith and Uranium is indicative of an electrojet tilted to the north-west. The relatively uniform negative D in the profile is also a characteristic of such a tilted electrojet and the D/H ratio yields an estimate of the tilt angle to be  $25^\circ \pm 5^\circ$ . The latitude profile at this time (A in figure 3.32) shows the north to south variations. This profile is typical of antiparallel eastward and westward electrojets. The Z component profile indicates, from the transition point, that the center of the westward electrojet is at  $\sim 66^\circ$  N latitude. The Z behaviour to the south is consistent with the existence of an eastward electrojet which is also indicated by the positive H region in the southern portion of the profile. The Z transition at  $61^\circ$  N latitude marks the location of the center of the eastward electrojet. The station at Newport (not shown) detects a positive H perturbation associated with the eastward electrojet. The H/Z ratio here is  $-.23$  indicating that the equatorward border of this jet is  $3^\circ$  north near  $58^\circ$  N latitude. Also, using magnetograms (not shown) from College and Sitka (in



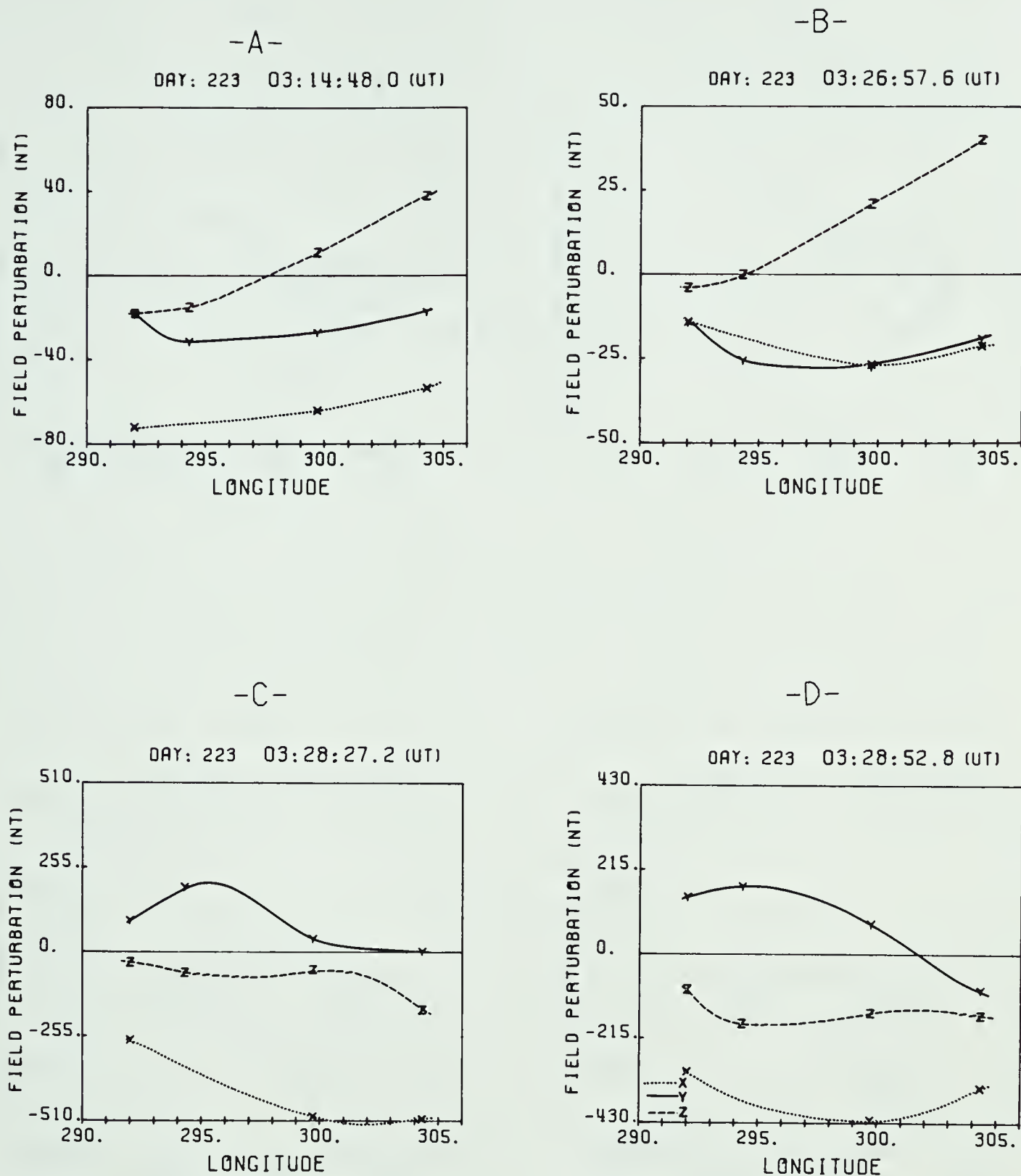
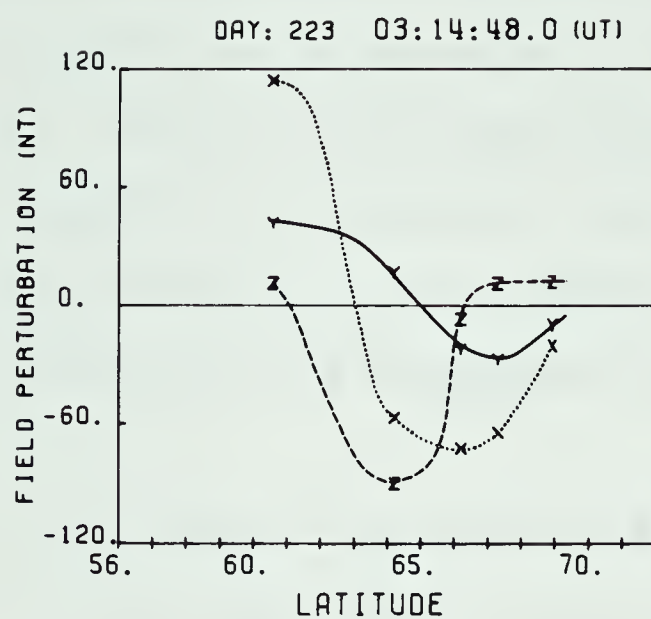


Figure 3.31  
 Longitude profiles at indicated times for Day 223, 1977. Profiles are referred to in text by the indicated label. Note that X, Y, and Z refer to magnetic components H, D, and Z.

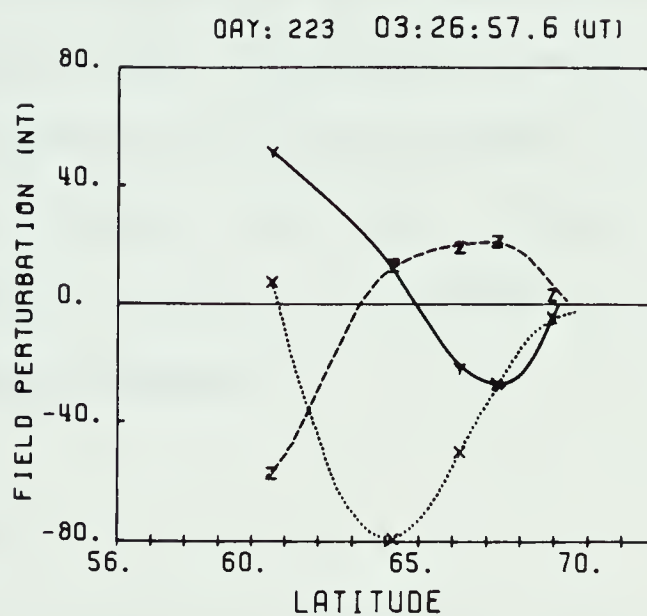




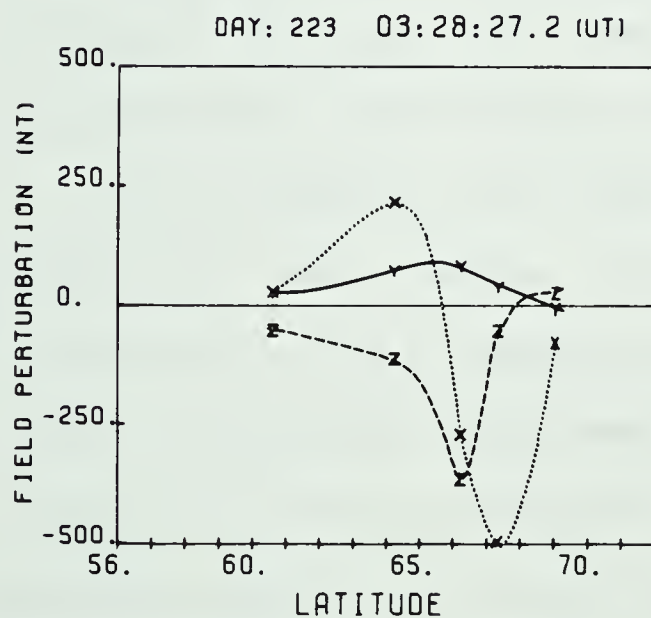
-A-



-B-



-C-



-D-

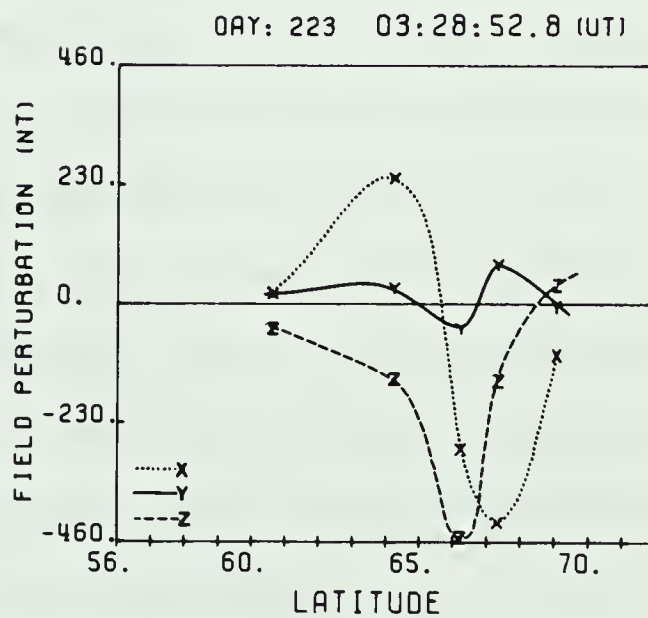


Figure 3.32

Latitude profiles at indicated times for Day 223, 1977. Profiles are referred to in text by the indicated label. Note that X, Y, and Z refer to magnetic components H, D, and Z.



Alaska) the location of this eastward electrojet can be more accurately located. The resultant picture of the pre-onset electrojets is given in A of figure 3.35. The Alberta sector is seen to lie at the region of overlap of the eastward and westward electrojets. This is known as the Harang Discontinuity (see Heppner, 1972) and is a steady-state feature of the ionospheric current systems.

### 3.5.3 Surge Onset and Development

We have stated earlier that a surge is generally marked by a sharp, short-lived magnetic perturbation. On Day 223, 1977 the surge activity is very distinct. At 0327:30 each component at every station shows a dramatic change. Until 0333 surge-related effects clearly dominate. Although a westward electrojet is also intensifying during this time, the profiles will be interpreted in terms of a surge system.

The baseline for the surge analysis is taken at 0325. This time was chosen since at this time the magnetic activity at most stations has reached a relatively constant level. If we make the assumption that the current systems active at this time remain constant, then the differential profiles will display any additional activity.

Prior to the major surge effects seen at 0328 there is an indication of weak but consistent activity (see figures 3.23 - 3.28). In particular, the positive D spike at Fort Smith is preceded by a weak negative D perturbation. The question we must address is whether or not this initial



activity is surge-related. The latitude profile at 0327 (profile B in figure 3.32) indicates a weak but very distinct westward electrojet centered at  $64^{\circ}$  N latitude. Both the magnitude and asymmetry of the D component are very typical of those found near the westward edge of such an electrojet. The Z component displays an asymmetry which is atypical of a simple westward electrojet. An eastward electrojet to the south is likely to be responsible for this. The longitude profile at this time (profile B in figure 3.31) supports the existence of a westward electrojet. The Z component profile shows a distinct linear trend. This could be indicative of a current system tilted to the north-west with the station at Hay River positioned near its center. The H and D component perturbations are approximately equal, implying a tilt of  $45^{\circ}$ . The negative D, however, is not likely to be due simply to the tilt of the current system. We know that the station line is in the northern portion of the westward electrojet, near its westward boundary. This, as we have noted with regards to the latitude profile, is a region of significant negative D. The amount of negative D which will be contributed because of this depends strongly on the position of the westward edge of the electrojet. The nearer the station is to the edge, the greater will be the contribution. The uniformity of the H and D profiles suggests that the contribution might be small, nevertheless, the estimate of a  $45^{\circ}$  tilt is undoubtedly an overestimate. Finally, we again note that





while this electrojet will obviously influence the character of the profiles, the dominating effects for the next few minutes are surge-related.

The major increase in activity begins at 0327:30. Within one minute, at 0328:30, the longitude profile (profile C in figure 3.31) displays the positive D peak which we associate with the head of the surge. During this minute, the D component at Hay River increases positively by about 250 nT, the H component at Fort Smith drops about 450 nT and the Z component at Uranium City drops about 260 nT. As previously mentioned, the surge is characterized by a positive H region to the south and a negative H region to the north. The latitude profile at this time (profile C in figure 3.32) shows this transition at 65° N latitude. The stacked magnetogram of the H component (figure 3.26) shows the transition rather dramatically. The latitude profile also shows a smooth and extensive positive D region. This would suggest that the surge itself is a broad form, with its leading edge near the longitude of the Alberta magnetometer array.

Approximately 30 seconds later, the longitude and latitude profiles at 0329 (panel D in figure 3.31 and panel D in figure 3.32) show some interesting developments. The latitude profile changes little for the H and Z components; however, the D component shows the development of a negative regime. The surge has apparently moved westward leaving the station line in a region of negative D. The longitude





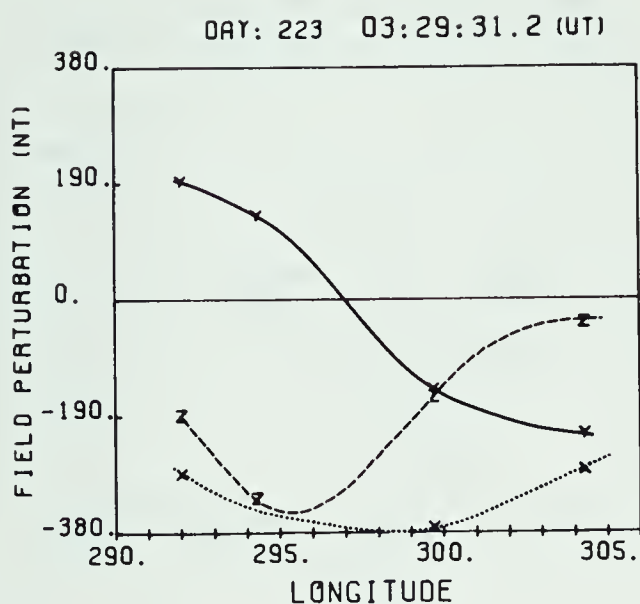
profile also shows this development. The cross-over point in the D component profile is now well defined near  $302^{\circ}$  E. The positive peak in D indicates that the head of the surge is located near  $296^{\circ}$  E longitude, west of the south-north station line. The longitude profile also shows a negative Z component with no well defined peak in Z being apparent at this time.

Both profiles at 0329:31 (E in figure 3.33 and E in figure 3.34) show an increasing negative D region. This suggests further westward motion of the surge. The longitude profile now shows a negative peak in Z. As with the Day 307, 1976 event, this peak is located near the cross-over point in the D component.

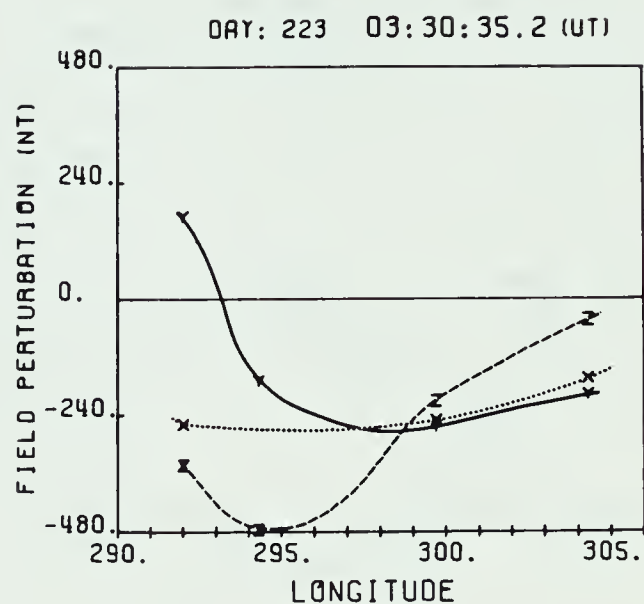
By 0330:35, the latitude profile (F in figure 3.34) shows that the positive to negative H transition has been lost. There is now a negative H region across the entire line. This is expected when the station line is east of the surge and under the influence of a westward electrojet. The general form of the profile is that of a broad westward electrojet with its center near  $69.5^{\circ}$  N ( $4^{\circ}$  north of its position at the onset of the substorm perturbations around 0327). The station at Cambridge Bay detects an H/Z ratio of .83 indicating that the poleward border of the westward electrojet is  $5^{\circ}$  to the south near  $72^{\circ}$  N latitude. The longitude profile at this time (F in figure 3.33) indicates the continued westward motion of the surge through the continued westward movement of the D component cross-over.



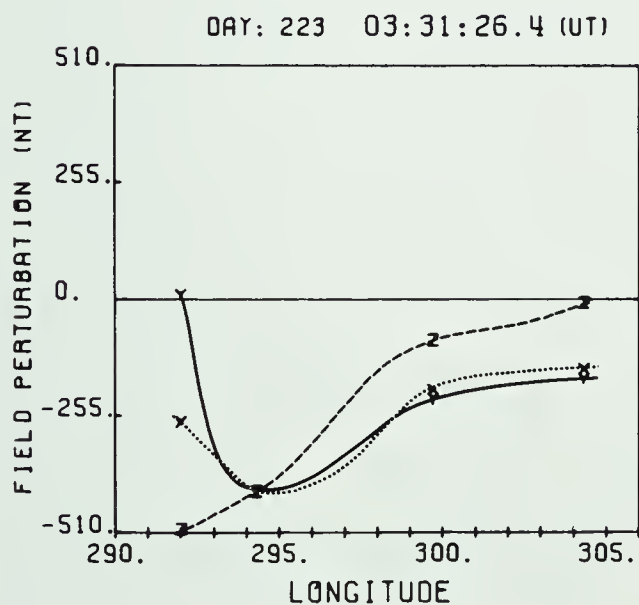
-E-



-F-



-G-



-H-

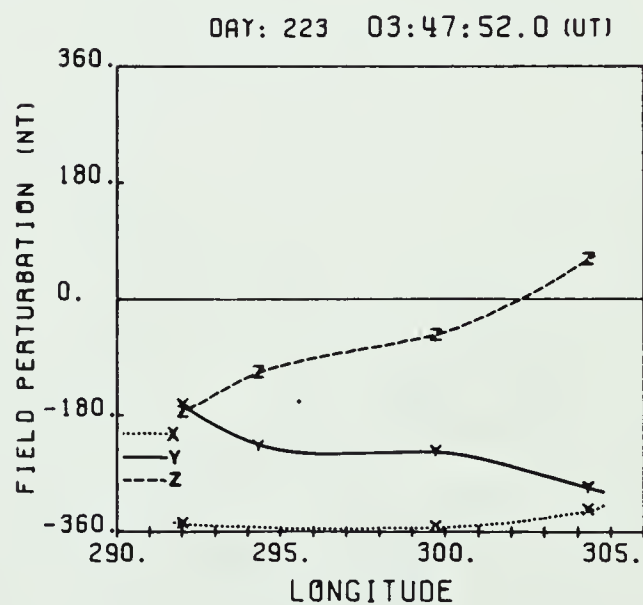
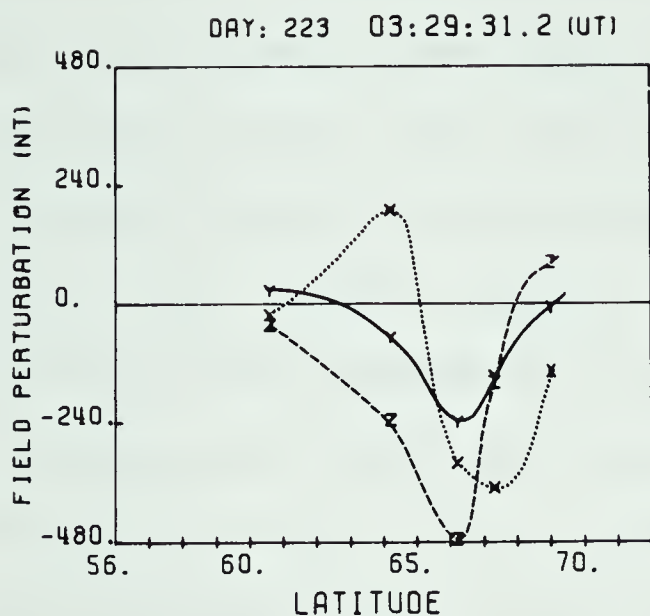


Figure 3.33

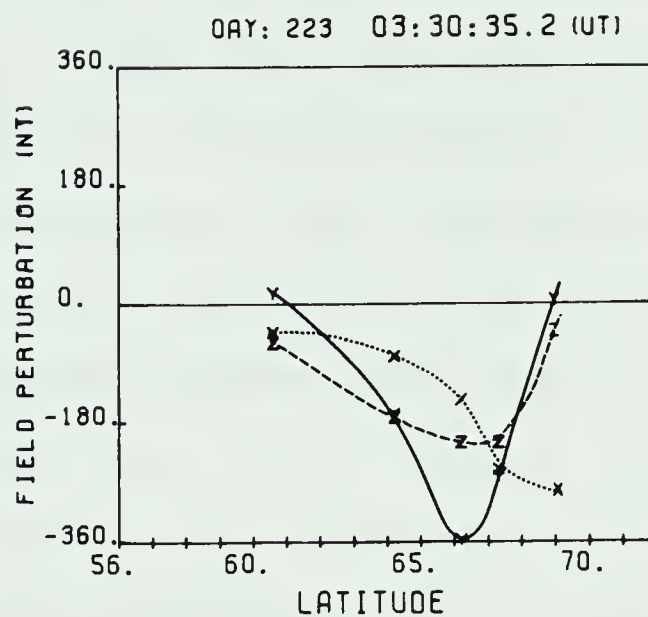
Longitude profiles at indicated times for Day 223, 1977. Profiles are referred to in text by the indicated label. Note that X, Y, and Z refer to magnetic components H, D, and Z.



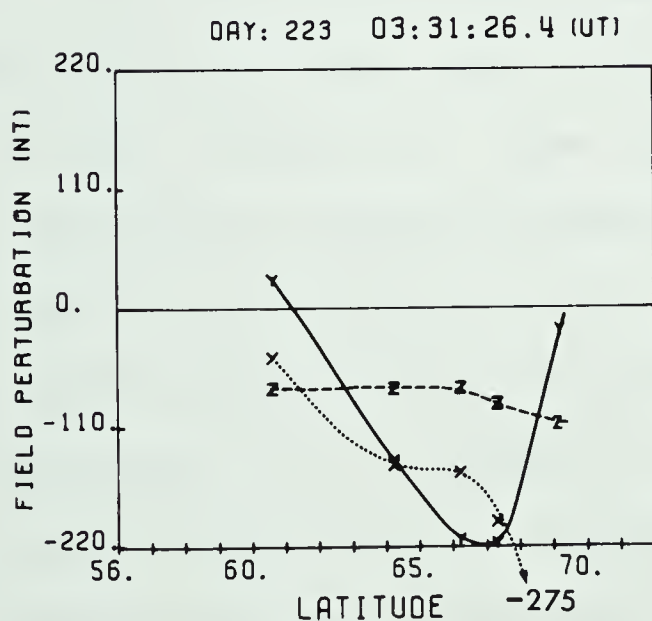
-E-



-F-



-G-



-H-

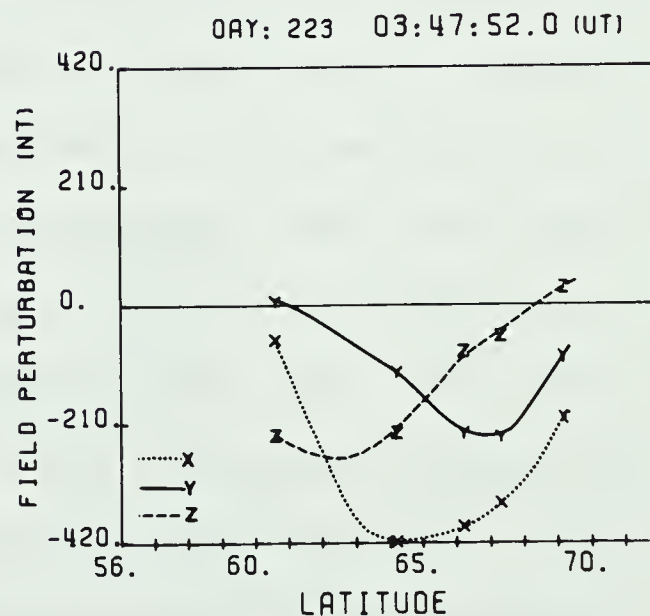


Figure 3.34

Latitude profiles at indicated times for Day 223, 1977. Profiles are referred to in text by the indicated label. Note that X, Y, and Z refer to magnetic components H, D, and Z.





The longitude profile at 0331:30 (G in figure 3.33) indicates further motion of the D component cross-over and, in particular, shows that the Z peak has now shifted westward along with the D component cross-over point. The latitude profile at this time (G in figure 3.33) indicates that the entire system has moved poleward. With the exception of Yellowknife, the magnitude of the perturbations has generally decreased along the line. The station at Cambridge Bay detects an H/Z ratio of .64 indicating that the poleward border of the westward electrojet is  $3^{\circ}$  to the south near  $74^{\circ}$  N latitude. The current systems have moved rapidly westward and poleward during this stage of the substorm development.

As with the event on Day 307, 1976, we must examine the possibility that the above effects have been produced through changes in the dimensions of the surge. If the surge-related current systems were changing, then we would expect the magnitude of the magnetic effect to change also. From the magnetograms, the negative D (seen in the later profiles) is undoubtedly caused by the surge. We can see that its peak magnitude remains relatively constant. This would seem to indicate that the system has remained stable. Again, from the knowledge of the motion and stability of the westward travelling surge we can suggest that it is the motion of the current system which is the source of the motion we see in the magnetic signature. From this, we can estimate the velocity of the surge from the change in



the D cross-over point in time. A calculation of this nature yields a value of  $5.6 \pm .5$  km sec<sup>-1</sup> for the D cross-over point and, using equation 3.1, a surge velocity of 4.8 km sec<sup>-1</sup>. This is a particularly fast speed for a surge but we must note that we are dealing with a particularly large event.

The riometer behaviour during this event is shown in figure 3.29 . The onset of absorption at 0338 is very sudden and intense. It is seen at all stations, indicative of a very broad region of precipitation. The initial period is short-lived but shows by far the most strong cosmic noise absorption. It corresponds directly to the development of the surge in the Alberta sector. There is even some indication that the peak in absorption at Fort Smith occurs prior to the peak at Fort Providence as one would expect from a westward travelling surge. There is also considerable absorption after the surge has passed indicating a continued precipitation of high energy particles.

#### 3.5.4 Following the Passage of the Surge

Over the next few minutes, the profiles (not shown here) remain quite constant and the perturbations become smoother and weaker. By 0348 all surge effects have certainly disappeared. The longitude profile at this point (H in figure 3.33) displays negative, relatively flat H and D components. The Z component profile has a definite linear trend suggesting that the stations are near the mid-region of a westward electrojet tilted to the north-west so that



all stations except Uranium City would be located south of the center of the electrojet. If we assume that the negative  $D$  is produced entirely from this tilt, then the tilt angle can be calculated. The  $D/H$  ratio implies a tilt angle of  $30^\circ \pm 10^\circ$ . We must emphasize that beyond the large measurement error the estimate of the tilt is subject to systematic errors. These errors arise primarily from the station's location within the westward electrojet and are difficult to determine precisely. Interestingly, during this event the electrojet altered its position considerably and yet the estimate of the tilt has remained reasonably constant ( $45^\circ$  when the electrojet was centered to the south and  $30^\circ$  when centered to the north of the line).

Finally an estimate of the width of this electrojet is of some interest. The edge of the electrojet can be estimated from the negative extremum of  $Z$  on the latitude profile to be at  $63^\circ$  N latitude. The center of the electrojet can be estimated from the cross-over point in the  $Z$  component to be at  $68.5^\circ$  N latitude. If we assume a  $30^\circ$  tilt this gives a full width of  $9.5^\circ$ . This is indeed a broad westward electrojet.

An estimate of the location of this westward electrojet is shown in B of figure 3.35. The effects are felt at great distances. For instance, in Honolulu the magnetogram displays a 4 hour growth of the cross-tail current (indicated by the increasingly negative  $H$  component) prior to the onset which it detects at 0325. Figure 3.36 shows



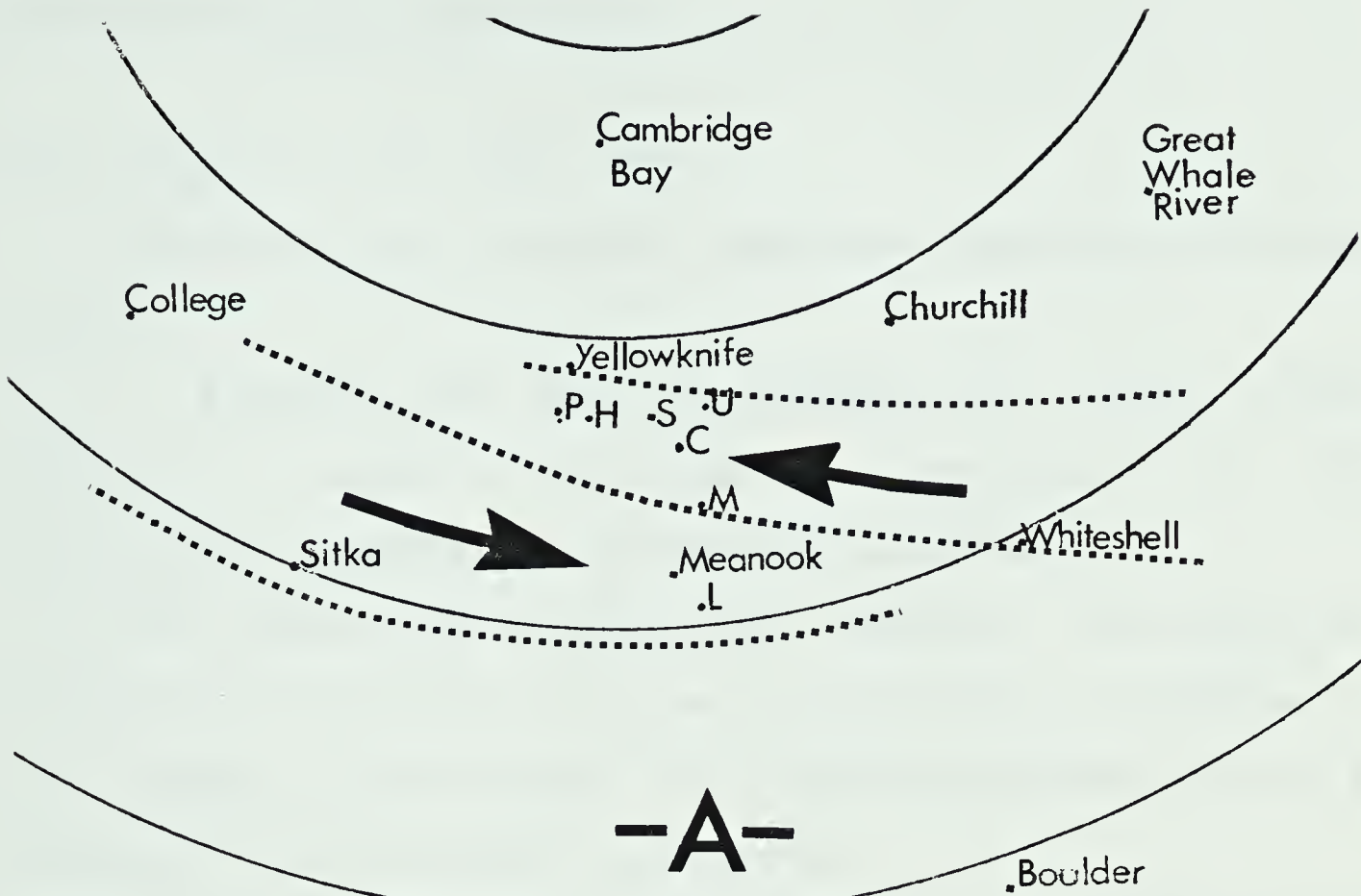




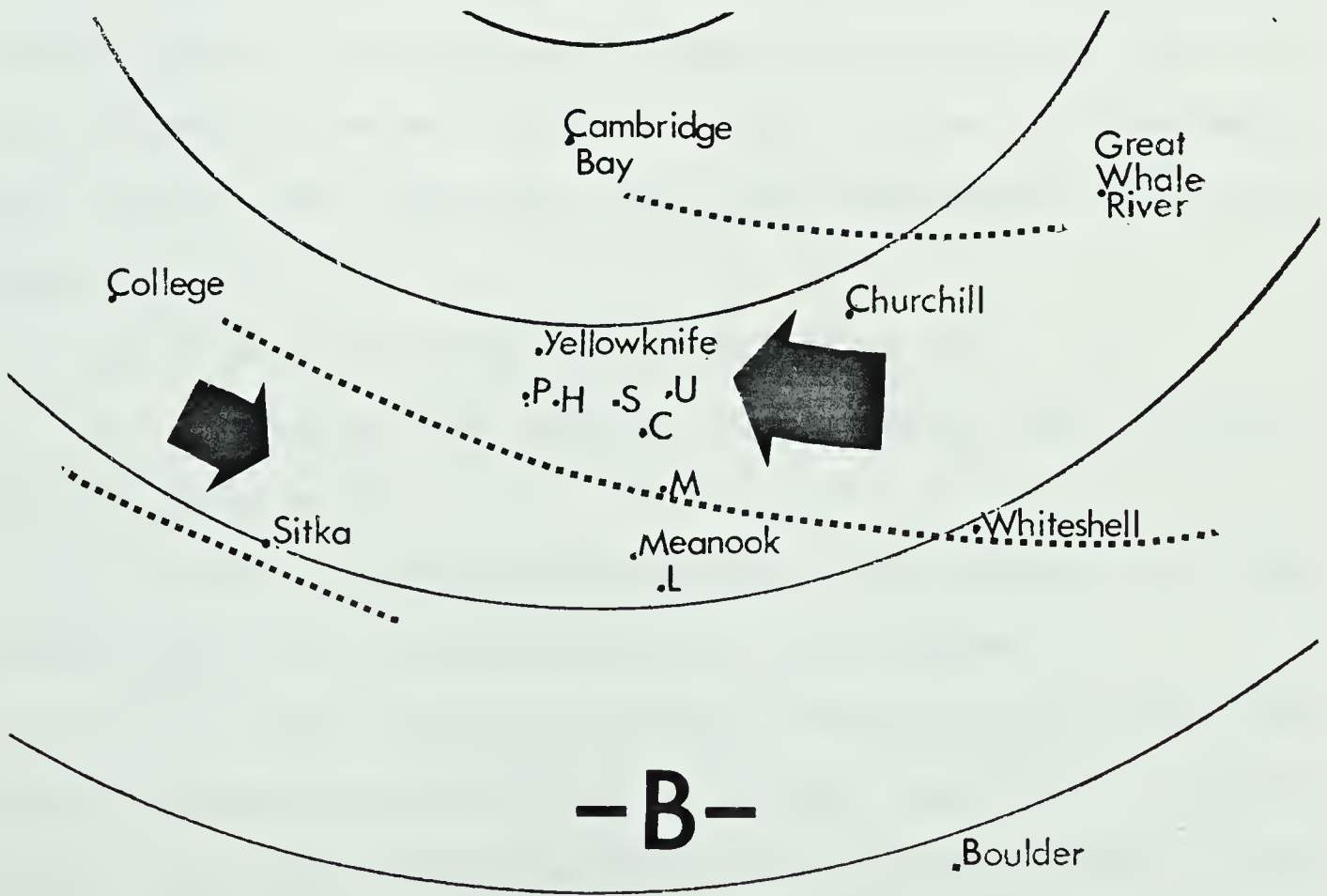


Figure 3.35

Estimated locations of electrojets before ('A')  
and after ('B') onset of event on Day 223, 1977.



-A-



-B-



both the magnetogram for this event and, for comparison, a magnetogram from a quiet day.

### 3.5.5 Summary of Day 223, 1977

We can now list the more important features of this event.

- 1.) Activity is seen to precede the onset of the substorm. It seems to represent an enhancement of the steady-state eastward and westward electrojets.
- 2.) The effect of a developing westward electrojet is detected just prior to the onset of the surge. A negative  $D$  seen prior to the surge at some stations seems to be a response to this westward electrojet.
- 3.) The onset of the surge is observed to develop very rapidly within the Alberta sector. It is centered south of the east-west line but affects a broad region. Nevertheless, the effects are distinct and the signatures are well defined.

The latitude profile is characterized by:

a) A positive  $H$  region to the south and a negative region to the north.

b) A broad negative  $Z$  across the line with its peak located near the central latitude of the surge.

c) A broad positive  $D$  region across the line when the surge is located overhead and a broad negative  $D$  region across the line when the head of the surge is west of the line. These also peak near the central latitude of the



## MAGNETIC FIELD: HONOLULU, 1977

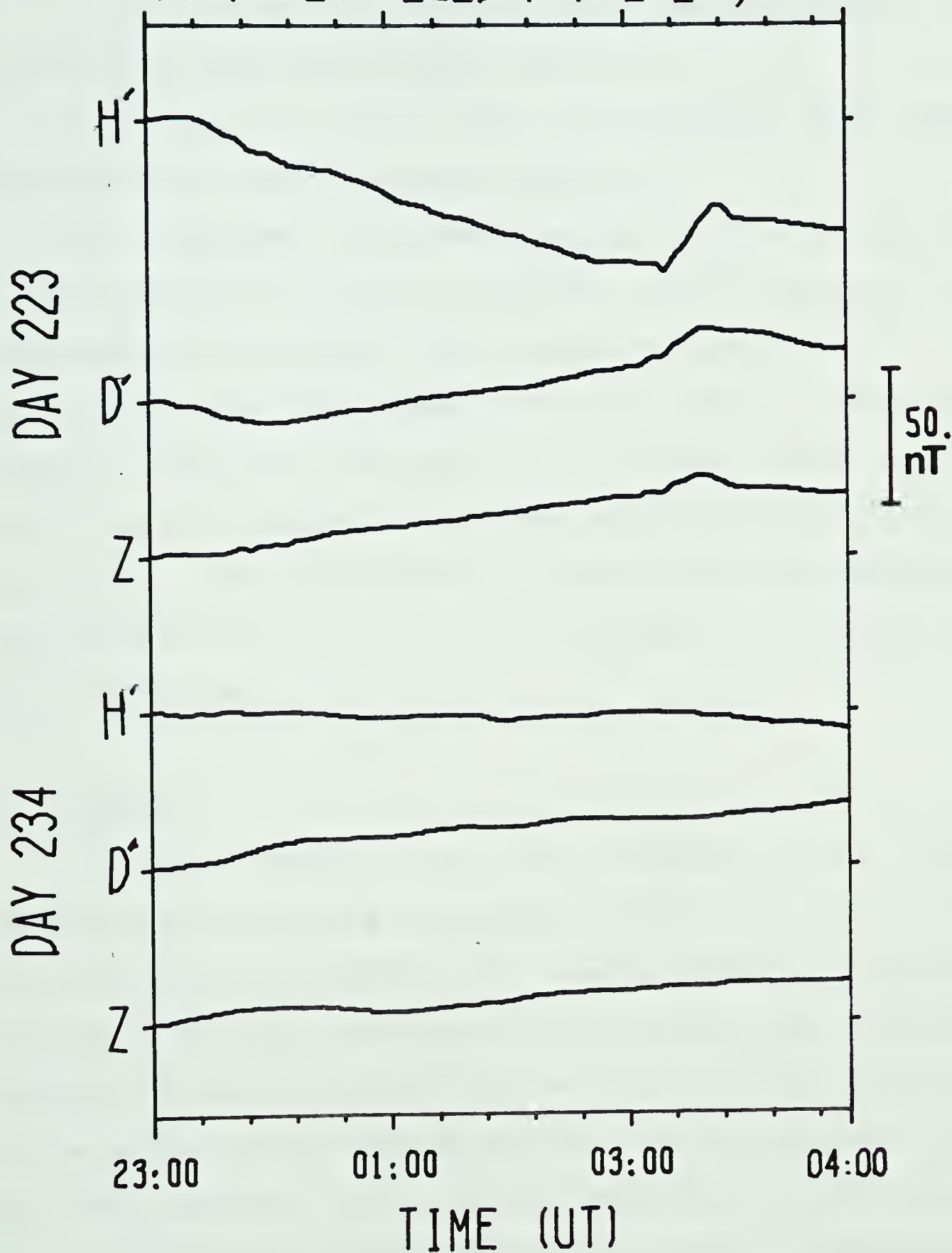


Figure 3.36

Magnetograms from station at Honolulu for event on Day 223, 1977 and also, for comparison, on a quiet day (Day 234, 1977)





surge.

The longitude profile is characterized by:

a) A positive D region located near the head of the surge with a negative D region behind it.

b) A negative Z region with a well defined peak which corresponds to the cross-over point in D.

The signature along the longitude profile is observed to move smoothly but rapidly westward. This suggests that the surge has propagated with a speed of  $4.8 \text{ km sec}^{-1}$ .

4.) Following the passage of the surge, a very broad westward electrojet dominates. It is centered much further north than the initial steady state electrojet seen prior to the onset. The electrojet is particularly broad and there are indications that it is tilted northwest with respect to the station line.

### 3.6 Summary

In this chapter, the surge activity within three substorm events has been analyzed. While each event has distinguishing features, all events gave a reasonably consistent magnetic signature for the surge. The important features of this signature and some aspects of the behaviour of the surge (either seen or implied) can now be summarized. We note, however, that a typical surge may be difficult to define since no two surges are exactly alike. Furthermore, the observed effects from any particular surge will depend dramatically on the observer's position relative to it.



1.) In terms of a longitude profile, the magnetic signature has the following characteristics.

a) A positive D regime with a well defined peak occurs in the westward portions of the surge form. This is generally followed by a region of negative D. This latter region is often altered by the effects of an expanding westward electrojet.

b) A positive Z regime in front of the surge leads into an extensive negative regime beneath the surge. The negative extremum of the Z component corresponds closely to the transition point in the D component.

c) In the westward portion of the surge the H component can be either positive (if it is in the southern portion) or negative (if it is in the northern portion). It generally displays a negative trend due to the influence of the expanding westward electrojet.

In terms of a latitude profile, the magnetic signature has the following features.

a) In the forward portions of the surge the H component undergoes a positive to negative transition as it goes from southern to northern regions of the surge. An extensive negative region occurs behind the surge.

b) The D component displays a broad positive regime in the forward region of the surge. This becomes a broad negative region in the trailing region. Both of these regions have peak values near the central latitude of the surge.



c) There is a broad negative Z regime beneath the surge. This is also seen to peak near the central latitude of the surge.

2.) The motion of the surge is reflected in the motion of transition points in the magnetic signature. In particular, motion of the D transition point on the longitude profiles was used as an indicator of the surge movement.

The surge which corresponded to the leading edge of the westward electrojet was indeed observed to travel westward. The motion, however, was not always smooth. On occasion the surge was seen to travel into the Alberta sector while at other times it developed within the sector and then progressed westward. On occasion, prior to the arrival of the westward electrojet, surge forms were observed to develop and decay without undergoing any significant motion.

3.) The effects of a localized westward current system were often detected prior to the onset of the surge. A north-westerly tilt of this system was observed. In these cases, a negative D perturbation detected prior to the surge was, at least in part, a response to this tilted system. The approaching surge system was also seen to contribute to this effect.

A north-west tilt of the substorm electrojet of 10 - 30 degrees, with respect to lines of constant geomagnetic latitude, does not seem to be uncommon in the evening sector. Moreover, the tilt remains relatively unchanged from



the moments prior to a substorm to the time at which the event begins to decay.





## CHAPTER 4

### MODELLING OF THE SUBSTORM EVENTS

#### 4.1 Introduction

In Chapter 3 the development of the westward travelling surge was presented. This development was described in terms of a proposed model current structure of the surge, as is shown in figures 3.2 and 3.3 .

In this chapter we will show that the model reproduces the major features of the observed longitude and latitude profiles of the magnetic field perturbation. We will compare theoretical (i.e. modelled) profiles with the observed profiles at selected times during each of the three events.

#### 4.2 The Model Current System

The general nature of the model current system was described in chapter 3. The primary feature of the system is a region of equatorward-flowing ionospheric current followed by a region of poleward-flowing current. The primary motivation for the model was empirical. The observation of a strong positive D perturbation has led others (Kisabeth and Rostoker, 1977; Hughes, 1978) to model the surge in terms of a current loop, closed in the ionosphere by a region of equatorward-flowing current. The frequent observation of a strong negative D perturbation following the positive D perturbation suggests the inclusion of a similar current



loop but closed in the ionosphere by a region of poleward-flowing current.

A westward current system, included in the model, reflects an enhanced region of the westward electrojet occurring during the substorm. In cases where the eastward electrojet was seen to intensify an eastward current system was included.

The locations and magnitudes of each current segment of the model were adjusted as required for each event. However, the equatorward-flowing system was always placed directly in front of the poleward-flowing system. Furthermore, these two systems were always of equal dimension and contained the same amount of current. The main reason for this was that the magnitude and duration of the positive and negative D component perturbations were usually seen to be nearly equal.

The westward current system was devised such that the downward field aligned current feeding it was introduced in two stages. Most of the current (~70%) flowed into the ionosphere at the eastern border and the rest flowed ~5° west of this border. Similarly the current was allowed to flow up field lines some 5° in from and at the western border. This was done as a first-step towards a distribution of the current. Note that the current density specified in the model parameters is an averaged value.

In the modelling of each event, all current systems were closed at a height of 100 km. in the ionosphere. Also,



a superconductor was placed at a depth of 200 km. beneath the Earth's surface in each case. As previously mentioned, the superconductor is used to model the effects of currents induced within the Earth. The depth of the superconductor is inversely related to the strength of the induced field and, therefore, to the rate at which the inducing currents change. In the case of the westward travelling surge and other substorm-related behaviour, a superconductor depth of 200-250 km has been found to give reasonable results (Kisabeth, 1972). Basically, the contribution of the induced field to the Earth's magnetic field is such that it adds to the H and D component perturbations and takes away from the Z component perturbations.

#### 4.3 Justification of the Model

The current flow in the ionosphere is understood in terms of the conductivity (i.e. the ratio of Hall-to-Pederson conductivity) and the electric field either observed or proposed to exist there. In particular, because the Hall-to-Pederson conductivity ratio is 3 in the pre-midnight sector, the westward electrojet is seen to be primarily a Hall current driven by a southward-directed electric field (see figure 4.1-a ).

Within the region of the auroral surge there is known to be intense electron precipitation (see chapter 1). Such a localized area of negative charge should result in an inward directed electric field to the east and west of it. If we





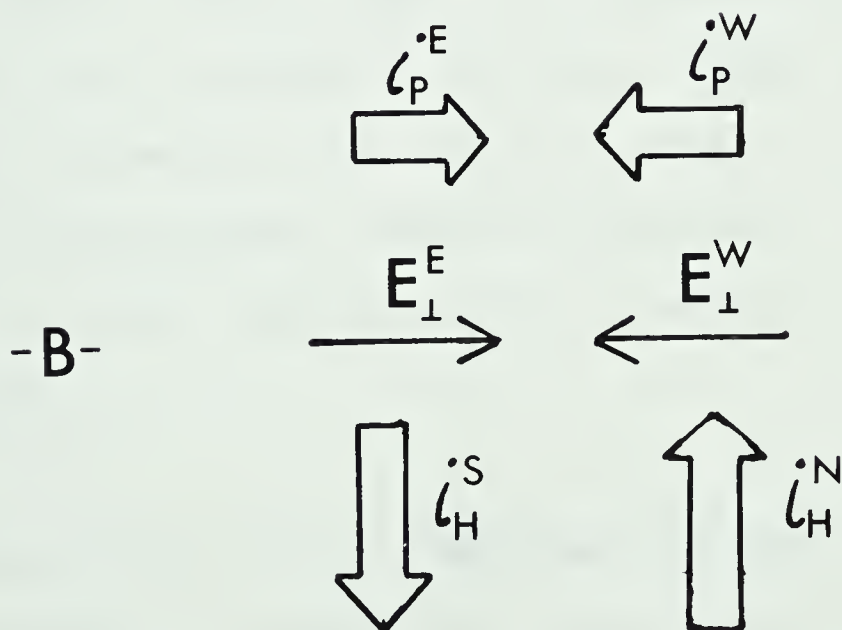
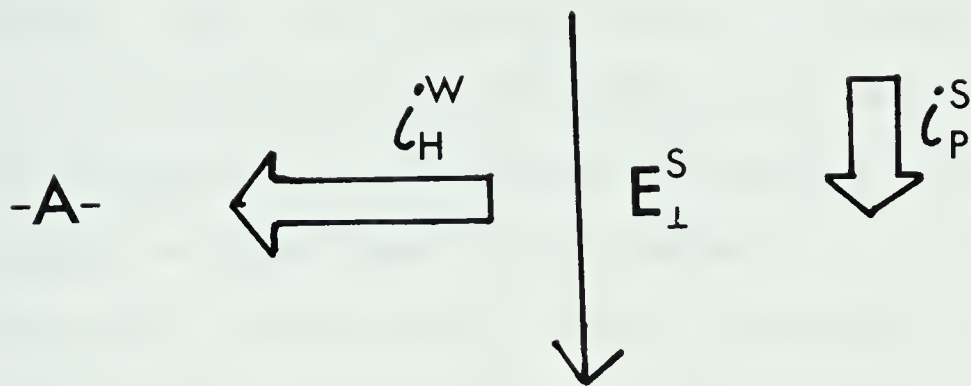


Figure 4.1

Hall and Pederson current flow for electric fields expected in westward electrojet ('A') and surge ('B') regions. Subscripts H and P refer to Hall and Pederson, respectively. N, E, W, and S refer to directions north, east, west and south.



consider only the resulting Hall currents (see figure 4.1-b) then a region of southward flowing current will develop followed by a region of northward flowing current. From symmetry considerations, these currents should be equal in magnitude. With a Hall conductivity of 40 mhos, an electric field of 25 millivolts/meter would be required to produce a current density of 1 amp/meter. Currents of this magnitude are typical of that used in the model.

Extensive measurements of the electric field in the surge region are not available. In one study (Horwitz et al, 1978),  $E$  was observed to rotate westward prior to and during the passage of a westward travelling surge. Also, northward directed electric fields were observed to the east of the surge. While there were no eastward directed  $E$  fields observed, the westward electric field does suggest a poleward flowing Hall current within the region of the surge. To this point, however, there is no direct evidence (i.e. in situ measurements) to support the model which we have used.

#### 4.4 General Approach to Modelling the Data

Profiles to be modelled were selected from each event. These were selected as being representative of different phases of the substorm development. The profiles were selected at points prior to, during and following the passage of the surge.

The initial locations of the model current systems were



determined according to the analysis presented in chapter 3. Variations in the position of the borders, the tilt and the relative magnitudes of the current system were then made in order to achieve the best fit. The small number of data points per profile and the large number of degrees of freedom make a standard statistical estimate of the goodness of fit difficult to determine and interpret. For this reason the control of the model parameters and the determination of the occurrence of the best fit was not automated.

For each event, the parameters defining the model for each modelled (theoretical) profile are listed in a table. In order to be consistent, the profile code (e.g. profile B-1) used in the figures of chapter 3 will also be used in this chapter. Each current system is defined with respect to the central point of the western edge. The length, therefore, is given in degrees of longitude from this reference point. The system is then tilted (if indicated) to the south-east, again with respect to this reference point.

Finally for a particular event, the position, dimension and current density of each current system were allowed to change from profile to profile. In general the degree of tilt was fixed throughout an event.

## 4.5 Modelling the Data

### 4.5.1 The Day 214, 1974 Event

The theoretical and the observed profiles chosen for





this event are shown in figure 4.2 . The model parameters are listed in table 4-1.

Profile B is taken just prior to the arrival of the surge. In the model we have placed the western edge of the system at  $308^{\circ}$  E,  $4^{\circ}$  east of Uranium City. While there is some disagreement between the theoretical and the observed profiles, the basic form does agree. The most significant discrepancy occurs as the H component approaches the baseline, however it is in this region, near the baseline, that the values will be most prone to error because of the effects of current systems which were not incorporated into the model. The key feature of this profile is the indication of a positive D regime as the poleward current system (and the surge) approaches.

Profile D is taken when the surge is overhead. In the model the western edge of the poleward current system has been placed  $1^{\circ}$  west of Fort Smith. In the theoretical profile we can see the positive D and the negative Z regimes associated with this system. In this case, the theoretical profile might be shifted slightly to the west but it has a form which agrees basically with the observed profile.

Because the theoretical profile is slightly off-set, one can clearly see the development of a negative D regime behind the positive D regime and also that the negative extremum of the Z component corresponds to the cross-over point in the D component. These features have been noted as being characteristic of the surge form.

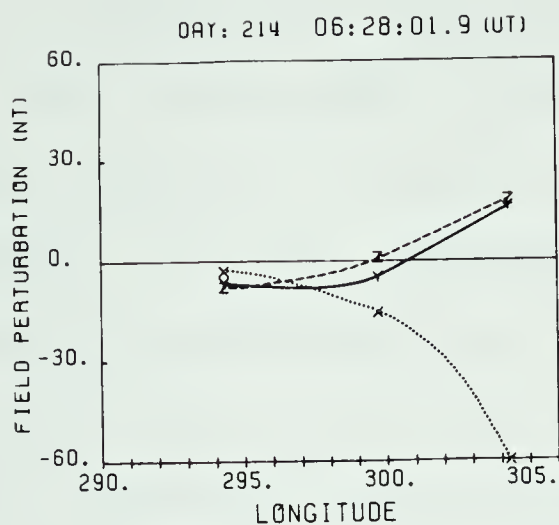




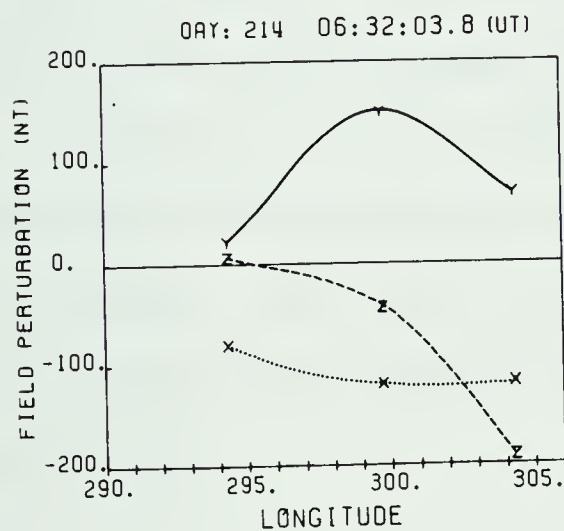
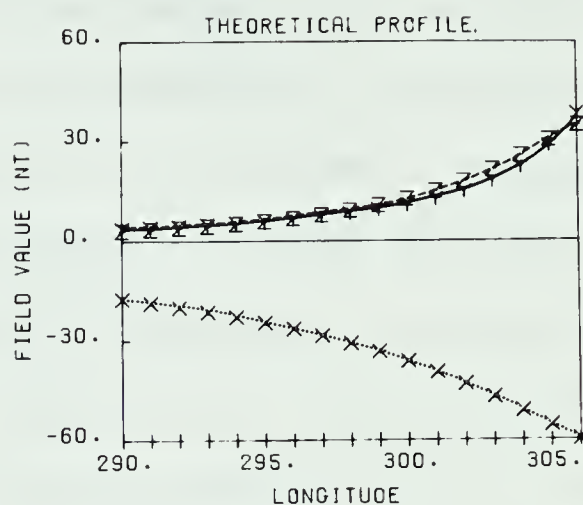
Table 4.1  
Current System Parameters; Surge Model for Day  
214, 1974

PROFILE	POLEWARD/EQUATORWARD CURRENT SYSTEM					WESTWARD CURRENT SYSTEM				
	WEST. EDGE CNTR. ( <sup>o</sup> E) ( <sup>o</sup> N)	LNQTH (DEG.)	WDTH (DEG.)	TILT ( <sup>o</sup> SE)	CUR. DENS. (A/M)	WEST. EDGE CNTR. ( <sup>o</sup> E) ( <sup>o</sup> N)	LNQTH (DEG.)	WDTH (DEG.)	TILT ( <sup>o</sup> SE)	CUR. DENS. (A/M)
B	308.0 68.0	14.0	6.0	0	.25	308.0 68.0	20.0	6.0	0	.35
D	296.5 70.0	14.0	6.0	0	.40	294.0 70.0	25.0	6.0	0	.45
E	278.0 69.5	12.0	7.0	-10	.90	278.0 69.5	30.0	7.0	-10	.70

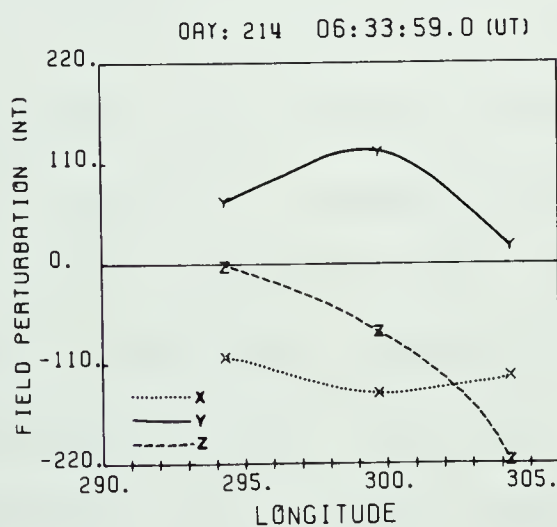
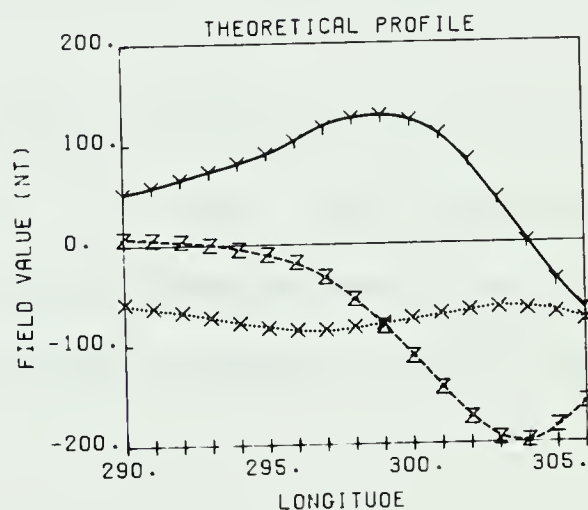




-B-



-D-



-E-

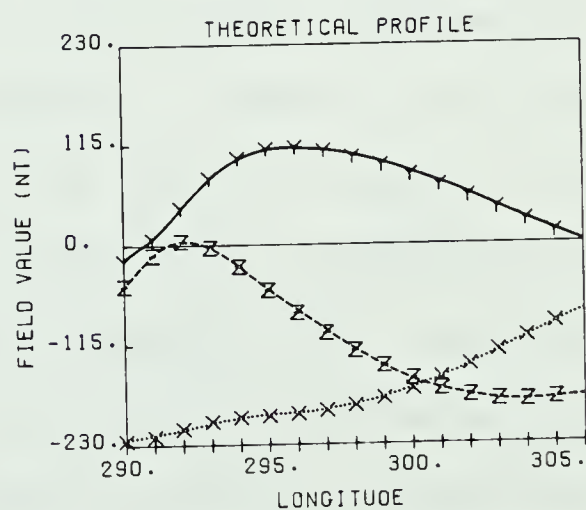


Figure 4.2

Observed and theoretical longitude profiles at indicated times for Day 214, 1974. Profiles are referred to in text by the indicated label. Note that X, Y, and Z refer to magnetic components H, D, and Z.



Profile E is taken just after the passage of the surge. In the theoretical profile we have generated a positive D and a negative Z regime using only the westward current system. It was suggested in chapter 3 that this was a possible explanation for the observed behaviour. In order to produce this profile the westward edge of the system was not only placed to the north-east of the station line but also tilted  $10^\circ$  to the south-west. While such a tilt may seem somewhat unusual, the orientation of the arcs at this time (figure 3.5 ) does support it.

Finally, we note that the model has reproduced the key features of the magnetic signature in each data profile. Furthermore, features of the surge development and, in particular, the expansion westward and poleward have been reproduced.

#### 4.5.2 The Day 307, 1976 Event

For this event both longitude and latitude profiles are modelled. The chosen profiles are shown in figures 4.3, 4.4, 4.5, and 4.6 . The model parameters are given in table 4-2.

The longitude and latitude profiles A of figures 4.3 and 4.4 are taken prior to the development of the westward travelling surge. The model used to generate the theoretical profiles is a simple westward current system. An important feature of the system is that the westward electrojet is tilted by  $20^\circ$  to the north-west as was suggested by the analysis of chapter 3.

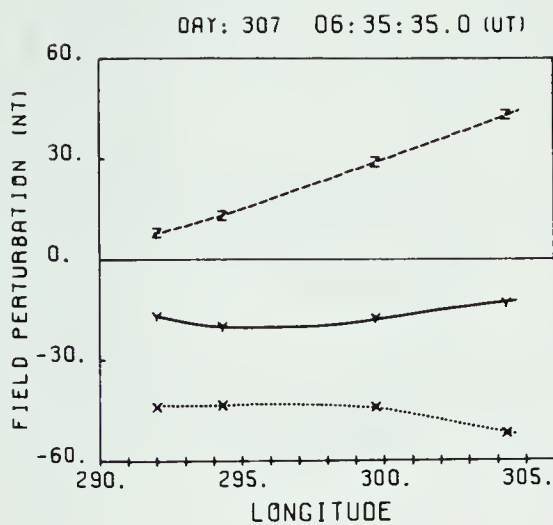




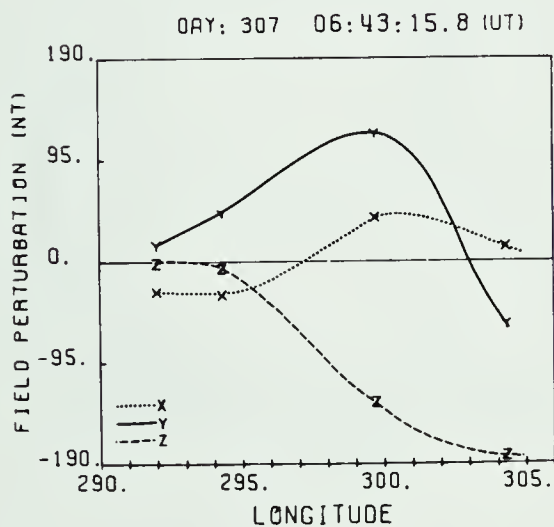
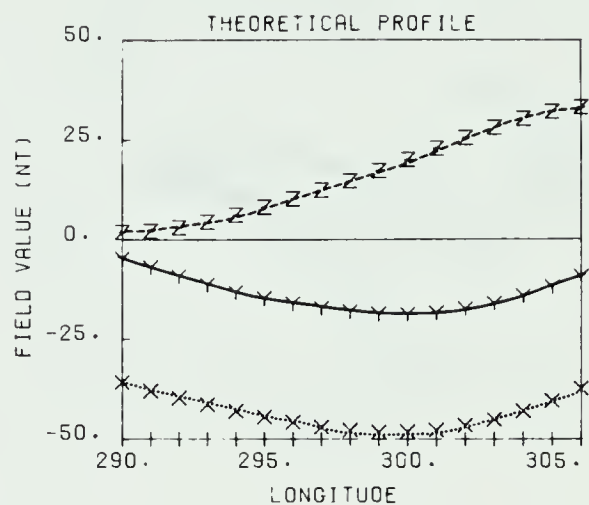
Table 4.2  
Current System Parameters; Surge Model for Day  
301, 1976

PROFILE	POLEWARD/EQUATORWARD CURRENT SYSTEM					WESTWARD CURRENT SYSTEM				
	WEST. EDGE CNTR. ( $^{\circ}$ N)	LN $\overline$ TH (DEG.)	WDTH (DEG.)	TILT ( $^{\circ}$ SE)	CUR. DENS. (A/M)	WEST. EDGE CNTR. ( $^{\circ}$ N)	LN $\overline$ TH (DEG.)	WDTH (DEG.)	TILT ( $^{\circ}$ SE)	CUR. DENS. (A/M)
A										
		290.0	25.0	4.0	20	.20				
		67.5								
B1	292.0	19.0	6.0	20	.55	290.0	25.0	6.0	20	.12
	71.5					71.5				
D6	284.0	20.0	7.0	20	.45	284.0	26.0	7.0	20	.50
	72.5					72.5				
E										
		278.0	30.0	7.0	20	.75				
		72.5								





-A-



-B1-

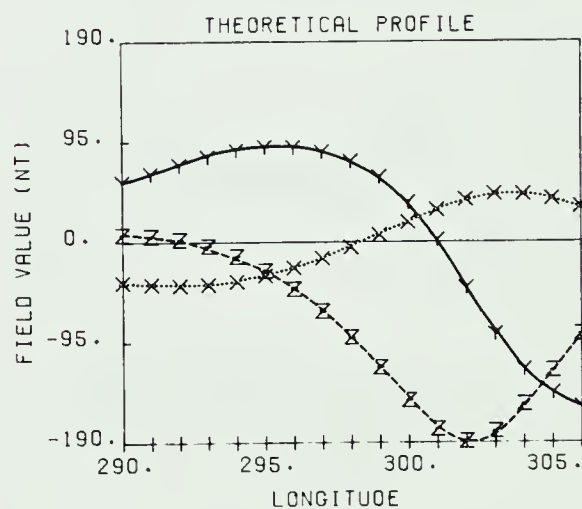
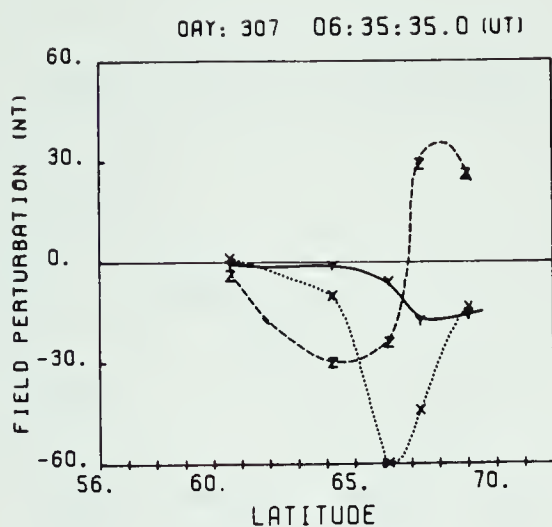
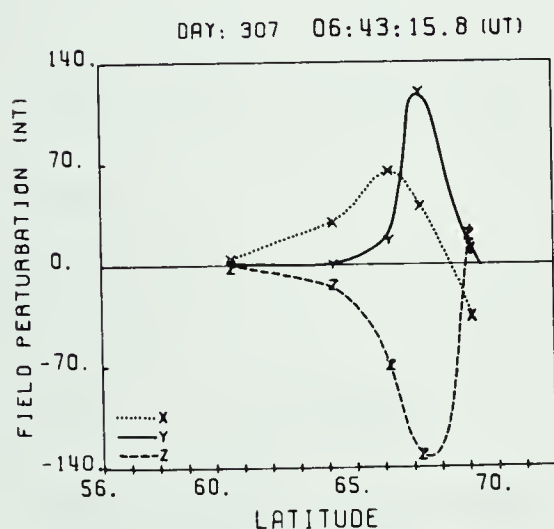
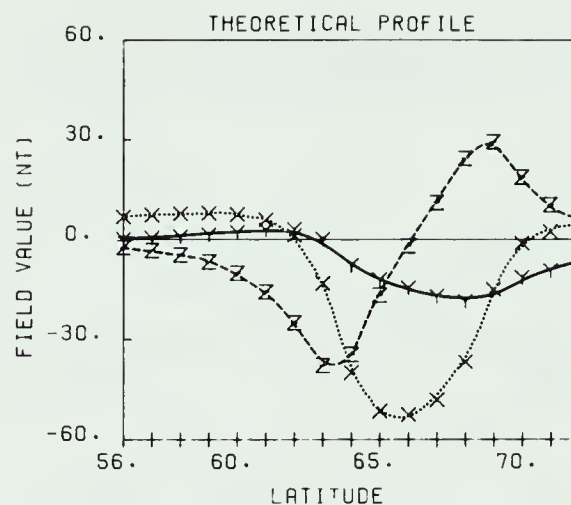


Figure 4.3  
Observed and theoretical longitude profiles at indicated times for Day 307, 1976. Profiles are referred to in text by the indicated label. Note that X, Y, and Z refer to magnetic components H, D, and Z.

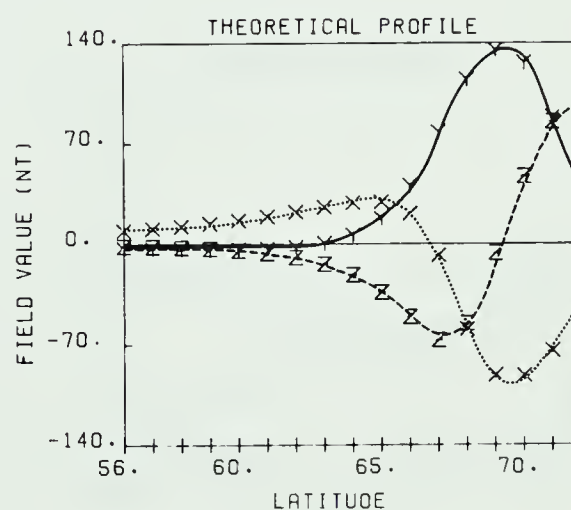




-A-

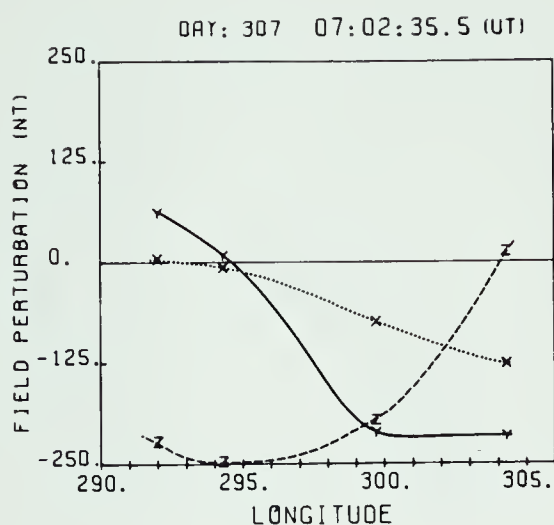


-B1-

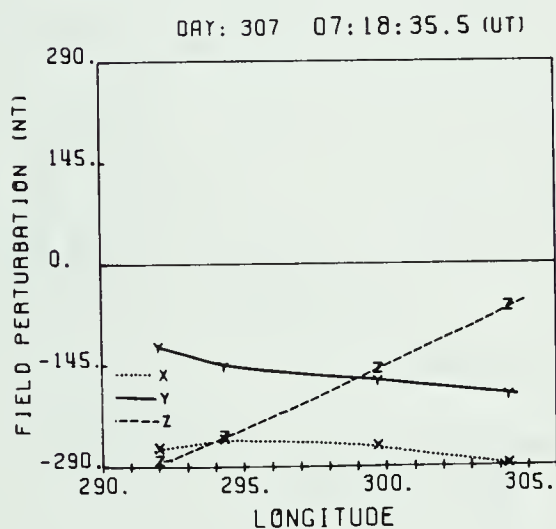
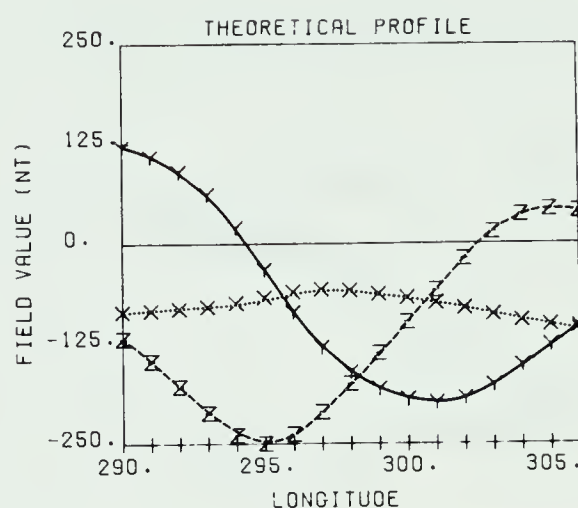
Figure 4.4

Observed and theoretical latitude profiles at indicated times for Day 307, 1976. Profiles are referred to in text by the indicated label. Note that X, Y, and Z refer to magnetic components H, D, and Z.





-D6-



-E-

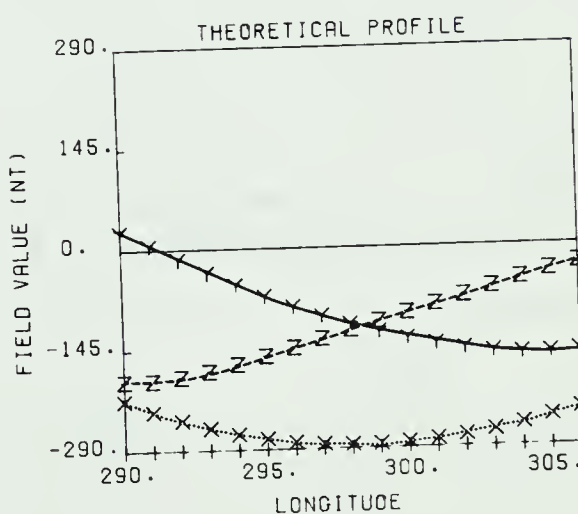
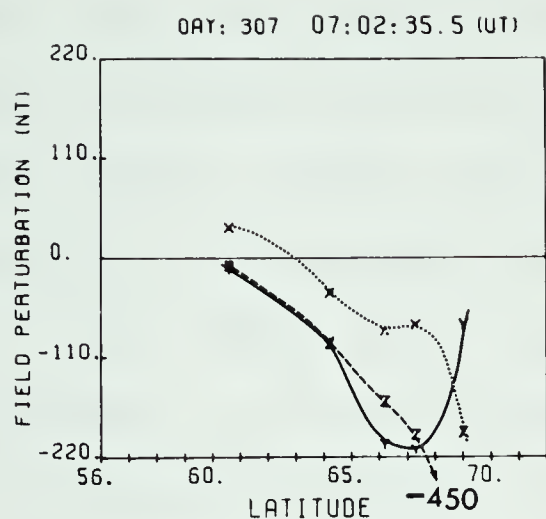


Figure 4.5

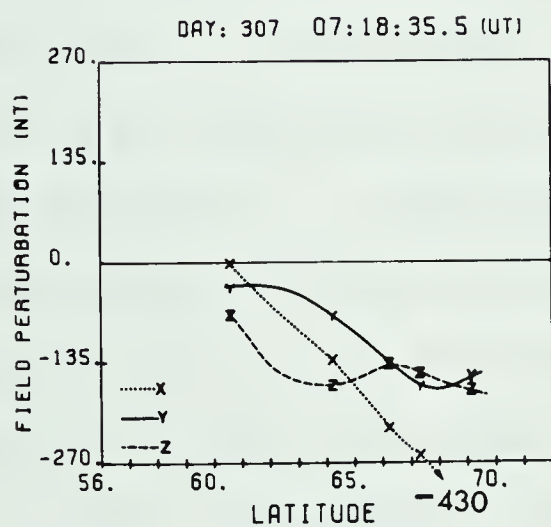
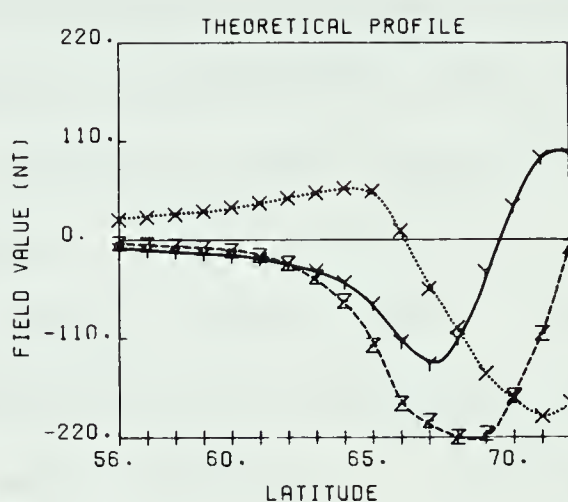
Observed and theoretical longitude profiles at indicated times for Day 307, 1976. Profiles are referred to in text by the indicated label. Note that X, Y, and Z refer to magnetic components H, D, and Z.







-D6-



-E-

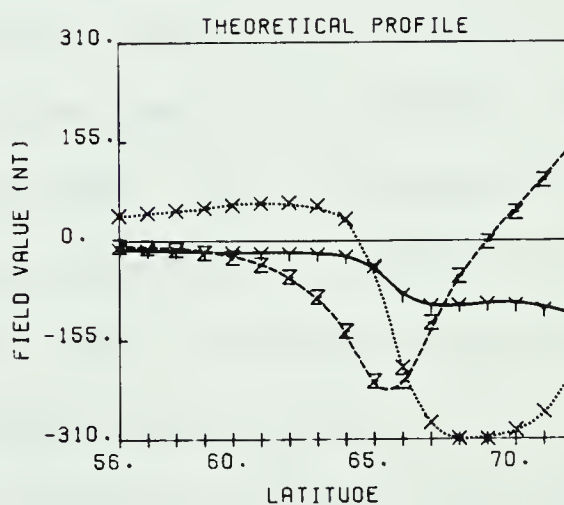


Figure 4.6

Observed and theoretical latitude profiles at indicated times for Day 307, 1976. Profiles are referred to in text by the indicated label. Note that X, Y, and Z refer to magnetic components H, D, and Z.



The theoretical longitude profile shows good agreement with the data profile. The uniform H and D components have been reproduced and the tilted current system has generated the linear change in the Z component as a function of longitude in agreement with the data.

The theoretical latitude profile also shows good agreement. The basic form of the profile is consistent with the data profile while the data does indicate a somewhat narrower negative H regime and Z transition region.

The longitude and latitude profiles B-1 of figures 4.3 and 4.4 were (in the analysis of chapter 3) considered to represent a surge-like perturbation prior to the onset of the major substorm currents. The model used to generate the corresponding theoretical profiles is primarily a poleward/equatorward current system centered near  $301^{\circ}$  E. A weak westward current system was also included. Both of these systems were tilted to the north-west by  $20^{\circ}$ .

The theoretical longitude profile compares very well with the data. The H component values are quite near the baseline and the position of the negative to positive transition is quite flexible in the data profile. The only discrepancy occurs as the D component approaches the baseline in the western region of the profiles.

The theoretical latitude profile does have the basic form of the observed profile. However, both the positive H and negative Z extrema are too low in magnitude and the width of the positive D regime seems to be too large.



The longitude and latitude profiles D-6 of figures 4.4 and 4.5 were chosen as the surge was passing overhead. The model used includes a poleward/equatorward system centered near  $294^{\circ}$  E and a strong westward current system.

The theoretical longitude profile closely matches the data profile. The only major discrepancy occurs as the observed H component returns to the baseline in the western region of the profile.

The theoretical latitude profile again follows the basic form of the data profile however all of its values are considerably too low. For instance in the theoretical profile the Z component peaks at -220 nT while the data indicates that it does not peak until at least -450 nT. Indeed it would seem that the theoretical values should be uniformly doubled. This would be equivalent to doubling the current density however such a procedure would greatly affect the behaviour of the theoretical longitude profile.

The longitude and latitude profiles E of figures 4.5 and 4.6 were taken long after the passage of the westward travelling surge. The model used to generate the theoretical profiles included only a broad westward current system placed further westward. The current system is still tilted  $20^{\circ}$  to the north-west.

In the western region of the theoretical longitude profile, the D and Z component values tend to be too large. Nevertheless, the basic form of the profile matches that of the observed profile.





While the D component of the theoretical latitude profile does show good agreement with the data, the H and Z components are not as successful. In the data profile the Z component is seen to remain at a reasonably constant negative level while in the theoretical profile the Z component becomes positive at higher latitudes. While the data profile does indicate that the H component drops from positive values at lower latitudes to negative values at higher values, the rate of decrease is considerably slower than that of the theoretical values.

Finally, we note that the model has reproduced many of the key features of the observations. In many cases the agreement is very good. However, for a few latitude profiles the agreement is less satisfactory.

#### 4.5.3 The Day 223, 1977 Event

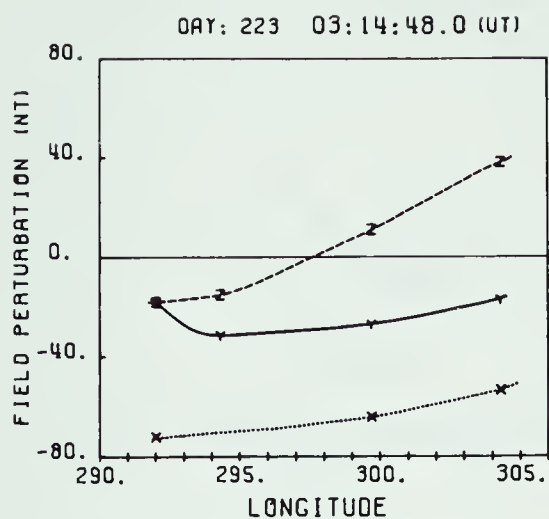
For this event both longitude and latitude profiles are available for modelling. The selected profiles and the corresponding theoretical profiles are given in figures 4.7, 4.8, 4.9, and 4.10 . The model parameters are given in table 4-3.

The longitude and latitude profiles A of figures 4.7 and 4.8 were taken prior to the development of the westward travelling surge. In chapter 3 these profiles were interpreted in terms of an intensification of both the eastward and westward electrojets. In modelling these profiles we have included both a westward current system and

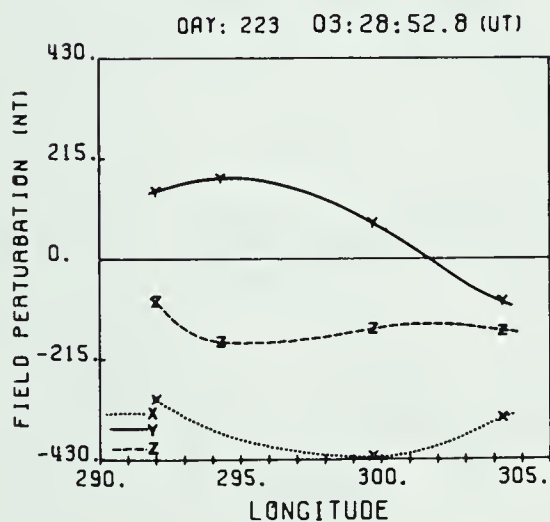
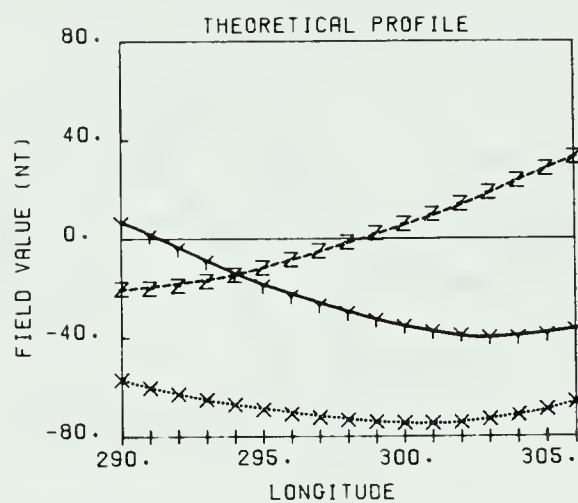








-A-



-D-

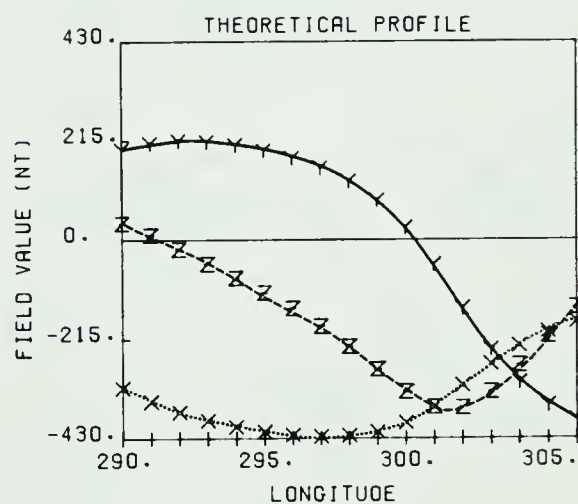
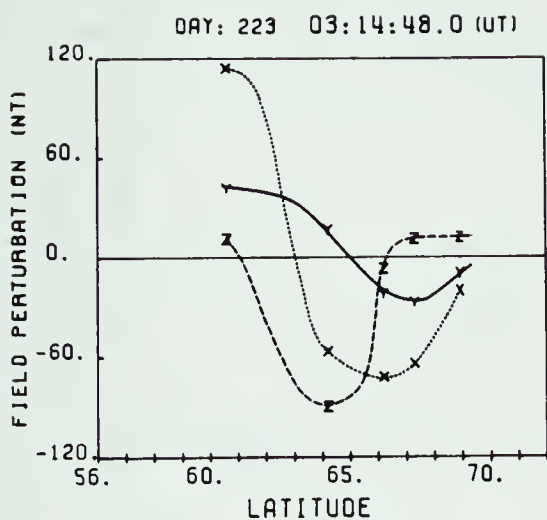


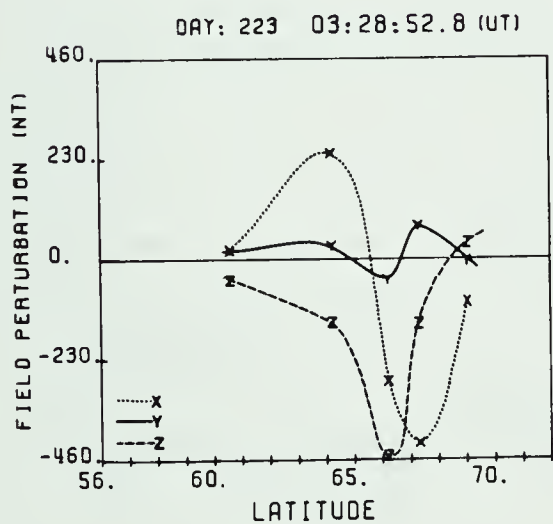
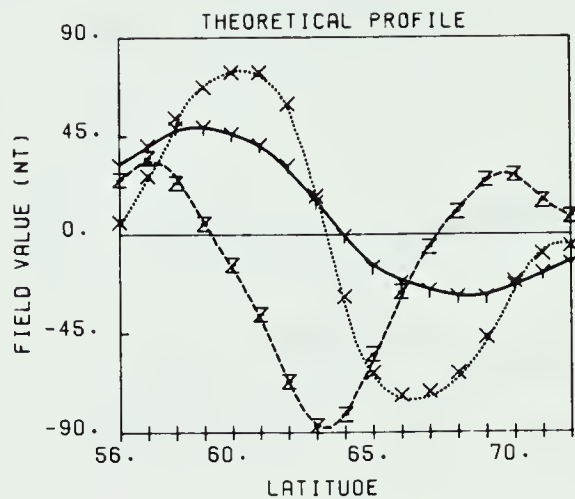
Figure 4.7

Observed and theoretical longitude profiles at indicated times for Day 223, 1977. Profiles are referred to in text by the indicated label. Note that X, Y, and Z refer to magnetic components H, D, and Z.





-A-



-D-

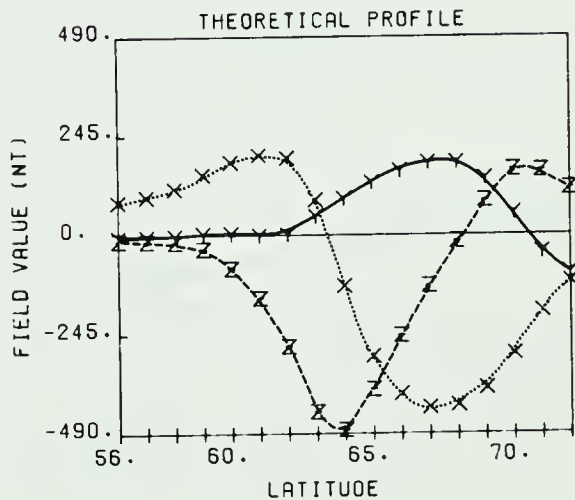
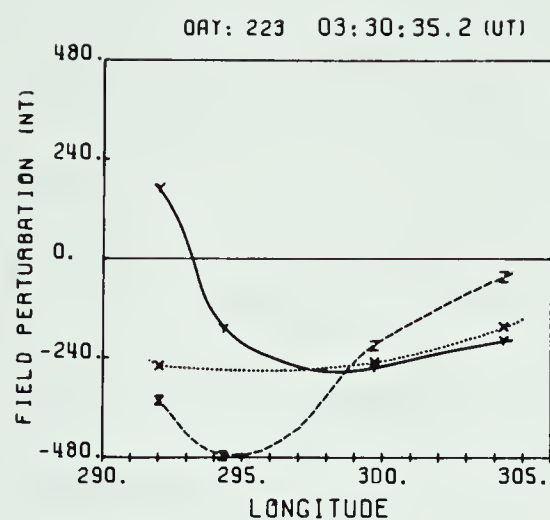


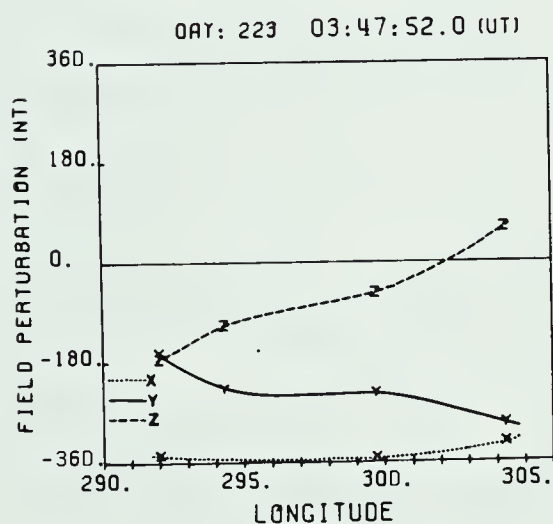
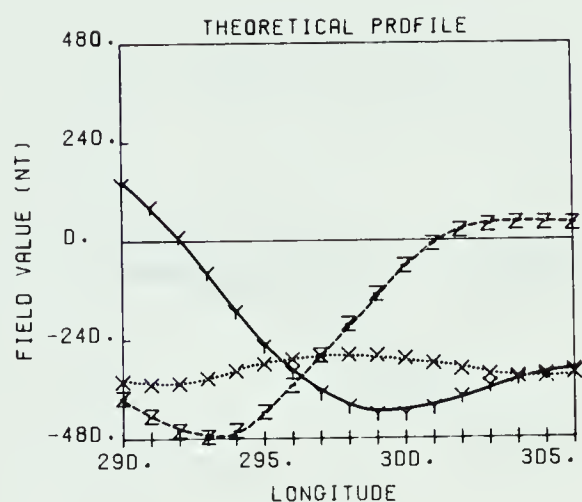
Figure 4.8  
Observed and theoretical latitude profiles at indicated times for Day 223, 1977. Profiles are referred to in text by the indicated label. Note that X, Y, and Z refer to magnetic components H, D, and Z.







-F-



-H-

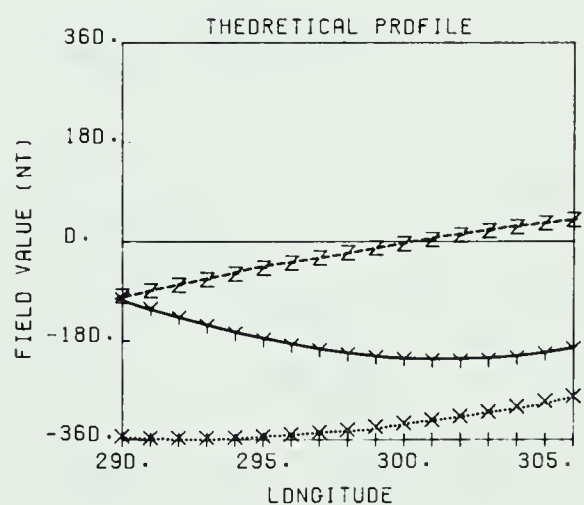
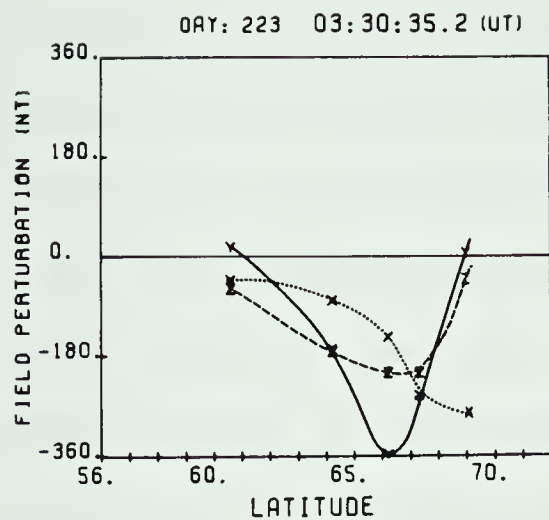
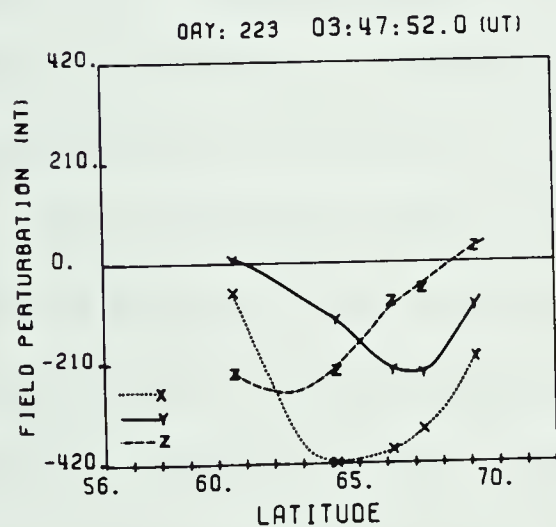
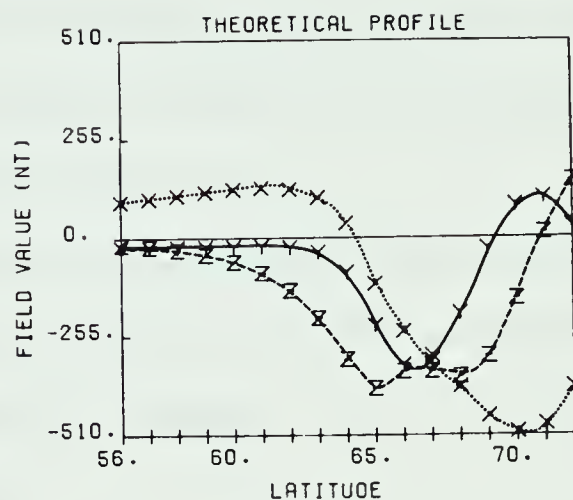


**Figure 4.9**  
Observed and theoretical longitude profiles at indicated times for Day 223, 1977. Profiles are referred to in text by the indicated label. Note that X, Y, and Z refer to magnetic components H, D, and Z.





-F-



-H-

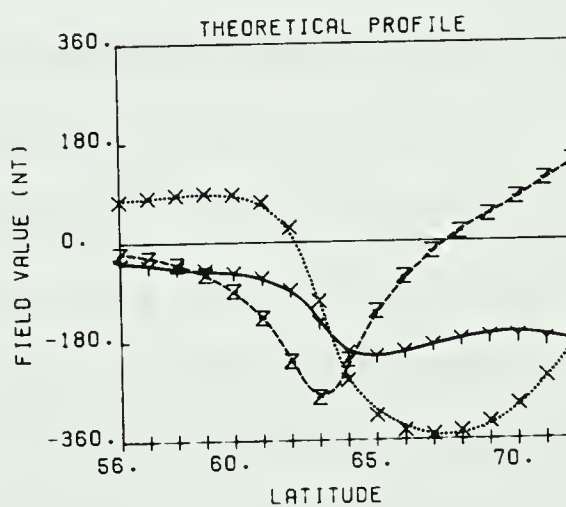


Figure 4.10

Observed and theoretical latitude profiles at indicated times for Day 223, 1977. Profiles are referred to in text by the indicated label. Note that X, Y, and Z refer to magnetic components H, D, and Z.



an eastward current system of equal magnitude. The eastward system has been placed directly south of the westward system and both have been tilted by  $30^\circ$  to the north-west. The westward current system has been placed so that the center of it crosses the station line near  $299^\circ$  E .

In the Z component of the theoretical longitude profile we can clearly see the result of the tilt in the westward current system. In all respects this profile is in good agreement with the observed profile.

In the theoretical latitude profile we must first note the difference in the scale size. The magnitude of the H component maximum near  $61^\circ$  N has not been reproduced by the model. Elsewhere, however, the form and the magnitude of the theoretical profile is in good agreement with the data.

The longitude and latitude profiles D of figures 4.7 and 4.8 were taken to represent an early stage of the surge development. In the model a very broad poleward/equatorward current system (each section is  $10^\circ$  long) was used and centered near the station line at  $300^\circ$  E. Both the westward and eastward current systems have been included but the westward system is now dominant. Both of these systems have been shifted poleward and the westward system has also been shifted westward. All systems have been tilted to the north-west by  $30^\circ$  .

The D and H components of the theoretical longitude profile match the data quite well, however the Z component shows a distinct discrepancy. While the data indicate that





the Z component remains relatively uniform, the theoretical Z component shows a definite negative extremum. In the analysis of this event it was noticed that while the negative Z extremum (which we have associated with the D component cross-over point in the surge signature) was not apparent in this profile, it did develop shortly afterward. The influence of some additional undefined current system could be responsible for this.

While the theoretical latitude profile agrees quite well in its basic form, the data profile has noticeably narrower regimes in each component. Nevertheless, the H component transition from positive to negative, which we associate with the westward travelling surge, has been reproduced.

In the longitude and latitude profiles F of figures 4.9 and 4.10 the surge has apparently moved westward. In the model we have used only the poleward/equatorward and the westward current systems. Both of these have been shifted westward and poleward. Both are still tilted by  $30^\circ$  to the north-west.

The theoretical longitude profile agrees very well with the data profile. There is some disagreement where the D component of the theoretical profile falls further negative than that of the data profile but on the whole the agreement is satisfactory. In these profiles we see that the negative Z extremum corresponds with the D component cross-over point. In the model these are associated with the transition



from poleward to equatorward flowing current.

For the theoretical latitude profile the agreement is not particularly good. First we note that the scale values are quite different. Taking this into account the D component has been reproduced quite well. Nevertheless, the theoretical Z values drop too far negative and return to the baseline too far to the north. The H component is also unsatisfactory. While the data values are negative throughout, the theoretical values are quite positive at lower latitudes and drop too negatively at higher latitudes. There are a number of probable causes contributing to this poor fit. For instance, during this period of the substorm there may have been significant changes in the local current structure or a new current system may have developed locally. Although it cannot explain all of the observed effects, the eastward electrojet (which we have neglected) may still be contributing significantly. It is also possible that the contribution from induced currents (viz, the rate of change of the magnetic field) may have altered substantially.

The latitude and longitude profiles H of figures 4.9 and 4.10 were taken well after the passage of the surge. The model used was simply a broad westward current system. The system is still tilted by  $30^\circ$  to the north-west and has been shifted considerably westward.

The agreement between the theoretical longitude profile and the observed profile seems quite satisfactory.



The theoretical latitude profile does not show as good agreement as is desired. While the basic form is similar, there are discrepancies. Again we note the scale differences. The H component does match quite well. In the Z component the theoretical values do indicate a sharper negative peak however this is not entirely inconsistent with the data (considering the paucity of data points). In the D component, however, the theoretical values do not recover at the higher latitudes in the fashion of the data values.

Finally, we again note that the model has been reasonably successful in reproducing the data. Again, the poorest agreement occurs for the latitude profiles particularly for those taken late in the substorm development.

#### 4.6 Summary of the Model and Modelling

In general the agreement between the model generated profiles and the observed profiles can be considered reasonable. The key features of the surge signature have been reproduced by the model thereby giving support to the analysis of the surge behaviour given in chapter 3. Furthermore, the suggestion that the electrojets are often tilted with respect to a line of constant geomagnetic latitude has been supported by reproducing these situations with tilted current systems.

In situations where the comparison between the model and the observations is not particularly good, the





differences could have been caused by the effects of current structures which were not included in the model. We have also noted that the cases with poorest agreement were the latitude profiles taken late in the substorm development. Since the magnetometer stations used in producing the latitude profiles do not lie along a line of constant longitude as precisely as the longitude profile stations lie along a line of constant latitude, more difficulties in obtaining good agreement with latitude profiles would be expected. Moreover, since our latitude profile simply spans a greater distance than our longitude profile, variations caused by fluctuations in the current structure would be more significant. We also note that since all data profiles are taken from the same baseline, which was chosen at a point prior to the surge onset, the effects of current variations will become more significant at times late in the substorm development. Finally, in the latter parts of the expansion phase and during the recovery phase the rate of change of the magnetic field decreases. The contribution from the induced currents will, therefore, decrease and a corresponding increase in the depth of the superconductor should have been made in the model. These, then, are possible reasons for the difficulties in obtaining good agreement.

Finally, a significant result from the modelling process is the scale size of the current structures we have used in the model. If we interpret the combination of the





leading current loops (the one with equatorward and the one with poleward ionospheric current) to correspond with the auroral surge form, then the magnitude of the form ranges from  $14^{\circ}$ - $20^{\circ}$  of longitude (at  $67.5^{\circ}$  N latitude). This gives us a scale length of 600-800 km. In describing their observations of the magnitudes of auroral spiral forms (which included the westward travelling surge), Hallinan and Davis (1976) suggest a scale size of 250-500 km. While our scale size is slightly larger, it is restricted to surges.



## CHAPTER 5

### CONCLUSIONS AND DISCUSSION

#### 5.1 Summary of Results

The purpose of this research was to investigate the development of the westward travelling surge during magnetospheric substorms. In particular, by examining the magnetic behaviour associated with this auroral form it was hoped that a magnetic signature for the surge could be identified and a model current system be developed.

Twelve substorm events were examined, three of which have been presented in chapter 3. By using a two-dimensional array of magnetometer stations it was determined that the nature of the magnetic perturbations associated with the surge was strongly dependent on the location of the observer relative to the surge. Only by utilizing both longitude and latitude profiles of the magnetic behaviour could the signature of the surge be completely described.

The precise nature of the profiles depends on the magnitude, location, and orientation of the surge. However, for a typical surge, located directly overhead, we can describe typical longitude and latitude profiles making up its signature.

The longitude profile features, from west to east, a positive D component regime followed by a negative D regime. The Z component behaves similarly but with the negative



extremum of the Z component occurring at the longitude at which the D component reverses its polarity. This correspondence continues throughout the development of the surge. The latitude profile features, from south to north, a transition from positive to negative regimes in the H component.

This feature of the latitude profile, along with the latitudinal behaviour of the D component, has previously been used in describing the westward travelling surge (Meng, 1965; Kisabeth and Rostoker, 1973). In this study, we also used this feature of the H component but found the positions of the peaks and points of polarity reversal in the longitude profiles of the D and Z components most useful in identifying and describing the behaviour of the surge.

We can classify the surges which we have examined according to their behaviour. Firstly, surges which had developed in a region east of our sector were observed to move westward across it at the head of an expanding westward electrojet. Secondly, surges were observed to develop within our sector. These forms increased in magnitude without displaying significant motion in any direction. With time these forms either simply decayed (remaining stationary) or moved off in a westward direction. In both cases these surges were seen prior to the appearance of the westward electrojet. Finally, surge forms were seen to "jump" into our sector. As opposed to the previous type, these forms appeared very suddenly showing little or no growth. These





surges then move westward at the head of an expanding westward electrojet. Multiple surges were also observed. In these cases surge-like signatures were observed to move westward through our sector during the expansion phase of the substorm.

The motion of the surge was not always uniform. While moving westward the velocity would generally remain constant but on occasion the surge would apparently slow down or stop entirely and subsequently continue to move westward, often at a different velocity. Measured velocities of the surge motion ranged from 0 to  $4.8 \text{ km sec}^{-1}$ .

A small negative perturbation in the D component was often observed prior to the arrival of the surge. Our analysis indicated that this could result from either the approaching surge itself or an intensification of a tilted, overhead, westward current (possibly associated with pre-existing arcs) oriented from the south-east to the north-west.

In modelling the westward travelling surge, three-dimensional current systems were used. The basic model is outlined in figure 3.2. It consists primarily of a current loop made up of anti-parallel Birkeland current sheets connected by equatorward-flowing ionospheric current positioned beside and to the west of a similar current loop made up of anti-parallel Birkeland current sheets but connected by poleward-flowing ionospheric current. A westward electrojet and, if necessary, an eastward



electrojet, both confined to flow between Birkeland current sheets, were superposed on the above system.

In general the modelled data agreed well with the observations. In particular the use of model current systems which were tilted with respect to a line of constant geomagnetic latitude was successful in modelling many of the observed magnetic perturbations. Furthermore, through the modelling process an ionospheric scale size for the surge of 600 to 800 km was obtained.

## 5.2 Comments and Discussion

With the observations of the surge behaviour in the ionosphere we would now like to investigate the behaviour in the plasma sheet. Rostoker and Boström (1976) utilized mapping factors to project ionospheric currents, fields and conductivities into the magnetotail. They suggested that an average Birkeland current region in the ionosphere having a thickness  $W_I = 440$  km and a width  $L_I = 2300$  km should map into a portion of the plasma sheet having a width  $W_p = 7.5$  Re and a length  $L_p = 20$  Re. The mapping factors are then given by;

$$M_w = W_p / W_I = 108 \quad (5.1)$$

$$M_L = L_p / L_I = 56$$

Using these mapping factors we can take "typical" parameters for the surge in the ionosphere and obtain parameters for the corresponding disturbed region in the plasma sheet.



TABLE 5.1

Ionospheric Surge Parameters Mapped to the Plasma Sheet

Ionosphere		Mapping Factor	Plasma Sheet	
Width	500 km	108	Thickness	8.5 Re
Length	700 km	56	Width	6.3 Re
Velocity	2 km/sec (west)	56	Velocity	110 km/sec (west)

From Table 5.1 two facts are immediately clear. Firstly, the half-thickness of the plasma sheet involved in the substorm process is equal to almost the entire half-thickness of the plasma sheet. Thus, in the late evening sector, most of the plasma sheet would map to the bps (Winningham et al , 1975) and very little to the cps. This would conform with the model of tail particle drifts and electric fields proposed by Hughes and Rostoker (1979) (see their figure 16) as an extension of the Rostoker and Bostrom (1976) picture. A second fact which is apparent is that the surge maps to a rather small portion of the tail (whose half-width is 20 Re). Thus the substorm disturbed region in the tail for any intensification is relatively confined in azimuthal extent and a satellite in the tail would have to be appropriately placed in order to be able to evaluate the behaviour of particles and electric fields on magnetic field lines which map to the acceleration region for auroral particles.





Insofar as the acceleration of auroral particles is concerned, there are two regions of space which have been considered. Firstly there is the neutral line in the magnetotail associated with the substorm breakup (see Nishida and Nagayana, 1973). Some researchers believe that an electric field along the neutral line can lead to particle acceleration, and Heikkila and Pellinen (1977) have suggested that the accelerating electric field may be of the induction type generated by the changing tail magnetic field. Secondly, there is considerable evidence for an acceleration region situated on auroral zone field lines 2,000 - 10,000 km above the Earth's surface. Theoretical studies by Evans (1975) and by Block (1975) predicted the existence of parallel electric fields in this altitude range on auroral zone field lines, and their presence was subsequently confirmed by barium cloud injection experiments (Wescott et al , 1976) and by direct probe measurements (Mozer et al , 1977). The electric field stems from potential double layers which accelerate electrons to energies of several keV and cause them to precipitate into the ionosphere. Protons are also accelerated to energies of the order of keV , their motion being directed away from the Earth into the magnetotail. Below the acceleration region, the field-aligned current flow out of the ionosphere is carried by the electrons while above the region it is carried by the ions (Kisabeth and Rostoker, 1979). The presence of net outward field-aligned current in a localized





region of space has been predicted by Hallinan (1976) to lead to the development of auroral spirals and loops, which suggests that the westward travelling surge may also tend to be associated with localized upward current flow.

The question of the westward motion (if any) of the leading edge of the surge form has been a great puzzle until this time. This is largely because most attempts to study substorms involved the use of dipole field geometry in which protons drift westward and electrons drift eastward. Since the auroral surge is definitely generated by high energy electrons, the westward motion of the surge would seem to be inconsistent with the eastward gradient and curvature drift of the electrons. However, it is important to note that the substorm acceleration processes occur on field lines which map to the magnetotail, where the field line geometry is most definitely not dipolar. In fact, the gradient in magnetic field is directed from the low latitude region to the high latitude region of the tail, so that electrons near the boundary of the tail lobe and the plasma sheet will have a gradient drift velocity from dawn to dusk (i.e. westward). However, in this region of space the electric field is directed so as to cause  $\vec{E} \times \vec{B}$  drift from dusk to dawn opposing the gradient drift of the electrons. Thus the electrons may, depending on the relative magnitude of the  $E \times B$  and gradient drift, move either westward, eastward or maintain a relatively fixed position in longitude. This may well account for the erratic behaviour of the westward



travelling surge.

Finally we note that our average value of the velocity of westward propagation of the leading edge of the surge can lead us to an estimate of the lower limit of the latitudinal gradient in magnetic field across the plasma sheet. The magnitude of the gradient drift velocity is given by Roederer (1970),

$$|\vec{V}_G| = (m v_L^2 / 2e) (\nabla B / B^2) \quad 5.2$$

where  $\vec{V}_L$  is the gyration velocity,  $e$  the electronic charge,  $B$  the magnetic field and  $\nabla B$  the gradient of the magnetic field normal to  $B$ . Using our velocity of 110 km/sec and an average tail plasma sheet field of 8 nT, we find an average value of the gradient in the magnetic field across the plasma sheet thickness of 4.5 nT/Re if one considers 10 keV electrons as being associated with the surge generation. Over a plasma sheet half thickness of 8.5 Re, this gradient would lead to a tail lobe field of  $\sim 40$  nT which is quite reasonable for conditions of moderate activity. However, we have neglected the eastward directed  $\vec{E} \times \vec{B}$  drift associated with the convection electric field. This drift has a velocity given by  $V = |E/B|$  and for  $E \approx 0.3$  mV/m it would be 40 km/sec which is considerably smaller than the electron gradient drift velocity and so our estimates can be considered reasonable as order of magnitude calculations.

In summary, we have not been able to determine whether



or not the auroral acceleration region is close to the Earth or in the deep tail. In either case, the energized electrons will gradient drift westward, and the irregularity of the drift motion may well relate to the size of the competing  $\vec{E} \times \vec{B}$  drift velocity. For large electric fields of the order of 100 mV/m in the ionosphere, the electron gradient drift might be effectively cancelled by the  $\vec{E} \times \vec{B}$  drift leading to a surge form which is essentially stationary after its generation.

Finally, some comment should be made regarding the nature of substorm development and our observations of the westward travelling surge. In particular, the observation of the sudden onset of the surge in our sector, as on Day 307, 1976 (see chapter 3), followed by the expansion of the westward electrojet tends to support the Wiens-Rostoker model of substorm development wherein the westward electrojet expands northward and westward in discrete steps. The sudden onset of the surge would characterize the onset of a particular step in the expansion. However, the observation of stationary surge forms (spirals) occurring prior to the onset of the expansion phase and the observation of multiple surges which propagate during the expansion phase, should be incorporated into the model of substorm development.







### 5.3 Final Comments

In this thesis we have successfully identified the magnetic signature of the westward travelling surge and investigated some of the features of its behaviour. To continue this investigation in more detail a more closely spaced array of magnetometer stations could be used. Furthermore, correlation of ground-based data with satellite data might result in a detailed description of the surge mechanism within the plasma sheet.

It is apparent that the westward travelling surge plays an important role in the magnetospheric substorm and further research into its behaviour will give a better understanding of the substorm processes.



## REFERENCES

- Akasofu, S.-I., The development of the auroral substorm, Planet. Space Sci., 12, 273, 1964.
- Akasofu, S.-I., Polar and Magnetospheric Substorms, D. Reidel Publishing Company, Boston, 278 pp., 1968.
- Akasofu, S.-I., A study of auroral displays photographed from the DMSP-2 satellite and from the Alaska meridian chain of stations, Space Sci. Rev., 16, 617, 1974.
- Akasofu, S.-I., Physics of Magnetospheric Substorms, D. Reidel Publishing Company, Boston, 599 pp., 1977.
- Akasofu, S.-I., Magnetospheric substorms, EOS, Transactions, American Geophysical Union, 59, 68, 1978.
- Akasofu, S.-I., C.I. Meng, and D. S. Kimball, Dynamics of the Aurora - 4: Polar magnetic substorms and westward traveling surges, J. Atmospheric and Terrest. Phys., 28, 489, 1966.
- Atkinson, G., The current system of geomagnetic bays, J. Geophys. Res., 72, 6063, 1967.
- Axford, W.I., The interaction between the solar wind and the earth's magnetosphere, J. Geophys. Res., 67, 3791, 1962.
- Axford, W.I. and C. O. Hines, A unifying theory of high latitude geophysical phenomena and geomagnetic storms, Can. J. Phys., 39, 1433, 1961.
- Behannon, K.W., Geometry of the geomagnetic tail, J. Geophys. Res., 75, 743.
- Biermann, L., Kometenschweife und solare korpuskular strahlung, Zeit. F. Astrophys., 29, 274, 1951.



- Block, L.P., Double layers, in Physics of the Hot Plasma in the Magnetosphere, edited by B. Hultqvist and L. Stenflo, 229 pp., Plenum, New York, 1975.
- Boström, R., A model of the auroral electrojets, J. Geophys. Res., 69, 4983, 1964.
- Chen, A.J. and G. Rostoker, Auroral-polar currents during periods of moderate magnetospheric activity, Planet. Space Sci., 22, 1101, 1974.
- Chapman, S. and J. Bartels, Geomagnetism, Oxford Univ. Press, London, 1940.
- Cladis, J.B., Multiple coupled oscillations of field lines in the magnetosphere: modulation of trapped particles and ionospheric currents, J. Geophys. Res., 76, 2345, 1971.
- Davis, T.N., Auroral Morphology, Planet. Space Sci., 20, 1369, 1972.
- Davis, T.N. and T.J. Hallinan, Auroral spirals 1. observations, J. Geophys. Res., 81, 3953, 1976.
- Dungey, J.W., Interplanetary magnetic field and the auroral zones, Phys. Rev. Lett., 6, 47, 1961.
- Evans, D.S., Evidence for the low altitude acceleration of auroral particles, Physics of Hot Plasma in the Magnetosphere, B. Hultqvist and L. Stenflo (eds.), p. 319, Plenum Press, New York, 1975.
- Fukunishi, H., Constitution of proton aurora and electron aurora substorms Part II: Dynamical morphology of proton and electron aurora substorms and phenomenological model for magnetospheric substorms, JARE Sci. Rep. Series A NO. 11, Polar Research Center, National Science Museum, Tokyo, 1973.
- Hallinan, T.J., Auroral spirals 2. theory, J. Geophys. Res., 81, 3959, 1976.





- Heikkila, W.J. and R.J. Pellinen, Localized induced electric fields within the magnetotail, J. Geophys. Res., 82, 1610, 1977.
- Heppner, J.P., The Harang discontinuity in auroral belt ionospheric currents, Geofys. Pub., 29, 105, 1972.
- Horwitz, J.L., J.R. Doupnik, and P.M. Banks, Chatanika radar observations of the latitudinal distribution of auroral zone electric fields, conductivities, and currents, J. Geophys. Res., 83, 1463, 1978.
- Hughes, T.J., A comprehensive model of ionospheric - magnetospheric current systems during periods of moderate magnetospheric activity, Ph.D. Thesis, University of Alberta, spring, 1978.
- Hughes, T.J. and G. Rostoker, A comprehensive model current system for high latitude magnetic activity - I. The steady state system, Geophys. J.R. astr. Soc., 58, in press, 1979.
- Iijima, T. and T. A. Potemra, Large scale characteristics of field-aligned currents associated with substorms, J. Geophys. Res., 83, 599, 1978.
- Kangas, J., L. Lukkari, and E.R. Heacock, On the westward expansion of substorm-correlated particle phenomena, J. Geophys. Res., 79, 3207, 1974.
- Kellogg, P.J., Flow of plasma around the earth, J. Geophys. Res., 67, 3805, 1962.
- Kisabeth, J.L., The dynamical development of the polar electrojets, Ph.D. Thesis, University of Alberta, 1972.
- Kisabeth, J.L. and G. Rostoker, Current flow in the auroral loops and surges inferred from ground-based magnetic observations, J. Geophys. Res., 78, 5573, 1973.





- Kisabeth, J.L. and G. Rostoker, Modelling of three-dimensional current systems associated with magnetospheric substorms, Geophys. J., 49, 655, 1977.
- Kisabeth, J.L. and G. Rostoker, Relationship of noise in the frequency range  $100 < f < 500$  kHz to auroral arcs and field-aligned current and implications regarding acceleration of auroral electrons, J. Geophys. Res., 84, 853, 1979.
- Lassen, K., J.R. Sharber, and J.D. Winningham, The development of auroral and geomagnetic substorm activity after a southward turning of the interplanetary magnetic field following several hours of magnetic calm, J. Geophys. Res., 82, 5031, 1977.
- Lui, A.T.Y., C.-I. Meng, and S.-I. Akasofu, Search for the magnetic neutral line in the near-earth plasma sheet: 1. Critical re-examination of earlier studies on magnetic field observations, J. Geophys. Res., 81, 5934, 1976.
- McPherron, R.L., C. T. Russell, and M. P. Aubry, Satellite studies of magnetospheric substorms on August 16, 1968: 9. Phenomenological model for substorms, J. Geophys. Res., 78, 3131, 1973.
- Meng, C.-I., A.L. Snyder, Jr., and H. W. Kroehl, Observations of auroral westward traveling surges and electron precipitations, J. Geophys. Res., 83, 575, 1978.
- Mozer, F.S., C.W. Carlson, M.K. Hudson, R.B. Torbert, B. Paraday, J. Yatteau, and M.C. Kelley, Observations of paired electrostatic shocks in the polar magnetosphere, Phys. Rev. Lett., 38, 292, 1977.
- Ness, N.F., The earth's magnetic tail, J. Geophys. Res., 70, 2989, 1965.
- Ness, N.F., Magnetometers for Space Research, Space Sci. Rev., 11, 459, 1970.



- Nishida, A. and N. Nagayana, Synoptic survey for the neutral line in the magnetotail during the substorm expansion phase, J. Geophys. Res., 78, 3782, 1973.
- Pellinen, R.J., P.O. Welling, and W. J. Heikkila, Energization of charged particles to high energies by an induced substorm electric field within the magnetotail, Report, TRITA-EPP-77-10, Royal Institute of Technology, Stockholm, Sweden, 1977.
- Piddington, J.H., Cosmic Electrodynamics, Wiley and Sons Inc. , New York, 305 pp., 1969.
- Pytte, T., R.L. McPherron and S. Kokubun, The ground signature of the expansion phase during multiple onset substorms, Planet. Space Sci., 24, 115, 1976.
- Pytte, T., R.L. McPherron, M.G. Kivelson, H.I. West, Jr., and E.W. Hones, Jr., Multiple-satellite studies of magnetospheric substorms: plasma sheet recovery and the poleward leap of auroral zone activity, J. Geophys. Res., 83, 5256, 1978.
- Ratcliffe, J.A., An Introduction to the Ionosphere and Magnetosphere, Cambridge Univ. Press, Cambridge, 256 pp., 1972.
- Roederer, J.G., Dynamics of Geomagnetically Trapped Radiation, Springer-Verlag, New York, 1970.
- Rostoker, G., Studies of magnetic substorms using ground-based, balloon, rocket and satellite observations, European Space Research Organization special publication, no. 107, page 125, 1975.
- Rostoker, G., Polar magnetic substorms, Rev. Geophys. and Space Phys., 10, 157, 1972.
- Rostoker, G. and R. Boström, A mechanism for driving the gross Birkeland current configuration in the auroral oval, J. Geophys. Res., 81, 235, 1976.



- Rostoker, G. and K. Kawasaki, East-west asymmetries in auroral zone current distribution during magnetic substorms, Final Report to the Dept. of Energy, Mines and Resources on EMR contract OSU-(77-00020), 37 pp., March, 1978.
- Schindler, K., A theory of the substorm mechanism, J. Geophys. Res., 79, 2803, 1974.
- Snyder, A.L., Jr. and S.-I. Akasofu, Auroral oval photographs from the DMSP-8531 and 10533 satellites, J. Geophys. Res., 81, 1799, 1976.
- Swift, D.W., On the formation of auroral arcs and acceleration of auroral electrons, J. Geophys. Res., 80, 2096, 1975.
- Swift, D.W., An equipotential model for auroral arcs: 2. numerical solutions, J. Geophys. Res., 81, 3935, 1976.
- Swift, D.W., Stenbaek-Nielsen, H.C., and T.J. Hallinan, An equipotential model for auroral arcs, J. Geophys. Res., 81, 3931, 1976.
- Vasyliunas, V.M., Mathematical models of magnetospheric convection and its coupling to the ionosphere, in: Particles and Fields in the Magnetosphere, ed. B. M. McCormac, D. Reidel Publ., Boston, page 60, 1970.
- Wescott, E.M., H.C. Stenbaek-Nielsen, T.N. Hallinen, T.N. Davis, and H.M. Peek, The skylab barium plasma injection experiments. 2, Evidence for a double layer, J. Geophys. Res., 81, 4495, 1976.
- Wiens, R.G. and G. Rostoker, Characteristics of the development of the westward electrojet during the expansive phase of magnetospheric substorms, J. Geophys. Res., 80, 2109, 1975.





Winningham, J.D., F. Yasuhara, S.-I. Akasofu, and W. J. Heikkila, The latitudinal morphology of 10-ev to 10-kev electron fluxes during magnetically quiet and disturbed times at the 2100-0300 MLT sector, J. Geophys. Res., 80, 3148, 1975.















**B30256**